UC Irvine
UC Irvine Previously Published Works

Title

Summary of the ATLAS experiment's sensitivity to supersymmetry after LHC Run 1 — interpreted in the phenomenological MSSM

Permalink

https://escholarship.org/uc/item/4zg4j855

Journal

Journal of High Energy Physics, 2015(10)

ISSN

1126-6708

Authors

The ATLAS collaboration

Aad, G

Abbott, B

et al.

Publication Date

2015-10-01

DOI

10.1007/JHEP10(2015)134

Copyright Information

Peer reviewed

Summary of the ATLAS experiment's sensitivity to supersymmetry after LHC Run 1 — interpreted in the phenomenological MSSM

The ATLAS collaboration

E-mail: atlas.publications@cern.ch

ABSTRACT: A summary of the constraints from the ATLAS experiment on R-parity-conserving supersymmetry is presented. Results from 22 separate ATLAS searches are considered, each based on analysis of up to $20.3\,\mathrm{fb}^{-1}$ of proton-proton collision data at centre-of-mass energies of $\sqrt{s} = 7$ and $8\,\mathrm{TeV}$ at the Large Hadron Collider. The results are interpreted in the context of the 19-parameter phenomenological minimal supersymmetric standard model, in which the lightest supersymmetric particle is a neutralino, taking into account constraints from previous precision electroweak and flavour measurements as well as from dark matter related measurements. The results are presented in terms of constraints on supersymmetric particle masses and are compared to limits from simplified models. The impact of ATLAS searches on parameters such as the dark matter relic density, the couplings of the observed Higgs boson, and the degree of electroweak fine-tuning is also shown. Spectra for surviving supersymmetry model points with low fine-tunings are presented.

Contents

1 Introduction

During the first run of the Large Hadron Collider (LHC), the ATLAS [1] and CMS [2] Collaborations performed a wide range of searches for supersymmetry (SUSY) [3–11], using proton-proton (pp) collision data at centre-of-mass energies ($\sqrt{s}$) of 7 and 8 TeV. SUSY, a theoretically favoured framework for extending the Standard Model (SM), is able to address some of its unanswered questions, particularly the hierarchy problem [12–15], which is related to the fine-tuning needed to obtain the correct mass for the observed Higgs boson. SUSY can also provide credible dark matter candidates [16, 17] and can improve the unification of the electroweak and strong interactions [18–26].

The minimal supersymmetric extension of the Standard Model (MSSM) [27–31] predicts partners for each of the SM states. It predicts a pair of scalar partners — one for each fermion chirality — for each of the SM quarks and leptons. These spin-zero partner particles are known as squarks ($\tilde{q}$) and sleptons ($\tilde{\ell}$) respectively. In the first two generations the pair of chiral partners is largely unmixed, so the mass states can be labelled $\tilde{e}_\mathrm{L}$ and $\tilde{e}_\mathrm{R}$, where the L and R subscripts denote the scalar partners of the left- and right-handed Standard Model fermion states respectively. In the third generation of quarks and leptons the mixing between the scalars is larger, and the mixed states are labelled by their mass indices e.g. $\tilde{t}_1$ and $\tilde{t}_2$, where $\tilde{t}_1$ is lighter by construction. Each state in the SM gluon colour octet has a spin-half partner known as a gluino $\tilde{g}$. There are a total of eight spin-half partners of the electroweak gauge and Higgs bosons: the neutral bino (superpartner of the U(1) gauge field); the winos, which are a charged pair and a neutral particle (superpartners of the W bosons of the SU(2)$_\mathrm{L}$ gauge fields); and the Higgsinos, which are two neutral particles and a charged pair (superpartners of the Higgs field's degrees of freedom). The bino, winos and Higgsinos mix to form four charged states called charginos $\tilde{\chi}_{1,2}^\pm$, and four neutral states known as neutralinos $\tilde{\chi}_i^0$ (where the index i lies in the range 1 to 4, ordered by increasing neutralino mass). The charginos and neutralinos are collectively referred to as electroweakinos.

Since no statistically significant signals consistent with supersymmetry have yet been observed at the LHC, searches have been used to constrain the allowed supersymmetric model space. In the case of searches for supersymmetry, this typically results in setting lower limits on the masses of the pertinent supersymmetric partner particles (sparticles).

This paper presents the combined sensitivity and constraints from 22 separate ATLAS analyses of the Run 1 LHC dataset, using centre-of-mass energies of 7 and 8 TeV and an integrated luminosity of up to $20.3\,\mathrm{fb}^{-1}$. Direct searches for the decay products of the sparticles listed above are considered together with searches for disappearing tracks, long-lived charged particles, monojet signatures, and a dedicated search for the heavier neutral Higgs bosons, also expected in the MSSM. More details about the searches can be found in section 2.

The impact on the space of SUSY models has traditionally been presented in rather constrained frameworks, which have particular limitations when considering large numbers of analyses. One frequently used strategy for interpretation is in terms of models motivated by a particular mechanism of SUSY-breaking, for example via gravitational or gauge interactions. While such models can have theoretically appealing features, they assert relationships between SUSY-breaking parameters that may not be realised in nature, and they sample only a small part of the parameter space of the MSSM. SUSY searches at the LHC have also been interpreted using 'simplified' models. Such models attempt to capture the behaviour of a small number of kinematically accessible sparticles, assuming all others play no role. The simplest case corresponds to one specific SUSY production process with a fixed decay chain. Such models provide insight into the experimental constraints on the individual sparticle and decay mode, but fail to capture the complex effects that can result from large numbers of competing production and decay processes.

The MSSM has over a hundred parameters that describe the pattern of sparticle masses and their decays. This parameter space is too large to be scanned exhaustively and compared to ATLAS data. By applying a series of assumptions motivated by either experimental constraints or general features of possible SUSY breaking mechanisms, the number of parameters can be reduced to 19. This is known as the phenomenological MSSM (pMSSM) [32–34]. This model is assumed to conserve R parity,[1] which ensures that sparticles are produced in pairs and the lightest supersymmetric particle (LSP) is stable. The parameters are assumed to be real so that new CP violation does not occur in the sparticle sector. Parameters that would give rise to additional flavour-changing neutral currents are absent. The LSP provides a dark matter candidate if colourless and electrically neutral. In this paper, the LSP is required to be the lightest neutralino. Its production at the LHC gives rise to missing transverse momentum (whose magnitude is denoted $E_{\mathrm{T}}^{\mathrm{miss}}$), which is required by most of the ATLAS searches considered in this paper. There is no theoretical upper bound on the parameters characterising the sparticle masses. However, since the experiments have no sensitivity to sparticles with very large masses, the following additional restriction is applied before a specific set of parameters is considered: all sparticle masses must be less than 4 TeV. A specific set of the 19 parameters is referred to as a model point in parameter space; 310,327 such model points, each consistent with a range of previous experimental results, are considered. More details about the selection of pMSSM points can be found in section 3.

---

[1] $R = (-1)^{3B+L+2S}$ where B is baryon number, L is lepton number and S is spin.

Several groups have advocated the use of the pMSSM for interpretation of LHC results [33–52]. Most of these studies use estimated experimental efficiencies and acceptances for pMSSM points, and compare them to the model-independent limits from a selection of LHC searches to constrain the pMSSM parameter space. Previous ATLAS analyses have also used the pMSSM for interpretation of individual searches [53–57] by fixing most of the parameters, and varying just two or three: they therefore explore only a small part of the parameter space. This paper makes full use of the ATLAS experimental simulation, reconstruction and analysis tools. It represents the most comprehensive assessment of the ATLAS constraints on supersymmetry models to date.

The paper is organised as follows. The relevant ATLAS Run 1 analyses are summarised in section 2. A description of the pMSSM parameter space can be found in section 3, along with the direct and indirect constraints applied prior to the generation of the 310,327 model points. Monte Carlo simulation of those model points is described in section 4. The effect of the ATLAS searches on this pMSSM space is described in section 5. Discussion and conclusions can be found in section 6.

2 ATLAS searches

A total of 22 distinct ATLAS analyses are considered, spanning a wide range of different search strategies and final states, as listed in table 1. Each analysis has several signal regions — for example the analysis requiring events with zero isolated electrons and muons and a minimum of 2–6 jets in association with large $E_{\mathrm{T}}^{\mathrm{miss}}$ [58] has 15 different signal regions, each with different requirements on kinematic parameters and/or multiplicities of jets. For each of the 22 analyses, most of the signal regions from the original analysis are considered. However, in some cases, for practical reasons it was necessary to leave out some specialised signal regions or more complex combined fits. This leads to a slight underestimate of the full reach of the search. In total, almost 200 distinct signal regions are considered.

The analyses are classified into the four broad categories shown in table 1. 'Inclusive' searches are those primarily targeting decays, including cascade decays, initiated by production of squarks of the first two generations or gluinos. 'Third-generation' searches are those targeted particularly at the production of top and bottom squarks, known as the stop ($\tilde{t}$) and sbottom ($\tilde{b}$). 'Electroweak' searches include those for direct production of electroweakinos and sleptons. Since each search involves multiple signal regions, and since different SUSY production and decay processes can contribute to each of those, this categorisation can only be considered to be a rough guide when interpreting the type of sparticles to which the analysis might show sensitivity. 'Other' searches are those for heavy, long-lived particles (which are only considered for a small subset of the model points) and the search for heavy Higgs bosons. The details of the analyses can be found in the corresponding papers (listed in table 1) and a brief summary for each is given below.

In what follows the term 'lepton' (ℓ) is used to refer specifically to the charged leptons $e^{\pm}$ and $\mu^{\pm}$ of the first two generations. Where $\tau^{\pm}$ leptons are also included — for the 3-leptons and 4-leptons electroweak searches — this is indicated explicitly.

Analysis	Ref.	Category
0-lepton + 2–6 jets + E_T^{miss}	[58]	
0-lepton + 7–10 jets + E_T^{miss}	[59]	
1-lepton + jets + E_T^{miss}	[60]	
$\tau(\tau/\ell)$ + jets + E_T^{miss}	[61]	Inclusive
SS/3-leptons + jets + E_T^{miss}	[62]	
0/1-lepton + $3b$-jets + E_T^{miss}	[63]	
Monojet	[64]	
0-lepton stop	[65]	
1-lepton stop	[56]	
2-leptons stop	[66]	
Monojet stop	[67]	Third generation
Stop with Z boson	[68]	
$2b$-jets + E_T^{miss}	[69]	
$tb+E_T^{miss}$, stop	[57]	
ℓh	[70]	
2-leptons	[54]	
2-τ	[55]	
3-leptons	[53]	Electroweak
4-leptons	[71]	
Disappearing Track	[72]	
Long-lived particle	[73, 74]	Other
$H/A \to \tau^+\tau^-$	[75]	

Table 1. The 22 different ATLAS searches considered in this summary. The term 'lepton' (ℓ) refers specifically to $e^\pm$ and $\mu^\pm$ states, except in the cases of the electroweak 3-leptons and 4-leptons analyses where τ leptons are also included.

2.1 Inclusive searches

The inclusive searches are designed to be sensitive to prompt decays of squarks, particularly those of the first two generations, and gluinos. Strongly interacting sparticles may decay directly to the LSP, via the decay $\tilde{q} \to q + \tilde{\chi}_1^0$ for the squark and via $\tilde{g} \to q + \bar{q} + \tilde{\chi}_1^0$ for the gluino. Alternatively, cascade decays may also occur involving one or more additional sparticles yielding final states with additional jets, large E_T^{miss} and possibly leptons, including τ leptons. The ATLAS searches targeting these final states are classified according to the different dominant signal signatures, as follows.

The 0-lepton + 2–6 jets + E_T^{miss} analysis [58] has wide-ranging sensitivity to strongly interacting sparticle production. It vetoes events with leptons in order to suppress the background from W boson and $t\bar{t}$ decays. Depending on the signal region, final states with a minimum jet requirement of 2–6 jets with large transverse momenta (denoted p_T in the fol-

lowing) are considered, each in association with large E_T^{miss}. Signal regions with small numbers of jets provide sensitivity to the direct production and decay of squarks, while those with higher jet multiplicities are sensitive to the production and direct decay of gluinos, and various cascade decays. The original analysis has two signal regions specifically targeting hadronic decays of high-p_T W bosons. These signal regions are not considered in this paper.

The 0-lepton + 7–10 jets + E_T^{miss} analysis [59] selects events with significant E_T^{miss} and with jet multiplicities ranging from 7 to 10 or more, depending on the signal region. It was designed to target, amongst others, models where each gluino of a produced pair decays through a (possibly virtual) top squark to $t + \bar{t} + \tilde{\chi}_1^0$. The four top quarks produced generally lead to large jet multiplicities in the final state. This search also has sensitivity to other models in which cascade decays generate large numbers of jets. It has a looser requirement on the E_T^{miss} than the 2–6 jet analysis described in the previous paragraph, because the many possible intermediate stages of the cascade decay tend to reduce the E_T^{miss}. Unlike the original analysis, where the disjoint signal regions could be statistically combined to improve sensitivity, in this paper signal regions are considered individually when determining whether or not a model point is excluded.

The 1-lepton + jets + E_T^{miss} analysis [60] explicitly requires one isolated lepton, several jets and high E_T^{miss} in the selection. Two sets of signal regions are used from this analysis — one set with relatively high p_T leptons (sensitive to SUSY scenarios with larger mass splittings between the produced sparticle and the LSP) and another set using low-p_T leptons (sensitive to smaller mass splittings). The signal regions requiring two leptons are not considered. Overall, it is sensitive to decay chains where leptons can be produced through the cascade decay of squarks and gluinos.

The $\tau(\tau/\ell)$ + jets + E_T^{miss} search [61] targets final states arising from cascades producing hadronically decaying τ leptons — with signal regions requiring either one or two τ leptons, and including large E_T^{miss}, jets and either exactly zero or one additional light lepton. This search can be sensitive to long decay chains in models with light staus.

Cascade decays of squark and gluino pairs can also lead to final states with multiple leptons, or with two leptons of the same electric charge, known as same-sign (SS) leptons. Those final states are addressed by the SS/3-leptons + jets + E_T^{miss} analysis [62], which requires multiple jets in the final state, and either two SS leptons — with or without jets containing b-hadrons (b-jets) in the final state — or at least three leptons.

For models where many b-jets are expected, the specially designed 0/1-lepton + 3b-jets + E_T^{miss} analysis [63] is sensitive. This analysis is designed around the definition of two sets of signal regions: one set with no isolated leptons, and another with at least one isolated lepton.

The Monojet analysis [64] selects events where the leading jet's p_T is as large as 50% of the E_T^{miss}, and there is large E_T^{miss} and no leptons. The single jet can originate from initial-state QCD radiation (ISR), providing sensitivity to collisions in which no decay products from sparticle decays are observed. This can occur either for direct pair production of invisible LSPs, or if the produced sparticles are only a little heavier than the LSP (up to a few GeV) and their decays therefore produce SM particles of too low an energy to be detected in the other searches.

2.2 Third-generation searches

This set of analyses is focused on searches for direct production of third generation squarks. Their masses are generally expected to be at the TeV scale or below if the Higgs boson(s) are to be protected from large unnatural loop corrections. The decay of $\tilde{t}$ and $\tilde{b}$ squarks also leads to distinctive experimental signatures, typically involving the production of t- or b-quarks in association with large $E_{\mathrm{T}}^{\mathrm{miss}}$.

The 0-lepton stop search [65] is optimised for the direct production of pairs of top squarks decaying directly to a top quark and neutralino, leading to an all-hadronic final state with at least two b-jets and large $E_{\mathrm{T}}^{\mathrm{miss}}$. Most of the signal regions rely on variables related to the reconstructed top quarks present in the final state and on lepton vetoes, but there are also signal regions that target the case where one of the pair of top squarks decays to a top quark and a neutralino and the other decays to a bottom quark and a chargino.

The 0-lepton stop search is complemented by the 1-lepton stop search [56], in which all of the signal regions are characterised by exactly one isolated lepton, at least two jets and large $E_{\mathrm{T}}^{\mathrm{miss}}$. The presence of a b-jet is used in both signal regions targeting $\tilde{t}_1 \to b\tilde{\chi}_1^{\pm}$ and those targeting $\tilde{t}_1 \to t\tilde{\chi}_1^0$, while the latter also use variables related to reconstructed top quarks. The dedicated signal regions targeting top squark decays with soft leptons or boosted top quarks are not included in this paper.

The 2-leptons stop search [66] is designed for final states containing two isolated leptons and large $E_{\mathrm{T}}^{\mathrm{miss}}$, primarily targeting top squarks decaying through an intermediate chargino. Only the so-called "leptonic m_{T2}" signal regions, targeting charginos decaying through on-shell W bosons, are included in this paper.

The Monojet stop analysis [67] looks for final states characterised by large $E_{\mathrm{T}}^{\mathrm{miss}}$, at least one high-$p_{\mathrm{T}}$ jet (vetoing events with more than three jets), and no leptons. The signal regions of this search were designed in the context of a search for top squarks, each decaying into an undetected charm quark and a neutralino which is relevant for cases where the LSP mass is close to the top squark mass. The $E_{\mathrm{T}}^{\mathrm{miss}}$ requirement is less stringent than that of the Monojet analysis described in section 2.1. The signal regions targeting reconstructed and tagged charm jets are not included in this paper.

The search for top squarks with a Z boson in the final state [68] is motivated by the decay of $\tilde{t}_2 \to \tilde{t}_1 Z$, which can produce many leptons in the final state. The leptons are required to form a pair with a mass consistent with the Z boson, with at least one b-jet and large $E_{\mathrm{T}}^{\mathrm{miss}}$.

The $2b$-jets $+$ $E_{\mathrm{T}}^{\mathrm{miss}}$ analysis [69] searches for SUSY scenarios that produce events containing exactly two b-jets, significant $E_{\mathrm{T}}^{\mathrm{miss}}$ and no isolated leptons, for example those coming from decays of bottom squarks to a b-quark and the LSP and from top squark to a b-quark and chargino.

The $tb + E_{\mathrm{T}}^{\mathrm{miss}}$, stop analysis [57] was designed for a mixed scenario: direct production of pairs of top or bottom squarks each decaying (with various branching ratios) to neutralinos or charginos, and yielding final states consisting of a top quark, bottom quark and large $E_{\mathrm{T}}^{\mathrm{miss}}$.

2.3 Electroweak searches

This section details the analyses considered in this paper which target sparticles produced via electroweak interactions. This includes the production of pairs of sleptons or electroweakinos which typically decay into final states containing several high-p_T leptons and significant E_T^{miss}.

The lepton plus Higgs boson (ℓh) analysis [70] is designed to search for direct pair production of a chargino and a neutralino, which decay to final states with large E_T^{miss}, an isolated lepton, and a Higgs boson h which is identified by requiring either two b-jets, or two photons, or a second lepton with the same electric charge (targeting $h \to WW$ decays). Only the signal regions for Higgs boson decays to bottom quarks are considered in this paper.

The 2-leptons analysis [54] targets electroweak production of charginos and/or neutralinos, or sleptons in events with exactly two leptons, large E_T^{miss} and, for some signal regions, two or more jets in the final state.

A complementary search targeting the third-generation leptons is the 2-τ analysis [55] searching for SUSY in events with at least two hadronically decaying τ leptons, large E_T^{miss} and a jet veto.

The 3-leptons analysis [53] is a search for the direct production of charginos and neutralinos in final states with three leptons — which here may include up to two hadronically decaying τ leptons — and large E_T^{miss}, which can come through the decays via sneutrinos, sleptons or W, Z or Higgs bosons.

The 4-leptons analysis [71] looks for SUSY in events with four or more leptons, of which at least two must be electrons or muons. The leptons may also include hadronically decaying τ leptons in this case. Such high lepton multiplicity final states can occur if a degenerate $\tilde{\chi}_2^0 \tilde{\chi}_3^0$ pair is produced which subsequently decay via sleptons, staus or Z bosons to $\tilde{\chi}_1^0$ and many leptons.

The Disappearing Track analysis [72] is motivated by scenarios with a wino-like LSP in which the charged wino is typically only ~ 160 MeV heavier than the LSP. In such models the $\tilde{\chi}_1^\pm$ can have decay lengths of order a few tens of centimetres before it decays to a $\tilde{\chi}_1^0$ and a charged pion. The low-momentum pion track is typically not reconstructed, so the distinctive signature is that of the high-p_T chargino track apparently disappearing within the detector volume.

2.4 Other searches

The long-lived particle searches [73, 74] are designed to detect heavy long-lived particles by measuring their speed β using the time-of-flight to the calorimeters and muon detectors and $\beta\gamma$ (where γ is the relativistic Lorentz factor) from the specific ionisation energy loss in the pixel detector. Only the direct production of pairs of long-lived top or bottom squarks, gluinos, staus or charginos are considered in this paper. The search using 7 TeV data from 2011 [73] considered sparticles as light as 200 GeV, whereas in most cases the later analysis [74] only considered sparticles above 400 GeV. Both searches are therefore included for maximal sensitivity.

The $H/A \to \tau^+\tau^-$ search [75] is designed to detect the heavy, neutral Higgs bosons predicted in the MSSM if they decay to τ-pairs.

3   pMSSM points and indirect constraints

An overview of the method of selecting signal model points is provided in this section. A summary of the scan of the pMSSM parameter space, the software employed, and the constraints applied to determine the final selection are described.

3.1   pMSSM points generation

The model set is generated by selecting model points within the pMSSM using methods similar to those described in ref. [34], but with several important changes. The modifications are made after taking into account new experimental results, updated calculational tools, knowledge gained from the study described in ref. [34], and the improved capabilities of the ATLAS simulations. The full details of the method by which the model points are selected, including the sampling procedure, the codes employed, and the constraints applied to determine the final selection of 'surviving' model points may be found in the appendices.

The model points are selected after making the following assumptions about the MSSM. They are motivated both by constraints from experimental observations and a desire for theoretical simplicity:

(*i*)   *R*-parity is exactly conserved.

(*ii*)   The soft parameters are real, so that no new sources of CP violation exist beyond that present in the CKM matrix.

(*iii*)   Minimal Flavour Violation [76] is imposed at the electroweak scale.

(*iv*)   The first two generations of squarks and sleptons with the same quantum numbers are mass degenerate, and their Yukawa couplings are too small to affect sparticle production or precision observables.

(*v*)   The LSP is the lightest neutralino.

This approach remains agnostic about the presence of non-minimal particle content at higher scales, the mechanism of SUSY breaking, and the unification of sparticle masses. Assumptions *ii–iv* are motivated by the necessity of imposing some organising principle on SUSY flavour-violating parameters to allow TeV-scale masses for the squarks and sleptons. Combining assumptions *i–v* reduces the large MSSM parameter space to the 19-dimensional subspace considered here. The parameters and the ranges used to sample them are listed in table 2. The 4 TeV upper bound on most of the mass parameters is chosen to make all states kinematically accessible at the LHC. As might be expected, decreasing the value of this upper limit restricts the space, resulting in an increase in the apparent fraction of the pMSSM space to which ATLAS analyses are sensitive. Further increasing any physical mass above 4 TeV has little effect on the LHC phenomenology in most cases. An exception

Parameter	Min value	Max value	Note
$m_{\tilde{L}_1}(=m_{\tilde{L}_2})$	90 GeV	4 TeV	Left-handed slepton (first two gens.) mass
$m_{\tilde{e}_1}(=m_{\tilde{e}_2})$	90 GeV	4 TeV	Right-handed slepton (first two gens.) mass
$m_{\tilde{L}_3}$	90 GeV	4 TeV	Left-handed stau doublet mass
$m_{\tilde{e}_3}$	90 GeV	4 TeV	Right-handed stau mass
$m_{\tilde{Q}_1}(=m_{\tilde{Q}_2})$	200 GeV	4 TeV	Left-handed squark (first two gens.) mass
$m_{\tilde{u}_1}(=m_{\tilde{u}_2})$	200 GeV	4 TeV	Right-handed up-type squark (first two gens.) mass
$m_{\tilde{d}_1}(=m_{\tilde{d}_2})$	200 GeV	4 TeV	Right-handed down-type squark (first two gens.) mass
$m_{\tilde{Q}_3}$	100 GeV	4 TeV	Left-handed squark (third gen.) mass
$m_{\tilde{u}_3}$	100 GeV	4 TeV	Right-handed top squark mass
$m_{\tilde{d}_3}$	100 GeV	4 TeV	Right-handed bottom squark mass
$|M_1|$	0 GeV	4 TeV	Bino mass parameter
$|M_2|$	70 GeV	4 TeV	Wino mass parameter
$|\mu|$	80 GeV	4 TeV	Bilinear Higgs mass parameter
M_3	200 GeV	4 TeV	Gluino mass parameter
$|A_t|$	0 GeV	8 TeV	Trilinear top coupling
$|A_b|$	0 GeV	4 TeV	Trilinear bottom coupling
$|A_\tau|$	0 GeV	4 TeV	Trilinear τ lepton coupling
M_A	100 GeV	4 TeV	Pseudoscalar Higgs boson mass
$\tan\beta$	1	60	Ratio of the Higgs vacuum expectation values

Table 2. Scan ranges used for each of the 19 pMSSM parameters. Where the parameter is written with a modulus sign both the positive and negative values are permitted. In the above, "gen(s)" refers to generation(s).

is when decays proceed via virtual heavy sparticles, when increasing that sparticle mass would lead to further suppression of those decays. A larger range is permitted for $|A_t|$, a parameter which affects loop corrections to the mass of the the Higgs boson. The larger range increases the fraction of model points having the mass of the lightest Higgs boson close to the measured value.

Given the large dimensionality of the pMSSM, a grid sampling technique at regular intervals is impractical. The space is therefore sampled by choosing random values for each parameter. It should be noted that in many cases only some of the parameters are relevant for a given observable, in which case the scan is effectively more comprehensive within the subspace of relevant parameters. The value of each parameter is chosen from a flat probability distribution, with lower and upper bounds given in table 2. The lower and upper limits of the parameter ranges are chosen to avoid experimental constraints and to give a high density of model points with masses at scales accessible by the LHC experiments, respectively.

Condition iv imposes the constraints that the soft mass terms for the second generation are equal to those in the first, as shown in table 2. This means, for example, that $\tilde{u}_L$ and $\tilde{c}_L$ have the same soft mass term in the Lagrangian so that their physical masses are very close. Furthermore the scalar partners of the left-handed fermions, such as $\tilde{e}_L$ and $\tilde{\nu}_{e_L}$, have the same soft mass due to $SU(2)_L$ invariance, but D-terms related to electroweak symmetry breaking split their mass-squared values by $\mathcal{O}(m_W^2)$.

Parameter	Minimum value	Maximum value
$\Delta\rho$	-0.0005	0.0017
$\Delta(g-2)_\mu$	-17.7×10^{-10}	43.8×10^{-10}
$\mathrm{BR}(b \to s\gamma)$	2.69×10^{-4}	3.87×10^{-4}
$\mathrm{BR}(B_s \to \mu^+\mu^-)$	1.6×10^{-9}	4.2×10^{-9}
$\mathrm{BR}(B^+ \to \tau^+\nu_\tau)$	66×10^{-6}	161×10^{-6}
$\Omega_{\tilde{\chi}_1^0}h^2$	—	0.1208
$\Gamma_{\mathrm{invisible(SUSY)}}(Z)$	—	$2\,\mathrm{MeV}$
Masses of charged sparticles	$100\,\mathrm{GeV}$	—
$m(\tilde{\chi}_1^\pm)$	$103\,\mathrm{GeV}$	—
$m(\tilde{u}_{1,2}, \tilde{d}_{1,2}, \tilde{c}_{1,2}, \tilde{s}_{1,2})$	$200\,\mathrm{GeV}$	—
$m(h)$	$124\,\mathrm{GeV}$	$128\,\mathrm{GeV}$

Table 3. Constraints on acceptable pMSSM points from considerations of precision electroweak and flavour results, dark matter relic density, and other collider measurements. A long dash (—) indicates that no requirement is made. Further details may be found in the text.

Once each of the 19 parameters has been chosen, a variety of publicly available software packages are used to calculate the properties of each model point, as described in appendix A. In some cases the software is modified to produce accurate results for the wide range of models found in the pMSSM scan. The sparticle decays are calculated, again using a variety of codes and analytical techniques, as described in appendix B.

3.2 pMSSM point selection

Acceptable model points are furthermore required to have consistent electroweak symmetry breaking, a scalar potential that does not break colour or electric charge, and all particles' mass-squared values must be positive. Model points with theoretical pathologies, described in more detail in appendix C, are discarded. Further experimental constraints, shown in table 3, which indirectly affect the parameter space are applied and described below.

3.2.1 Precision electroweak and flavour constraints

Unless specified otherwise, the relevant observables are calculated using `microMEGAs` 3.5.5 [77, 78]. The constraint on the electroweak parameter $\Delta\rho$ uses the limit on ΔT (the parameter describing the radiative corrections to the total Z boson coupling strength, the effective weak mixing angle, and the W boson mass) in ref. [79] and $\Delta\rho = \alpha\Delta T$ with $\alpha = 1/128$. The allowed branching ratio (BR) of $b \to s\gamma$ is the union of the two standard deviation (2σ) intervals around the theoretical prediction and the experimental measurement from ref. [80]. For the branching ratio of $B_s \to \mu^+\mu^-$, the value calculated by `microMEGAs` is scaled by $1/(1 - 0.088)$ as proposed in ref. [81] for comparison with experiment. The

scaled value is required to lie within the 2σ interval around the combined result from the LHCb and CMS Collaborations [82]. The 2σ theoretical prediction for the SM (3.20 to 4.12) $\times 10^{-9}$ lies within this interval. The branching ratio $B^+ \to \tau^+\nu_\tau$ is calculated using ref. [83], which includes $\tan\beta$-enhanced corrections. The allowed range is the union of the 2σ intervals around the experimental results [84–87] and the SM prediction [88]. Finally, for the SUSY contribution to the anomalous magnetic moment of the muon, $\Delta(g-2)_\mu$, a very large range is allowed. This range in $\Delta(g-2)_\mu$ is the union of the 3σ intervals around the SM value, $(0.0 \pm 5.9) \times 10^{-10}$ from combining [89] the results of refs. [90–92] and the experimental measurement [93, 94] corrected to an updated value of the muon to proton magnetic moment ratio [95, 96] giving $\Delta(g-2)_{\mu,\mathrm{exp}} = (24.9 \pm 6.3) \times 10^{-10}$. Three-sigma intervals are used to obtain a continuous range from the union.

3.2.2 Dark matter constraints

Since R-parity is assumed to be exactly conserved, the LSP is stable and as a consequence has a non-zero cosmological abundance. It is assumed that the LSP abundance is determined thermally and is not diluted by other processes e.g. late-time entropy addition. No assumption is made about whether the LSP is the sole constituent of dark matter. As a result, the total cold dark matter energy density is used as an upper limit on the LSP abundance. The limit is based on the latest combined measurement from the Planck Collaboration of $\Omega_{\mathrm{CDM}}h^2 = 0.1188 \pm 0.0010$ (table 4 of ref. [97]).[2] The upper limit is set to the observed central value plus double the experimental uncertainty. The limit on the spin-independent cross-section is that for the interaction of a neutralino with a nucleus derived by the LUX experiment [98]. In the case of the LSP mass versus proton spin-dependent cross-section plane the limit is from the COUPP Collaboration [99], while in the LSP mass versus neutron spin-dependent cross-section plane, the XENON100 Collaboration [100] limit is applied. `MicrOMEGAs 3.5.5` is used to calculate the neutralino-nucleon cross-sections. These are scaled down by the ratio of the expected relic density from the LSP to the observed relic density to obtain the effective dark matter cross-sections, assuming the remaining non-LSP dark matter is invisible to the direct detection experiments. When accepting or rejecting models, the calculated value is allowed to be up to a factor of four higher than the limits obtained by the experiments, to account for nucleon form-factor uncertainties [33].

3.2.3 Collider constraints

Finally, constraints from LEP and from the measurement of the Higgs boson mass at the LHC are applied. To ensure consistency with LEP, model points are discarded if their additional contribution to the invisible width of the Z boson is above $2\,\mathrm{MeV}$ [101], or where any charged sparticle is lighter than $100\,\mathrm{GeV}$. For charginos, the bound is increased to $103\,\mathrm{GeV}$, provided that all sneutrinos are heavier than $160\,\mathrm{GeV}$ and the mass splitting between the chargino and the LSP is at least $2\,\mathrm{GeV}$. This constraint comes from the combined

---

[2]It should be noted that in the context of the dark matter relic density the symbol h corresponds to the normalised Hubble constant, rather than the Higgs boson.

LSP type	Definition	Sampled	Simulated Number	Simulated Fraction	Weight
'Bino-like'	$N_{11}^2 > \max(N_{12}^2, N_{13}^2 + N_{14}^2)$	480×10^6	103,410	35%	1/24
'Wino-like'	$N_{12}^2 > \max(N_{11}^2, N_{13}^2 + N_{14}^2)$	$\Big\} \, 20 \times 10^6 \, \Big\{$	80,233	26%	1
'Higgsino-like'	$(N_{13}^2 + N_{14}^2) > \max(N_{11}^2, N_{12}^2)$		126,684	39%	1
Total		500×10^6	310,327		

Table 4. Categorisation of the 310,327 model points by the type of the LSP (assumed to be the $\tilde{\chi}_1^0$) according to the neutralino mixing matrix parameters N_{ij}, where the first index indicates the neutralino mass eigenstate and the second indicates its nature in the lexicographical order $(\tilde{B}, \tilde{W}, \tilde{H}_1, \tilde{H}_2)$. For example, $N_{1,2}$ is the amplitude for the LSP to be $\tilde{W}$. The final two columns indicate the fraction of model points in that category that are sampled, and their weighted fraction after importance sampling.

LEP search [102]. First- and second-generation squarks are required to be heavier than 200 GeV, although this has only a very small effect given the scan range and the assumption of negligible first- and second-generation squark mixing. The lightest Higgs boson mass, as calculated by `FeynHiggs 2.10.0` [103, 104], is required to be in the range 124 to 128 GeV. This range is set around the central value of the Higgs mass at the time of generation, 126 GeV, and with a 2 GeV window that mainly reflects the typical theoretical uncertainty of the `FeynHiggs` calculation. The results are found not to depend on the exact value of the Higgs mass within this interval (as shown later in section 5.4).

3.2.4 Importance sampling by LSP type

Since low-mass SUSY models typically over-produce dark matter, the relic density constraint in table 3 sculpts the distribution of the allowed model points. The constraint depends strongly on the nature of the LSP. Except where particularly effective neutralino annihilation mechanisms are available, model points with a bino-like LSP generally tend to produce too much dark matter [105], meaning that such models are infrequently sampled and accepted in a random scan employing flat priors. The model points are therefore partitioned into three categories, bino-like, wino-like and Higgsino-like. The categorisation is made according to the dominant contribution to the LSP within the neutralino mixing matrix N_{ij} as shown in table 4. Model points are therefore selected, by importance sampling, in such a way that approximately equal numbers are obtained for each LSP type. In total 500 million model points are sampled randomly within the ranges listed in table 2. From the first 20 million sampled, 206,917 model points had a wino-like or Higgsino-like LSP and satisfied all of the constraints of table 3. To obtain a sufficiently high number with bino-like LSP, the remaining 480 million model points are used to find the 103,410 which had a bino-like LSP and satisfied the table 3 constraints. Generally models have a LSP dominated by one particular type, with over 87% of models having a LSP which is at least 90% pure. The phenomenology of each LSP type can be explored separately due to the large number of model points in each category. In the following
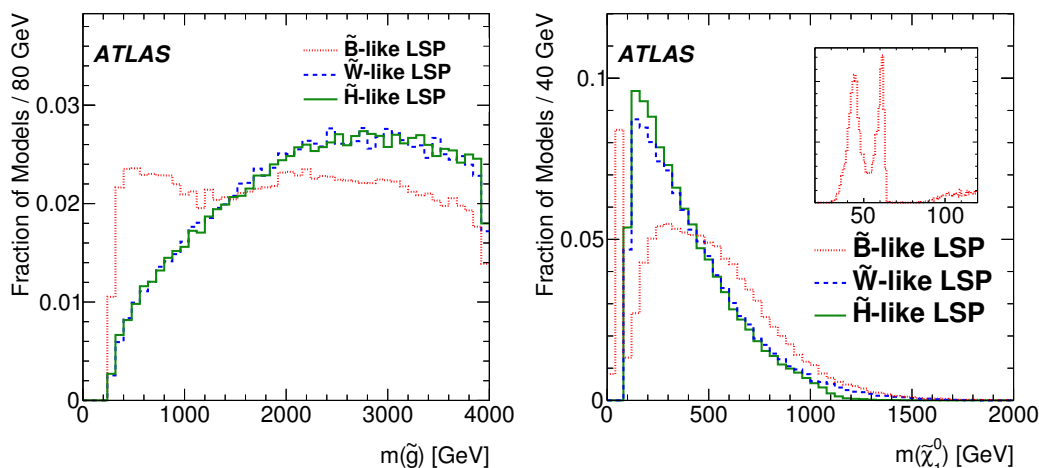
Figure 1. Distributions of the gluino and LSP masses, shown separately for models with a bino-like (dotted red), wino-like (dashed blue) or Higgsino-like (solid green) LSP. The constraints listed in table 3 have been applied, but not the constraints from the ATLAS searches. The distributions are normalised to unit area. The inset in the plot on the right shows in more detail the region of low neutralino mass for the models with bino-like LSP.
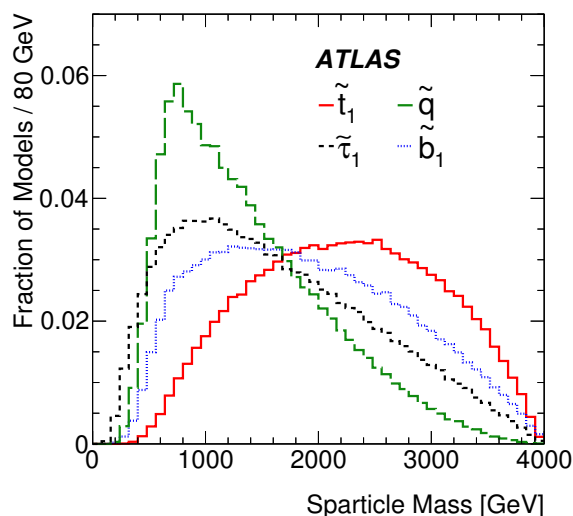
Figure 2. Normalised distribution of sparticle masses for the lightest top (solid red), bottom (dashed blue), first- or second-generation squark (dashed green) and stau (dot-dashed black) for all LSP types combined. The constraints listed in table 3 have been applied, but not the constraints from the ATLAS searches.

plots, where all LSP types are shown together the contribution from each LSP type is scaled according to the weights shown in table 4.

3.3 Properties of model points (before applying ATLAS constraints)

The distributions of the gluino and LSP masses for the model points satisfying the constraints from table 3 are shown in figure 1, separately for models with a bino-, wino- or Higgsino-like LSP. Light gluinos are more common among model points with bino-like LSP. Dark matter for model points with bino-like LSP is typically over-produced, so the presence of a gluino state close in mass to the LSP enables them to act as coannihilators with the dark matter in the early universe, reducing the relic density to a level that satisfies the constraint on $\Omega_{\tilde{\chi}_1^0} h^2$. The neutralino mass distribution for the bino-like LSP model points shows a sharp concentration of model points with $m(\tilde{\chi}_1^0) \lesssim 100 \, \text{GeV}$. This concentration corresponds to model points in which the dark matter relic density constraint can be satisfied due to enhanced neutralino pair annihilation via the Z or Higgs boson poles. A plot of the low-mass region for bino-LSP model points (shown in the inset to figure 1(a)) confirms this interpretation, showing two individual peaks corresponding to the separate Z and Higgs poles.

The identity of the next-to-lightest supersymmetric particle (NLSP) can be important for the phenomenology of a model point, and is strongly influenced by the LSP type. The NLSP is nearly always a chargino or neutralino for wino-like or Higgsino-like LSPs, as is expected given the small splittings between the different components of the wino or Higgsino multiplets. In particular, over 99% of wino-like LSP model points have a chargino NLSP. The small mass difference between the $\tilde{\chi}_1^\pm$ and the $\tilde{\chi}_1^0$ can lead to long $\tilde{\chi}_1^\pm$ lifetimes for wino-like and Higgsino-like LSPs, which result in the types of disappearing tracks searched for in the analysis described in ref. [72].

Bino-like LSP model points, by contrast, exhibit a much wider range of NLSP types, the distribution of which is determined by their effect on the LSP annihilation rate. Even for models with a bino-like LSP, charginos and neutralinos are still the most common NLSP type, since LSP-Higgsino mixing is important for many of the possible annihilation mechanisms. The remaining NLSP types are generally ordered by their effectiveness as coannihilators, with coloured NLSPs being the most prevalent and neutral NLSPs (sneutrinos) being the least so. The NLSP-LSP mass splitting for bino-like LSP model points is frequently less than $50 \, \text{GeV}$, supporting the assertion that light sparticles beyond the LSP are typically required to avoid over-production of bino-like LSPs.

In cases where a squark, gluino or slepton is almost mass degenerate with the LSP, the small available phase-space in the decay can lead to sparticles that are long-lived or even stable on the time scale for traversal of the ATLAS detector. In total 3,427 model points contain squarks, gluinos or sleptons with $c\tau > 1 \, \text{mm}$. The sensitivity of the SUSY searches targeting prompt decays (the first three categories in table 1, other than the Disappearing Track analysis) to these model points is reduced and therefore only the long-lived particle searches were considered for these model points.

The distributions of the mass of several other sparticles of phenomenological interest at the LHC can be found in figure 2. Even before ATLAS analyses are considered, the model set is depleted in light top squarks, and to a slightly lesser extent in light bottom squarks, by the requirement (in table 3) that the lightest Higgs boson mass be close to the experimentally observed value.

Production mode	Minimum cross section [fb]	Fraction of models generated		
		Bino LSP	Wino LSP	Higgsino LSP
Strong	0.25	82.5%	74.9%	76.7%
Mixed	0.25	52.6%	42.1%	13.9%
Electroweak	7.5	38.3%	72.5%	75.0%
Slepton pair	0.75	9.6%	7.9%	9.5%

Table 5. Minimum cross-sections required to do particle-level event generation for the four different production modes and the fraction of the models above this cross-section for each LSP type.

4 Signal simulation and evaluation of searches

For each of the 310,327 model points passing the preselection described in table 3 it has to be determined which, if any, of the ATLAS searches are sensitive to it and whether it can be excluded or not. Simulating and running the full set of ATLAS analyses on these would be extremely time and resource consuming. Each model point is therefore evaluated in three steps as described below. A special procedure is applied to evaluate the searches for long-lived particles and heavy Higgs bosons as described in the following sub-sections.

4.1 Supersymmetry signals

First, each model point is categorised based on its production cross-sections for SUSY particles, as calculated using `Prospino 2.1` [106–110]. The production processes are split into three separate groups: strong production, electroweak production (encompassing electroweakino and slepton pair production) and finally mixed production (e.g. of an electroweakino in association with a squark or gluino). Model points with cross sections for any of those processes larger than the minimum values in table 5 are subsequently retained, and any such processes are investigated in more detail as described below. For strong and mixed production, the minimum cross-section corresponds to just five signal events produced in the full $\sqrt{s} = 8\,\text{TeV}$ dataset. Sensitivity to such small cross-sections occurs only for model points with a very high fraction of events with four leptons in the final state, for which the 4-leptons analysis has a high acceptance (up to 50%). Production of electroweakinos is most effectively observed by using decays to leptons, which are often suppressed by the leptonic branching fractions of W, Z and h bosons, explaining the higher cross-sections limits. ATLAS searches have a greater sensitivity to low cross-section slepton pair production than to electroweakino production. Therefore, if the model point does not satisfy the higher cross-section criterion of the electroweak production group, a fourth group that allows for model points with lower cross-section slepton pair production is considered. Fewer than 10% of the model points have no process passing this selection and are thus not considered to be excludable.

For each of the model points satisfying one or more of the production mode cross-section criteria, a large sample of events is generated using `MadGraph5 1.5.12` [111] with

the `CTEQ 6L1` parton distribution functions (PDF) [112] and `Pythia 6.427` [113] with the `AUET2B` set of parameters [114]. `MadGraph5` is used to generate the initial pair of sparticles and up to one additional parton in the matrix element, while `Pythia` is used for all sparticle decays and parton showering[3] MLM matching [115] is used with up to one additional jet in the `MadGraph` matrix element, a `MadGraph` kT measure of $100\,\mathrm{GeV}$, and a `Pythia` jet measure cut off of $120\,\mathrm{GeV}$. Both `Tauola 1.20` [116] and `Photos 2.15` [117] are enabled to handle the decays of τ leptons and final-state radiation of photons, respectively.

To reduce the amount of computationally expensive detector simulation and reconstruction that is required, a Monte Carlo particle-level selection corresponding to each of the SUSY searches in the first three categories in table 1 is used to process the generated events. In this step, inefficiencies from the detector-level reconstruction are parameterised using a single efficiency factor for each signal region, determined from previously simulated signal samples. Exceptions to this are made for the τ reconstruction efficiency in the $\tau(\tau/\ell)$ + jets + $E_{\mathrm{T}}^{\mathrm{miss}}$ and 2-τ searches, for which p_{T}-dependent efficiencies are applied for each signal τ. Similarly, the Disappearing Track search applies the reconstruction efficiency for decaying charginos as a function of the distance from the centre of the ATLAS detector and the angular coordinates as published in ref. [72]. The expected event yield in each signal region is calculated for each model point. For most analyses the categorisation is performed by directly comparing the expected signal yield N_{sig} to the model-independent 95% confidence level (CL) upper bound on the number of beyond-the-SM events N_{max}^{95} in each signal region of that analysis. Model points are then partitioned into three categories, on the basis of that particle-level simulation, using criteria determined to be appropriate for each individual analysis. The first category comprised those already excluded at this stage on the basis that N_{sig} is sufficiently larger than N_{max}^{95} for at least one signal region of one analysis. The expected sensitivity of all other analyses to such model points is calculated using particle-level yields, and using average reconstruction efficiencies. The second category corresponds to those found not to be excludable, consisting of points with N_{sig} materially smaller than N_{max}^{95} for all analyses. The exact relationship between N_{sig} and N_{max}^{95} for the categorisation is determined separately for each signal region and depends on the accuracy with which the particle-level evaluation reproduces the results of a full simulation. In total 35.9% (44.7%) of the model points fall in the first (second) category and are deemed to have been excluded (not excluded) at the 95% CL. The validity of this classification was confirmed using the full simulation and reconstruction procedure described below for approximately 5% of the model points in the first category for each analysis. A final category of model points — those with N_{sig} close to N_{max}^{95} (typically within a factor of a few) for the most sensitive analyses — are subject to more detailed investigation, as follows.

For the 44,559 model points for which the overall exclusion is uncertain based on the particle-level simulation described above, the final step is a fast, `GEANT4`-based [118] simulation using a parameterisation of the performance of the ATLAS electromagnetic and hadronic calorimeters [119] and full event reconstruction. The simulation includes a realistic description of multiple pp interactions per bunch crossing, and is corrected

---

[3]Polarisation from the decay of the initial sparticles is not taken into account in this analysis.

for identification efficiencies and resolution effects. For each such model point, signal events are generated corresponding to four times the integrated luminosity recorded (i.e. $81.2\,\mathrm{fb}^{-1}$). The simulation is limited to those production modes which could contribute to the analyses of interest. For these processes, the nominal cross-section and the uncertainty are taken from an envelope of cross-section predictions using different parton distributions and factorisation and renormalisation scales, as described in ref. [120]. The addition of the resummation of soft gluon emission at next-to-leading-logarithm accuracy (NLL) [106, 121–124] is performed in the case of strong production of sparticle pairs.

The status of each previously inconclusive model point is then determined for each of the analyses using the same procedure [125] as used in the original analyses. In each analysis the signal region with the best expected sensitivity is identified and the "CLs method" [126] is used to determine if the model point is excluded or not at 95% CL. It should be noted that for the exclusion fits, the nominal signal cross-sections are used, without any theoretical uncertainties on the signal, except for the Monojet stop and Monojet analyses. These two analyses are particularly sensitive to the modelling of ISR as they rely on a high-p_{T} ISR jet in their event selection. Therefore an additional 25% ISR signal uncertainty is applied in those cases, based on the observed variance in acceptance in signal samples with modified parameters for the ISR modelling [67]. For the 0-lepton + 7–10 jets + $E_{\mathrm{T}}^{\mathrm{miss}}$, 0/1-lepton + 3$b$-jets + $E_{\mathrm{T}}^{\mathrm{miss}}$ and 2-leptons stop analyses, it is not possible to apply the full combined fit procedure of the original analyses. Instead only the individual signal regions are considered, resulting in somewhat conservative modelling of the sensitivity for those three analyses. For the overall exclusion, no attempt is made to combine the individual analyses. Instead the analysis with the best expected exclusion is used for each model point to determine its status.

4.2 Long-lived particle search

Model points with heavy long-lived particles require special treatment since such particles can traverse part or all of the ATLAS detector leaving rather distinct signatures. The dominant types of long-lived particles in the model points are the $\tilde{\chi}_1^+$ and the $\tilde{\chi}_2^0$ when they are almost mass-degenerate with the LSP. The decay of such long-lived particles is included in the simulation procedure described above and model points with such long-lived particles are considered using the same procedure.

Aside from the electroweakinos, 3,427 of the model points contain squarks, gluinos or sleptons with $c\tau > 1\,\mathrm{mm}$. These model points have not been simulated. Instead only the results from the Long-lived particle searches are used to constrain these model points.

The long-lived particle searches in refs. [73] and [74] provide limits on the production cross-section at 7 and 8 TeV, respectively, of bottom squarks, top squarks, gluinos, staus and charginos in the case where these live long enough to traverse the complete detector. Model points with bottom squarks, top squarks, gluinos, staus or charginos with a lifetime above 85 ns and production cross-sections exceeding the corresponding cross section limit from either the 7 or 8 TeV result are considered to be excluded. In all other cases — where the lifetime is shorter or the production cross-sections lower — the model point is considered not to be excluded.

4.3 Heavy Higgs boson search

Cross sections and branching ratios for heavy Higgs bosons are calculated for gluon fusion, or for production in association with b-quark(s) [127–129]. The high-m_A category ($m_A > 200$ GeV) of the ATLAS search [75] is used since this regime is relevant to all the model points in this study. It is assumed that b-quark associated production dominates and this calculation is performed for each model point in the pMSSM parameter space using the software SusHi 1.3.0 [103, 130–141]. The large value of m_A in all the model points has the effect that the A and H bosons are nearly mass degenerate, so both must be simulated. The quantity $\sigma(bbH) \times \mathrm{BR}(H \to \tau\tau) + \sigma(bbA) \times \mathrm{BR}(A \to \tau\tau)$ is calculated and is compared to the ATLAS 95% CL upper limits [75] for a scalar particle produced in association with b-quark(s) and decaying to $\tau\tau$. For the overall exclusion, this heavy Higgs boson search is considered only if none of the SUSY searches are expected to exclude the model point at the 95% CL.

5 ATLAS constraints from LHC Run 1

5.1 Impact of ATLAS searches on sparticle masses

The effect of the ATLAS search constraints are most easily presented as projections onto one-dimensional or two-dimensional subspaces of the full 19 parameter pMSSM space.[4] The most relevant parameters onto which to project are typically the sparticle masses. Production cross-sections for sparticles decrease rapidly when their masses are increased. When those initial sparticles decay, the masses of other sparticles affect the types of visible decay products and their kinematics. The mass of the LSP is particularly important since a decay to a high-mass LSP results in less energy being available for the observable decay products.

The fraction of surviving model points in the projected space necessarily depends both on the prior distribution of model points in the parameters that have been projected out, and on experimental constraints on sparticle masses other than those plotted. Thus, some care is needed in their interpretation. In particular the fractions of model points excluded can depend, in some cases sensitively, on the non-collider constraints shown in table 3, the choice of scan ranges shown in table 2, and on the choice of a flat prior. Nevertheless, some general features of the impact of the ATLAS Run 1 searches are clear.

The simplified-model limits shown on the plots throughout this section are the observed limits from the indicated analysis. In many cases there are several analyses interpreting their results in the same simplified models, and in this paper the observed limits from the most constraining analysis are shown. It should be noted that there is no minimum number of model points required in each bin.

The results are shown first for squark masses (of the first two generations) and the gluino mass in section 5.1.1, then for third-generation squark masses in section 5.1.2, and for the electroweak sparticles in section 5.1.3. A small subset of the model points contain long-lived squarks, gluinos or sleptons. These 3,427 model points are treated separately

---

[4]A full list of model parameters, observables and which analyses, if any, are excluding each model, are available from the ATLAS Collaboration website [142].

(a) Gluino / LSP. **(b)** Lightest ($1^{st}/2^{nd}$ gen) squark / LSP.
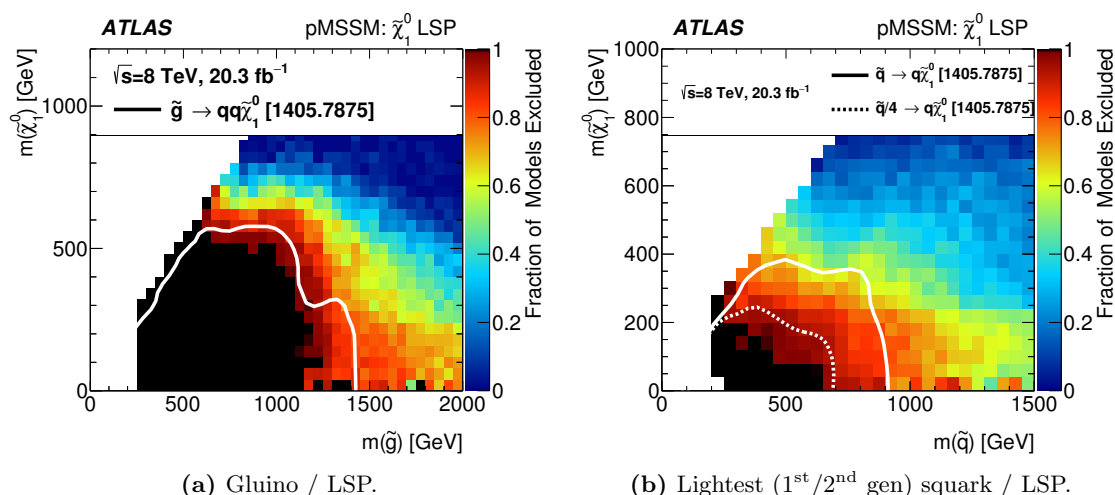
Figure 3. Fraction of pMSSM points excluded by the combination of 8 TeV ATLAS searches in the (a) $\tilde{g}$-$\tilde{\chi}_1^0$ and (b) the $\tilde{q}$-$\tilde{\chi}_1^0$ mass planes. The colour scale indicates the fraction of pMSSM points excluded in each mass bin, with black squares indicating 100% of model points being excluded. The white regions indicate places where no model points were sampled which satisfied the constraints of table 3. In both cases, the solid white lines overlaid are observed simplified-model limits from the 0-lepton + 2–6 jets + E_T^{miss} search [58] at 95% CL. In the $\tilde{g}$-$\tilde{\chi}_1^0$ case, the simplified-model limit is set assuming direct production of gluino pairs and that the squarks are decoupled, with gluino decaying to quarks and a neutralino, $\tilde{g} \to q + q + \tilde{\chi}_1^0$. In the $\tilde{q}$-$\tilde{\chi}_1^0$ plane, both lines are drawn assuming directly produced first/second-generation squark pairs, with each squark decaying to a quark and a neutralino, $\tilde{q} \to q + \tilde{\chi}_1^0$. The solid line corresponds to the case where all eight squarks from the first two generations are assumed to be degenerate. The dashed line has the squark production cross-section scaled down by a factor of four to emulate the effect of only two of those eight squarks being kinematically accessible.

in section 5.1.4 as only the long-lived particle search is considered for these model points. Section 5.1.5 describes the effect of a search for the decay of heavy neutral Higgs bosons to two τ leptons. The complementarity between the different ATLAS searches is described in section 5.1.6.

5.1.1 Squarks and gluinos

Figure 3(a) shows the fraction of model points excluded by the ATLAS searches as projected onto the two-dimensional space of the masses of the LSP and the gluino. As one would expect, light gluinos are robustly constrained by the ATLAS searches, whereas at larger gluino masses the fraction of model points excluded is reduced.

It is instructive to compare these observed pMSSM exclusions to the observed limits previously presented for simplified low-scale models. Superimposed on figure 3(a) is a line showing the 95% CL exclusion previously derived by the 0-lepton + 2–6 jets + E_T^{miss} analysis from a simplified model in which only the gluino and the LSP are kinematically accessible [58]. It can be seen that there is generally good congruence between the region

(a) All LSP types. **(b)** Bino-like LSPs.
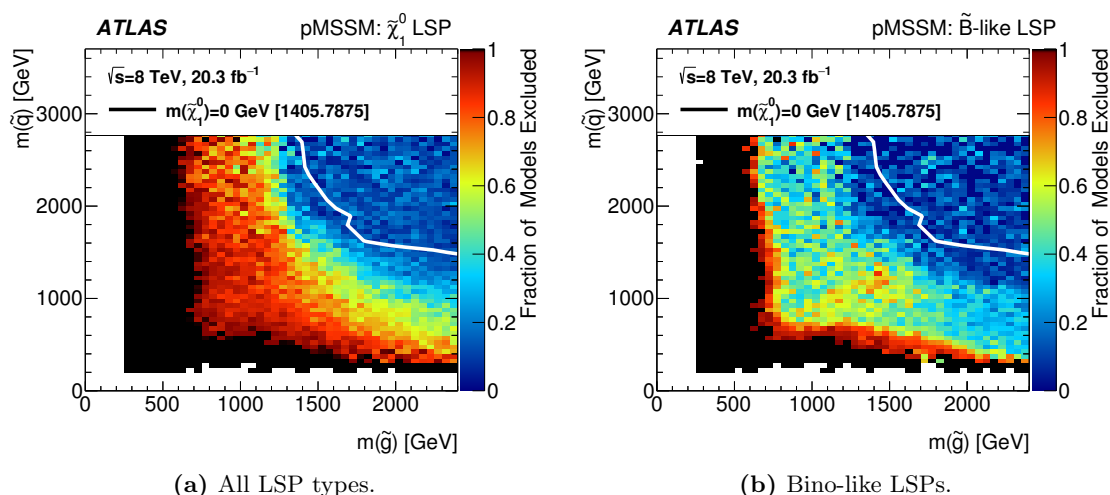
Figure 4. Fraction of pMSSM points excluded in the $\tilde{g}$-$\tilde{q}$ plane, where $\tilde{q}$ represents the lightest squark from the first two generations. The overlaid line shows a limit for a simplified model from the 0-lepton + 2–6 jets + $E_{\mathrm{T}}^{\mathrm{miss}}$ search [58] which assumes strong production of gluinos and eight-fold degenerate first- and second-generation squarks, with direct decays to quarks and massless neutralinos. The colour scale is as described in figure 3.

excluded in the two different scenarios, demonstrating that the simplified model is success-fully capturing the main pMSSM phenomenology in this case. Nevertheless, the pMSSM sensitivity does differ in detail from that of the simplified model. Not only is this because multiple analyses are considered here but also because of residual dependence on the masses of other sparticles. For example, the pMSSM permits the existence of additional particles with masses lying in between those of the gluino and the LSP, which can lead to cascade decays. In general such cascade decays can be expected to yield different jet p_{T} and $E_{\mathrm{T}}^{\mathrm{miss}}$ spectra, and perhaps additional leptons, which have different experimental acceptances.

Close to the diagonal line where $m(\tilde{g})$ is only a little larger than $m(\tilde{\chi}_1^0)$ (figure 3(a)) the simplified-model exclusion from ref. [58] underestimates the ATLAS sensitivity. The $\tilde{g} \to q\bar{q}\tilde{\chi}_1^0$ decays in this near-degenerate region produce low-energy quarks which typically fail to meet the kinematic requirements on jets. That ATLAS does indeed show good sensitivity in this region is instead due to the monojet analyses [64, 67]. These analyses were designed to capture the recoil of LSPs (or other, slightly heavier, SUSY particles) against initial-state QCD radiation.

Figure 3(b) shows a different projection, in this case to the mass of the LSP versus the mass of the lightest squark of the first two generations, $\tilde{q}_{\mathrm{L,R}}$ for $q \in \{u, d, s, c\}$, labelled here and in what follows as $\tilde{q}$. It can be observed that there is good sensitivity at low squark mass and no models with a squark mass below 250 GeV are allowed by the ATLAS analyses. The solid line superimposed on figure 3(b) shows the 95% CL exclusion obtained previously [58] for a simplified model in which the only kinematically accessible sparticles are the LSP and the eight squark states of the first two generations, where these squarks are all assumed to have the same mass. It can be seen that the region within the solid

simplified-model exclusion curve is only partially excluded within the pMSSM. This is primarily because the pMSSM-19 parameter space does not demand that the squarks be eight-fold degenerate, reducing the cross-section. There is a closer correspondence between the pMSSM sensitivity and that of an alternative simplified model (dashed line), in which the cross-section for direct (anti-)squark production has been reduced by a factor of four, to model the effect of only two of those eight squarks being mass degenerate.[5]

A noticeable excursion from the simplified-model lines, visible on both plots in figure 3 is a horizontal band of sensitivity to pMSSM points for LSP masses less than about 200 GeV stretching up to large gluino (or $\tilde{q}$) masses. Since such high-mass strongly interacting sparticles have small production cross-sections, one would not expect sensitivity to their production. Indeed these constraints are not the result of gluino or squark searches, but instead of searches for disappearing tracks from long-lived charginos. These long-lived chargino states are common for models with wino-like LSPs with mass splittings between the charged NLSP and the neutral LSP of less than about 200 MeV. The NLSP, when it decays inside the detector volume, produces an invisible LSP and a low-energy charged pion which itself often goes undetected. The search for such 'disappearing' charged-particle tracks is sensitive even in the absence of direct squark or gluino production, and hence sensitivity is observed for any mass of the strongly interacting sparticle.

Figure 4(a) shows the sensitivity as projected onto the plane of the gluino and squark masses, where now the LSP mass may take any value. One observes near-total exclusion by ATLAS analyses of gluinos with masses less than about 700 GeV, with a high fraction of exclusion up to about 1.2 TeV, for all values of the lightest squark mass. Light squarks are also strongly constrained, although those constraints weaken as the gluino mass increases, due to suppression both of direct squark-pair production via t-channel gluino exchange and of associated production of $\tilde{q} + \tilde{g}$.

The simplified model superimposed onto the squark-gluino plane is one that assumes an eight-fold degeneracy of squark masses in the first two generations and a massless LSP [58]. As one would expect, this simplified-model line lies close to the upper edge of the pMSSM sensitivity, since the pMSSM permits non-degenerate squarks, and a non-zero LSP mass, both of which reduce sensitivity, by reducing the signal cross-section and experimental acceptance respectively. The reduction in sensitivity caused by a non-zero LSP mass is more pronounced in the case of model points with a bino-like LSP, figure 4(b). These model points often have a small mass difference between the squark and the LSP in order to satisfy the dark matter relic constraint, as discussed earlier in section 3.3.

The pMSSM also allows one to explore how the sensitivity to direct squark production depends on the nature of the lightest squark. Figure 5 shows that the search reach depends on whether the squarks are left-handed or right-handed, and whether they are up-type or down-type squarks. Thus the assumption of equivalent sensitivity for all such squarks, common in presentation of LHC SUSY searches, is a simplification that is not justified in the more general context of the pMSSM. The production of down squarks is suppressed

---

[5]Reference [58] emulates the effect of a single kinematically accessible squark by dividing the cross-section by a factor of eight rather than four.

(a) Left up squark.
(b) Right up squark.
(c) Left down squark.
(d) Right down squark.
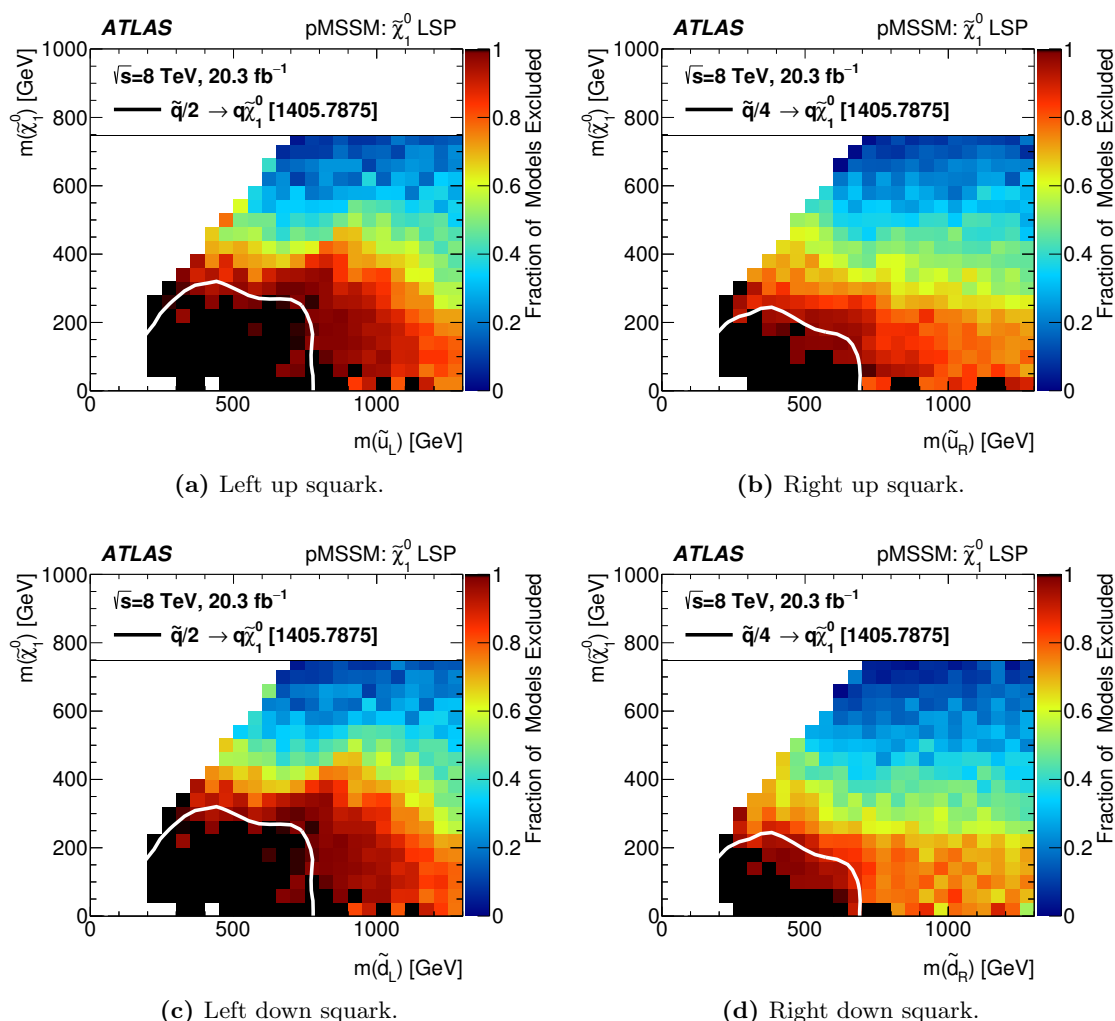
Figure 5. Fraction of model points excluded in the planes of the masses of the left-handed and right-handed squarks (of the first two generations) versus the neutralino mass. Both simplified-model limit contours are taken from the 0-lepton + 2–6 jets + $E_{\mathrm{T}}^{\mathrm{miss}}$ analysis (figure 10(c) of ref. [58]); however, for the left (right) handed squarks the assumption of four (two) degenerate squarks is emulated by dividing the cross-section for production of the eight degenerate squark states by a factor of two (four). The colour scale is as described in figure 3.

relative to up squarks since there are fewer valence down quarks than up in the proton. The results for left-handed squarks also differ from those for right-handed squarks. The $\tilde{u}_{\mathrm{L}}$ and $\tilde{d}_{\mathrm{L}}$ squarks form a SU(2) doublet and so are degenerate in mass up to electroweak symmetry breaking effects. This means that if the lightest squark is a $\tilde{q}_{\mathrm{L}}$, there would be another squark with similar mass — a statement not usually true for $\tilde{q}_{\mathrm{R}}$, which have no similar constraint. For a particular value of the lightest squark mass, the presence of a pair of left-handed squarks effectively increases the overall squark production cross-section, leading to larger apparent sensitivity. The improved sensitivity to left-handed squarks is further enhanced by the dominant squark decay modes. Right-handed squarks, which lack
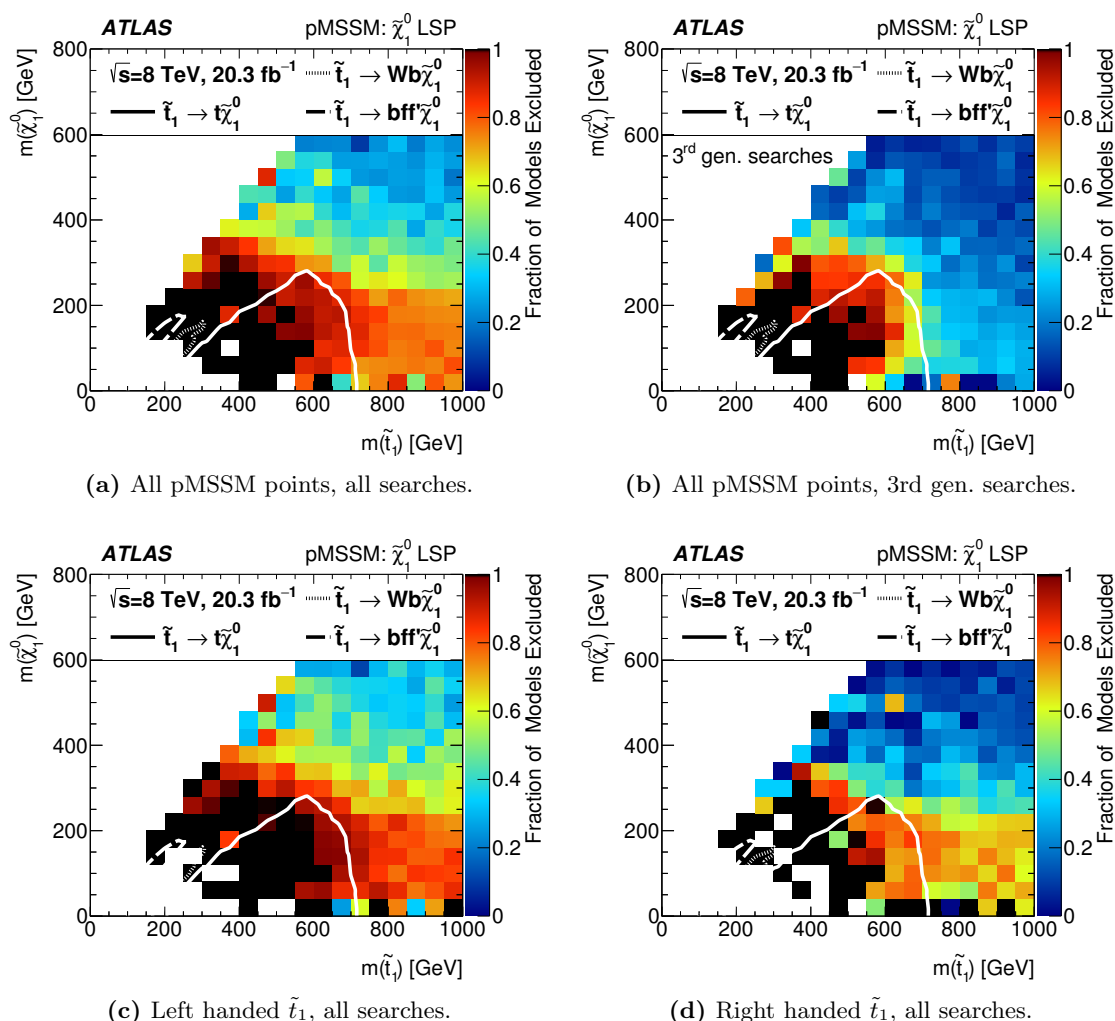
Figure 6. Fraction of pMSSM points excluded in the $\tilde{t}_1$-$\tilde{\chi}_1^0$ plane in various cases. The top two plots show the full model set, with impact of all searches on the left and only the third-generation searches on the right. The bottom row of plots separates the models according to whether the $\tilde{t}_1$ is either mostly (c) left handed or (d) right handed. There are relatively few pMSSM points at low $\tilde{t}_1$ mass for the reasons described in the text. The simplified-model limit overlaid [56, 57] is set assuming directly produced top squark pairs, with each decaying to a top quark and neutralino, $\tilde{t}_1 \to t\tilde{\chi}_1^0$. The colour scale is as described in figure 3.

weak couplings and have small Yukawa couplings, have suppressed decays to the wino-like or Higgsino-like LSPs which dominate the model sample. Instead right-handed squarks generally cascade decay via other electroweakino states resulting in events with smaller E_T^{miss}, a greater number of lower-p_T jets, and generally a smaller experimental sensitivity.

5.1.2 Third-generation squarks

The third-generation squarks are of particular phenomenological interest, since light top squarks (and to a lesser extent bottom squarks) are usually required if SUSY is to solve the

naturalness problem associated with the Higgs boson mass. They have been the subject of several dedicated searches, listed as 'third-generation' in table 1. Within the 19-parameter pMSSM the masses of these third-generation squarks are controlled by different parameters than for the first two generations, allowing the $\tilde{t}_{1,2}$ and $\tilde{b}_{1,2}$ masses to differ substantially both from one another and from the squarks of the first two generations.

Figure 6(a) shows the fractional exclusion of model points as projected onto the plane of the mass of the lighter of the two top squarks and that of the LSP. As discussed in section 3.3, there are relatively few model points at low top squark mass. This is because a large $m(\tilde{t})$ (and/or a large trilinear coupling A_t) is required to obtain the large quantum corrections needed to obtain the observed Higgs boson mass. Despite there being relatively few points in the initial sample with small top squark masses, one observes that when $m(\tilde{t})$ is below about 600 GeV, most points are excluded by ATLAS analyses.

The sensitivity to direct production of top squarks can be seen by considering the ATLAS exclusion using only those analyses from table 1 that target direct production of third-generation squarks. The results, presented in figure 6(b), show that when only these third-generation ATLAS searches are considered, good sensitivity continues to be observed for a lightest top squark mass up to about 700 GeV.

A reasonable correspondence is found between the sensitivity to the pMSSM points and those of the simplified-model decay considered in ref. [57], in which the top squark was assumed to decay with certainty to $t + \tilde{\chi}_1^0$ (including off-shell top decays). For larger top squark masses, in the range 600 GeV to 700 GeV, this example simplified-model line extends into a region where the observed fraction of pMSSM points that are excluded is less than 100%. This can be understood, since in ref. [57] it was shown that the sensitivity of the $\tilde{t}$ search analyses depends on the branching ratio of the top squark to the LSP. When the decay proceeds via the two-step process $\tilde{t}_1 \to b + \tilde{\chi}_1^\pm$ followed by $\tilde{\chi}_1^\pm \to W^{(*)} + \tilde{\chi}_1^0$, with the assumption that $m(\tilde{\chi}_1^\pm) = m(\tilde{\chi}_1^0)$, the 95% CL exclusion limit did not extend beyond $m(\tilde{t}_1) = 540$ GeV. Since a range of such branching ratios is found in the pMSSM model sample, it is to be expected that there is partial sensitivity in this intermediate region.

The lower two plots in figure 6 again show that the sensitivity of the ATLAS analyses can depend in a non-trivial way on sparticle properties that are not captured by simplified models. The dependence of the sensitivity on the left versus right chirality of the top squark is caused in part by different branching ratios for decays both to and from that squark. The branching ratios of decays involving wino-like gauginos are affected by the SU(2) coupling of the top squark, resulting in significant differences in the sensitivity depending on whether the $\tilde{t}_1$ is dominantly left- or right-handed. Furthermore, if the $\tilde{t}_1$ is mostly left-handed then the top squark's SU(2) partner, the $\tilde{b}$, would have a similar mass, allowing analyses targeting sbottom production to become relevant in constraining the models.

Figure 7(a) shows the sensitivity of ATLAS analyses as projected onto the mass plane of the lightest bottom squark versus the LSP. The sensitivity is generally well captured by a simplified model containing only an additional bottom squark and the LSP [69]. When searches for sparticles other than those of the third generation are omitted (figure 7(b)) the similarity of the pMSSM with the simplified model becomes still clearer. The sensitivity of the ATLAS searches was found to be similar regardless of whether the bottom squark was dominantly left- or right-handed.

(a) All searches.

(b) Third-generation searches.
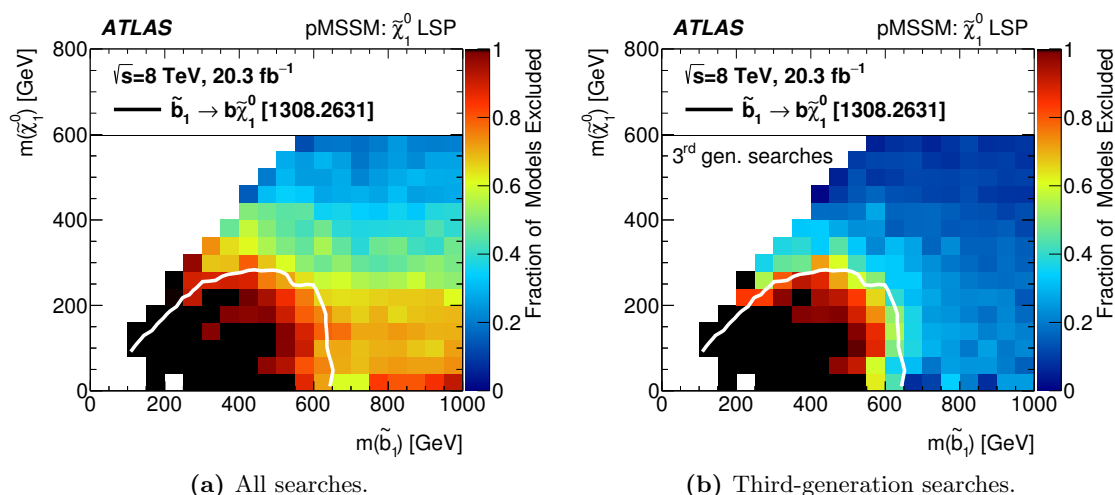
Figure 7. The fraction of pMSSM points excluded by (a) all the listed ATLAS Run 1 searches and (b) just the third-generation searches in the $\tilde{b}$-$\tilde{\chi}_1^0$ mass plane. The white line shows a simplified-model limit [69] made assuming directly produced bottom squark pairs, with bottom squarks decaying to a bottom quark and a neutralino, $\tilde{b} \to b + \tilde{\chi}_1^0$. The colour scale is as described in figure 3.
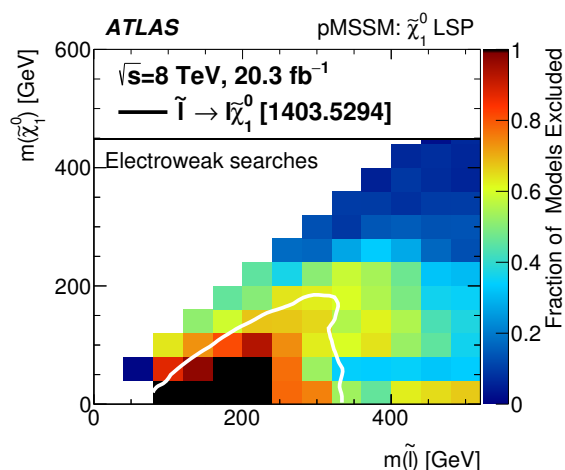
Figure 8. The fraction of pMSSM points excluded by just the electroweak ATLAS searches listed in table 1, projected onto the $\tilde{\ell}$-$\tilde{\chi}_1^0$ mass plane, where $\tilde{\ell}$ is the lightest slepton of the first two generations. The white line reflects one of the simplified-model limits (figure 8(c) of ref. [54]) made for direct slepton pair production assuming that left- and right-handed selectrons (or smuons) are mass-degenerate and that each decays via $\tilde{\ell}^{\pm} \to \ell^{\pm} + \tilde{\chi}_1^0$. The colour scale is as described in figure 3.

5.1.3 Electroweak sparticles and sleptons

The sensitivity to selectrons, smuons, and their sneutrino counterparts (here denoted collectively by $\tilde{\ell}$) is displayed in figure 8. It can be seen that the ATLAS searches have good sensitivity to slepton masses up to about 200 GeV, particularly when the LSP mass is lighter than about 75 GeV, where only bino-like LSPs survived the preselection of table 3. Nevertheless, the reduced sensitivity in the near-degenerate region where the slepton decay
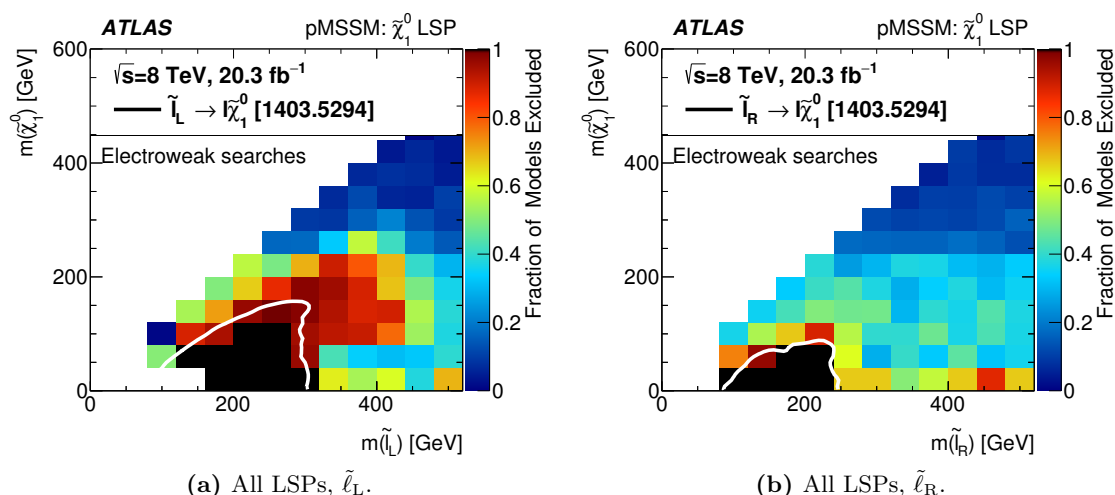
Figure 9. Impact of electroweak searches (as listed in table 1) in (a) the $\tilde{\ell}_{\mathrm{L}}$-$\tilde{\chi}_1^0$ and (b) $\tilde{\ell}_{\mathrm{R}}$-$\tilde{\chi}_1^0$ projections. It should be noted that in the 19-parameter pMSSM, the first- and second-generation sleptons of each handedness are required to be degenerate. The simplified-model limit in the $\tilde{\ell}_{\mathrm{L}}$ ($\tilde{\ell}_{\mathrm{R}}$) case is set assuming directly pair-produced left (right) handed selectrons/smuons, decaying to an electron/muon and neutralino. The simplified-model limits are from figures 8(a) and 8(b) of ref. [54]. The colour scale is as described in figure 3.

produces soft leptons and small $E_{\mathrm{T}}^{\mathrm{miss}}$ means that existing ATLAS searches cannot place any lower bound on the slepton mass. The region of sensitivity in the pMSSM projected plane is found to have a degree of correspondence with one of the simplified models of ref. [54]. Generally, reduced sensitivity is found in the pMSSM when compared to the more-constrained simplified model. This can be understood by recognising that this particular model presupposes that the left- and right-handed selectrons and smuons are all mass degenerate, and that each has a 100% branching ratio to a lepton and a LSP. Breaking these assumptions reduces the number of signal events, and hence allows more models to evade detection.

When the assumption of degenerate left- and right-handed states is dropped from the simplified model, the resulting limits are similar to those of the pMSSM. This can be seen in figure 9, showing the pMSSM space projected separately onto the mass of the left-handed or right-handed slepton. The fraction of model points excluded is compared to simplified models in which either only left- or right-handed sleptons ($\tilde{e}$ and $\tilde{\mu}$) are produced. ATLAS searches have more sensitivity to the production of left-handed sleptons since right-handed states lack SU(2) couplings and so have a smaller $\tilde{\ell}^+\tilde{\ell}^-$ production cross-section.

Figure 10 shows the fraction of model points excluded by just the electroweak ATLAS searches listed in table 1, projected onto the plane of LSP and lightest stau mass. It can be seen that the Run 1 sensitivity to staus is limited, with large fractions of model points surviving even at the lowest stau masses. This is largely because it is difficult to trigger on events resulting from direct stau production, and backgrounds to stau searches are much larger than for the equivalent search for sleptons of the first two generations. No definitive lower bound can be placed on the stau mass by ATLAS after Run 1.
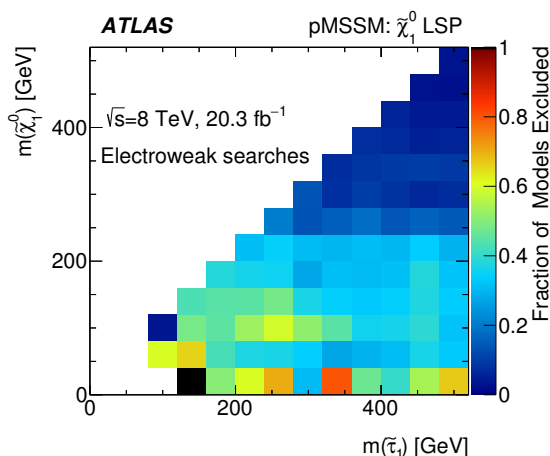
Figure 10. Impact of electroweak searches (as listed in table 1) on the $\tilde{\tau}$-$\tilde{\chi}_1^0$ plane. The colour scale is as described in figure 3.
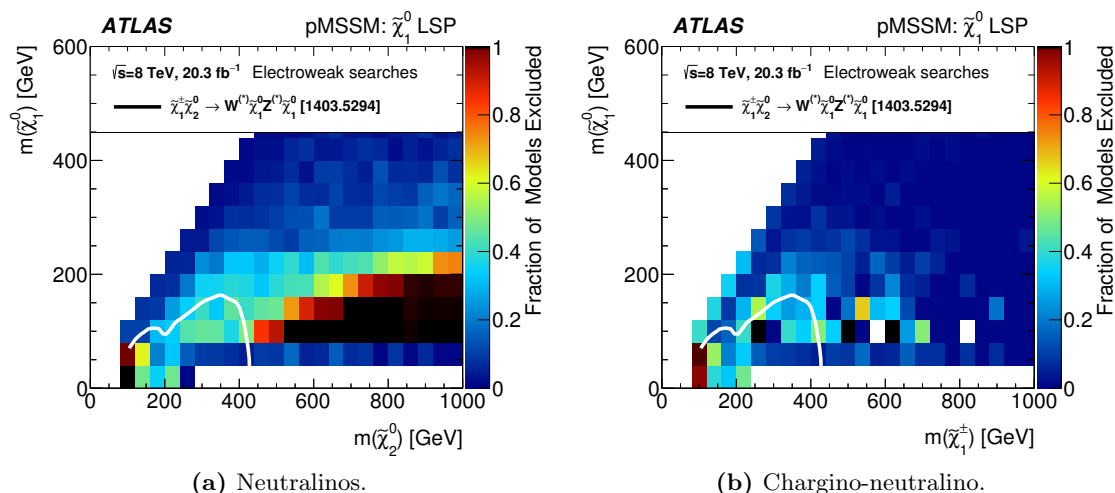
(a) Neutralinos. **(b)** Chargino-neutralino.

Figure 11. Impact of electroweak searches (as listed in table 1) (a) on the $\tilde{\chi}_2^0$-$\tilde{\chi}_1^0$ plane and (b) on the $\tilde{\chi}_1^\pm$-$\tilde{\chi}_1^0$ plane. The 95% CL observed exclusion limit from ref. [54] is for a simplified model that assumes pure-wino $\tilde{\chi}_1^\pm + \tilde{\chi}_2^0$ production, followed by the decays $\tilde{\chi}_1^\pm \tilde{\chi}_2^0 \to W^* \tilde{\chi}_1^0 Z^* \tilde{\chi}_1^0$. The colour scale is as described in figure 3.

Figure 11(a) shows the fraction of models excluded by only the electroweak ATLAS searches (see table 1), this time projected onto the plane of the masses of the lightest two neutralinos. Two prominent features are visible. For $\tilde{\chi}_1^0$ masses lighter than about 200 GeV, a large fraction of models are excluded, particularly as $m(\tilde{\chi}_2^0)$ becomes large. The dominant exclusion mechanism for large $m(\tilde{\chi}_2^0)$ is due to the Disappearing Track analysis and is strongest when the LSP is wino-dominated. The gaugino mass difference $\Delta m_\chi = m(\tilde{\chi}_1^\pm) - m(\tilde{\chi}_1^0)$ is typically less than a few hundred MeV for winos and of order a few GeV for Higgsinos. As the $\tilde{\chi}_2^0$ mass decreases, approaching that of the $\tilde{\chi}_1^0$, there is more neutralino mixing, leading to a larger Δm_χ, and a shorter $\tilde{\chi}_1^\pm$ lifetime, hence the Disap-

Long-lived	Bino LSP		Wino LSP		Higgsino LSP	
Particle	Models	Excluded	Models	Excluded	Models	Excluded
$\tilde{g}$	899 (5.2%)	5.1%	58 (3.4%)	3.4%	9 (0.0%)	0.0%
$\tilde{b}_1$	1252 (99.6%)	76.4%	51 (100.0%)	78.4%	67 (100.0%)	80.6%
$\tilde{t}_1$	345 (56.8%)	36.5%	6 (100.0%)	66.7%	17 (82.4%)	47.1%
$\tilde{\tau}_1$	406 (100.0%)	37.4%	2 (100.0%)	0.0%	41 (100.0%)	14.6%

Table 6. Number of model points with long-lived particles and their exclusion fraction. The percentages in parenthesis are the fractions of these model points where the long-lived particle has a lifetime long enough to traverse the entire detector.

pearing Track analysis loses sensitivity. The figure 11(a) row in which $m(\tilde{\chi}_1^0) \sim 50\,\text{GeV}$ has lower sensitivity for the Disappearing Track analysis. This region is dominated by models for which the relic density is controlled by the Z and h boson funnels, so has bino-like LSPs with a Higgsino admixture. Such models do not typically feature long-lived charginos.

For $m(\tilde{\chi}_2^0) \lesssim 400\,\text{GeV}$ and $m(\tilde{\chi}_1^0) \lesssim 200\,\text{GeV}$, direct production of $\tilde{\chi}_2^0$ (and/or $\tilde{\chi}_1^\pm$) states provides sensitivity via the 2-leptons, 3-leptons and 4-leptons analyses. The sensitive region for these multi-lepton analyses is similar to that shown from the simplified model of ref. [54]. Nevertheless there remain many viable pMSSM points within the region excluded in the simplified-model scenario. For example, many points in the Z and h boson funnel regions ($m(\tilde{\chi}_1^0) \sim 50\,\text{GeV}$) have little sensitivity in the multi-lepton analyses as the $\tilde{\chi}_2^0$ is predominantly Higgsino-like, leading to a lower production cross-section.

The equivalent plot for the projection onto the plane of the lightest chargino and the LSP is shown in figure 11(b), again showing the fraction excluded by the electroweak ATLAS searches. In this figure the Disappearing Track analysis has sensitivity to models with wino-like LSPs which lie close to the leading diagonal where $m(\tilde{\chi}_1^\pm)$ is only a little larger than $m(\tilde{\chi}_1^0)$. Models with Higgsino-like LSPs also lie close to that diagonal, but have larger mass splittings and so little sensitivity from the Disappearing Track analysis. Away from that diagonal only bino-dominated LSPs are found. Here the best sensitivity is from the multi-lepton electroweak search analyses (2-leptons, 3-leptons and 4-leptons), particularly for $m(\tilde{\chi}_1^\pm) \lesssim 400\,\text{GeV}$ and $m(\tilde{\chi}_1^0) \lesssim 200\,\text{GeV}$. The region with sensitivity to the multi-lepton searches again shows some similarity with the simplified-model limit from ref. [54], but again no region is totally excluded.

5.1.4 Long-lived squarks, gluinos and sleptons

As described in section 4.2, model points with long-lived squarks, gluinos and sleptons are treated separately as the sensitivity to these models of the regular searches for prompt decays is difficult to assess. Instead only the Long-lived particle searches [73, 74] are considered. These analyses have very good sensitivity to these model points as can be seen from table 6. Particularly good sensitivity is found in cases where the bottom squarks are long lived. The sensitivity to gluinos is quite poor as these are usually too short-lived to be picked up by the long-lived particle searches.
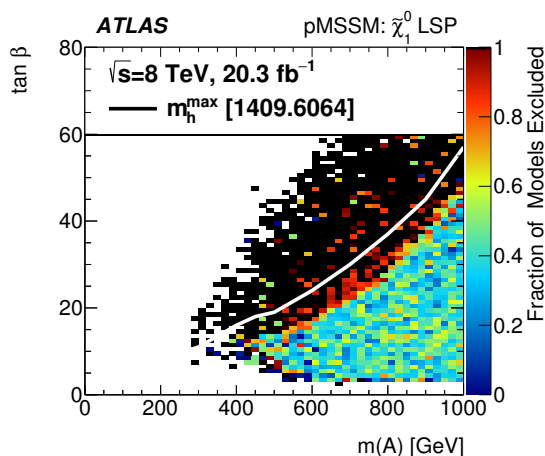
Figure 12. The fraction of model points excluded by ATLAS Run 1 searches, including those for heavy Higgs bosons, projected into the m_A-$\tan\beta$ plane. The white line overlaid is the observed limit for the m_h^{max} scenario from the $H/A \to \tau\tau$ search of ref. [75] where the region above the line is excluded.

5.1.5 Heavy neutral Higgs bosons

Figure 12 shows the fraction of model points excluded by the ATLAS Run 1 searches (which include searches for heavy Higgs bosons) when projected into the m_A-$\tan\beta$ plane. The white line overlaid is the observed limit from the ATLAS search [75] for heavy neutral Higgs boson(s), H or A, decaying to $\tau\tau$, as interpreted in the m_h^{max} scenario. A close correspondence can be observed between the limit obtained in that scenario and the region of the pMSSM space excluded by the Run 1 searches in the general pMSSM-19 space. The m_h^{max} scenario is seen to give a slightly conservative limit compared to the pMSSM space as it has light electroweakinos leading to a lower branching fraction for $A/H \to \tau\tau$ than for most pMSSM points with similar $m_A, \tan\beta$ values.

5.1.6 Complementarity of searches

The ATLAS searches are designed to be sensitive to different final states, or different kinematic regions. Nevertheless it is often the case that a model which produces an excess in one search can have a significant signal expectation in others, since related cascade decays can lead to complementary final states. The degree of complementarity is explored in figure 13, which shows the fraction of model points excluded (at 95% CL) by one analysis that are also excluded by another. For example, one can observe that of the model points that were excluded by the 1-lepton + jets + E_T^{miss} analysis (fourth row from bottom), 93% were also excluded by the 0-lepton + 2–6 jets + E_T^{miss} analysis (first column).

Figure 13 demonstrates that there is a good complementarity — relatively small overlap in sensitivity — between searches for strongly interacting particles, which are characterised by final states with jets, and searches for electroweak production. Further study shows that, for the sampling of pMSSM points made in this paper, the analyses with the largest regions of unique sensitivity are the 0-lepton + 2–6 jets + E_T^{miss} analysis [58], and the Disappearing
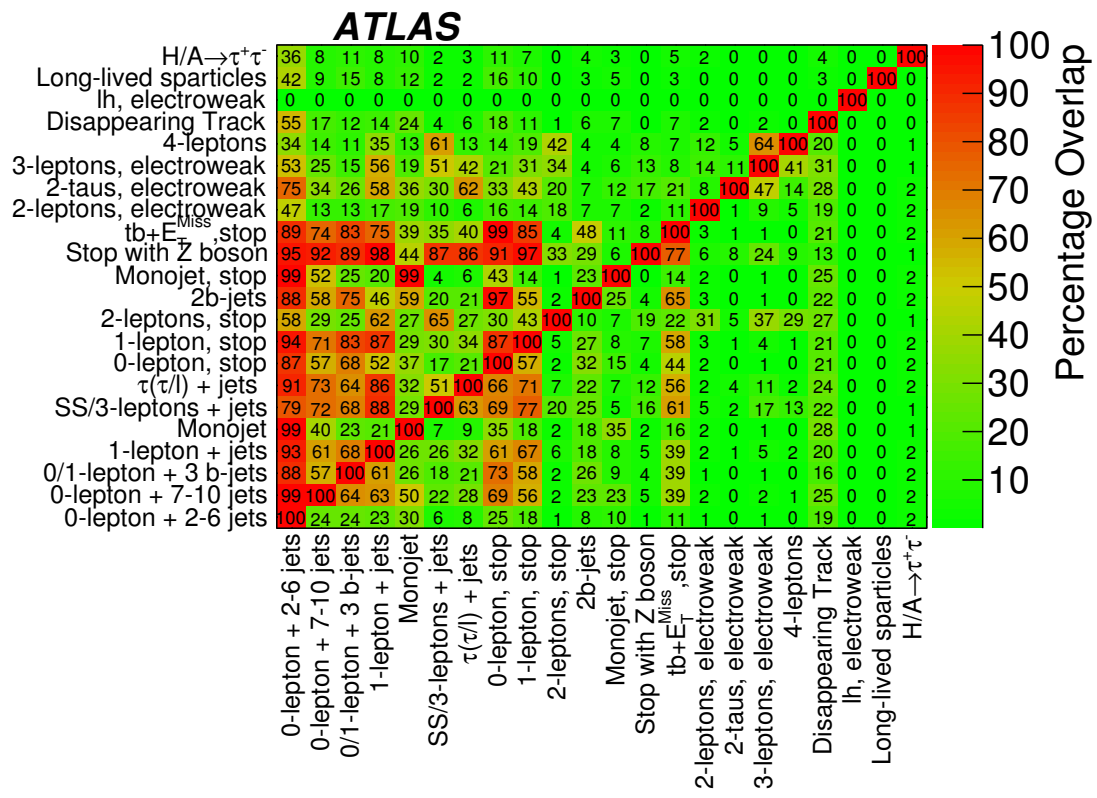
Figure 13. Complementarity of ATLAS searches: the figure shows the percentage of model points excluded by the analysis on the *y*-axis that were also excluded by the analysis on the *x*-axis. References for the individual analyses can be found in table 1. As none of the models considered are excluded by the ℓh analysis, it has no overlap with any other search.

Analysis	All LSPs	Bino-like	Wino-like	Higgsino-like
0-lepton + 2–6 jets + E_T^{miss}	32.1%	35.8%	29.7%	33.5%
0-lepton + 7–10 jets + E_T^{miss}	7.8%	5.5%	7.6%	8.0%
0/1-lepton + $3b$-jets + E_T^{miss}	8.8%	5.4%	7.1%	10.1%
1-lepton + jets + E_T^{miss}	8.0%	5.4%	7.5%	8.4%
Monojet	9.9%	16.7%	9.1%	10.1%
SS/3-leptons + jets + E_T^{miss}	2.4%	1.6%	2.4%	2.5%
$\tau(\tau/\ell)$ + jets + E_T^{miss}	3.0%	1.3%	2.9%	3.1%
0-lepton stop	9.4%	7.8%	8.2%	10.2%
1-lepton stop	6.2%	2.9%	5.4%	6.8%
$2b$-jets + E_T^{miss}	3.1%	3.3%	2.3%	3.6%
2-leptons stop	0.8%	1.1%	0.8%	0.7%
Monojet stop	3.5%	11.3%	2.8%	3.6%
Stop with Z boson	0.4%	1.0%	0.4%	0.5%
$tb+E_T^{miss}$, stop	4.2%	1.9%	3.1%	5.0%
ℓh, electroweak	0	0	0	0
2-leptons, electroweak	1.3%	2.2%	0.7%	1.6%
2-τ, electroweak	0.2%	0.3%	0.2%	0.2%
3-leptons, electroweak	0.8%	3.8%	1.1%	0.6%
4-leptons	0.5%	1.1%	0.6%	0.5%
Disappearing Track	11.4%	0.4%	29.9%	0.1%
Long-lived particle	0.1%	0.1%	0.0%	0.1%
$H/A \to \tau^+\tau^-$	1.8%	2.2%	0.9%	2.4%
Total	40.9%	40.2%	45.4%	38.1%

Table 7. Percentage of model points excluded by the individual analyses. It should be noted that the fraction of model points that can be excluded will depend on the model employed and range of input masses initially generated. The reader is reminded (table 2) that the sparticle mass terms in this paper extend to 4 TeV. References for the individual analyses can be found in table 1.

(a) Before ATLAS Run 1. **(b)** After ATLAS Run 1.
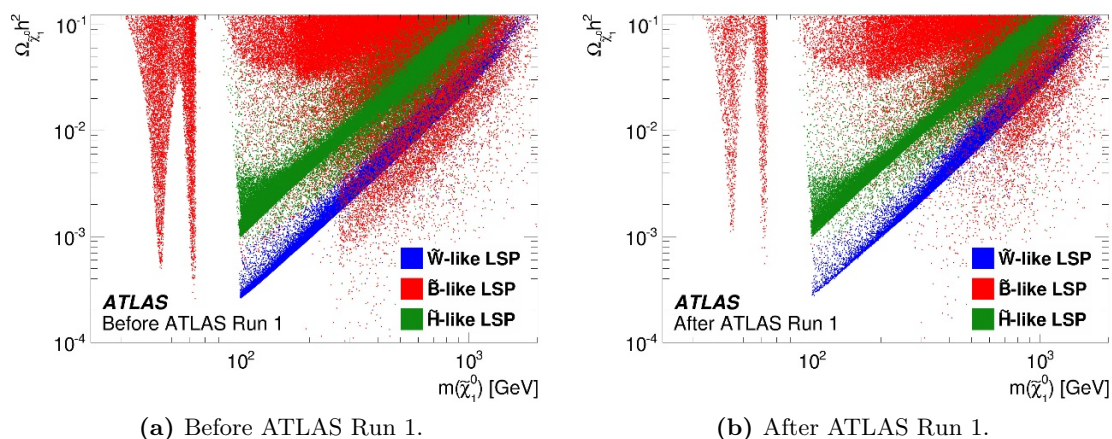
Figure 14. The density of pMSSM points projected onto the plane of dark matter relic density versus LSP mass, before and after the constraints from the search analyses. The colours labelling the different LSP types, as defined in table 4.

Track analysis [72]. Nevertheless some care is required in interpreting these results. The degree of apparent overlap is subjective, in that it depends, in some cases sensitively, on the metric used when sampling the pMSSM space. Even in cases where the apparent overlap appears to be large, for example between the 0-lepton + 2–6 jets + E_T^{miss} and 0-lepton + 7–10 jets + E_T^{miss} analyses, both searches are found to have regions of pMSSM space in which they provide unique sensitivity. The Disappearing Track analysis is mostly sensitive to model points with a wino-like LSP, so an alternative prior (or weighting by LSP type) of the sample model points would directly affect the apparent relative sensitivity of this analysis.

The overall fraction of model points within the pMSSM space excluded by each analysis for each of the LSP types is shown in table 7. Only the ℓh analysis is unable to constrain the pMSSM set with the luminosity available. The lack of sensitivity for that analysis is not unexpected since for simplified models it excludes only points with very light LSPs [70]. It should again be noted that the absolute values of the fractions of model points excluded is strongly affected by the prior sampling, in particular by the upper mass bounds used for the scan in selecting the pMSSM input parameters (see table 2). The relative fractions of model points excluded by each analysis are a little more informative, but again care is necessary in their interpretation since they too are sensitive to changes to the assumptions or constraints applied to the initial model set. Nevertheless, the high sensitivity of the 0-lepton + 2–6 jets + E_T^{miss} analysis for all LSP types, and the Disappearing Track analysis for models with a wino-like LSP is unambiguous.

5.2 Impact of ATLAS searches on dark matter

The nature of the LSP has a strong influence on the expected dark matter relic density. For the pMSSM points, the initial mass spectrum of the LSP — before applying any AT-LAS SUSY search constraints — is sculpted by the requirement that the dark matter relic density, as predicted from thermal production and annihilation calculations in the early uni-

verse, should not be larger than that observed. As discussed in section 3.2.2, the LSP is not required to account for all of the dark matter density, since other particles may contribute.

The effect of the relic density preselection can be seen in figure 14(a), which shows the density of pMSSM points in the plane of the $\tilde{\chi}_1^0$ relic density $(\Omega(\tilde{\chi}_1^0)h^2)$ versus the mass of the $\tilde{\chi}_1^0$. The model points with a bino-like LSP are shown in red, while those with wino-like and Higgsino-like LSPs are in blue and green respectively. The features at low LSP mass are due to the effective annihilation of LSPs through s-channel Z or Higgs bosons — the so-called Z-funnel and Higgs-funnel regions. There are few wino- or Higgsino-dominated LSPs at low mass since in such cases the $\tilde{\chi}_1^0$ is expected to be accompanied by an almost degenerate chargino, which would have been observed at LEP [102]. Most of the models with wino- and Higgsino-dominated LSPs lie on bands which are almost straight lines on the logarithmic plot, since the thermally averaged annihilation cross-section is expected to be proportional to the inverse square of the LSP mass, resulting in almost exact proportionality between $\Omega(\tilde{\chi}_1^0)h^2$ and $m(\tilde{\chi}_1^0)^2$.

Figure 14(b) shows the distribution of model points in the same plane after applying the constraints from the ATLAS SUSY searches. Considering first the bino-dominated LSP model points, one observes that model points are excluded by the ATLAS searches across a wide range of LSP masses (and expected relic densities). It is found that the ATLAS searches have some sensitivity up to $m(\tilde{\chi}_1^0) \lesssim 800\,\text{GeV}$, while at low bino mass about two-thirds of the LSP model points in the Z- and Higgs-funnel regions are excluded. For wino-dominated LSPs, the overall range of sensitivity in $m(\tilde{\chi}_1^0)$ again extends up to about $800\,\text{GeV}$. Model points with $m(\tilde{\chi}_1^0) \lesssim 220\,\text{GeV}$ are particularly depleted by the ATLAS searches with about 80% of model points with wino-like LSPs in this mass range being excluded, mostly by the sensitivity of the Disappearing Track analysis to the charged wino. For Higgsino-dominated LSPs, the ATLAS sensitivity is smaller as the $\tilde{\chi}_1^\pm$-$\tilde{\chi}_1^0$ mass splittings are mostly too large to have an observable $\tilde{\chi}_1^\pm$ lifetime.

Focusing on model points with bino-dominated LSPs, figure 15 shows the model point density before and after ATLAS Run 1 searches. In this figure the colour code now corresponds to the dominant annihilation mechanism of the dark matter — for example an orange point has at least one squark of the first two generations, or the gluino, close in mass to the LSP, allowing annihilation mechanisms such as $\tilde{q} + \tilde{\chi}_1^0 \rightarrow q + \gamma$ to proceed effectively. The vertical cut-offs for each coannihilator correspond to the preselection from previous experimental constraints — for example charged sparticles lighter than $100\,\text{GeV}$ are forbidden. The different minima seen for the relic dark matter energy density for each coannihilator correspond to the different coupling strengths.

The ATLAS searches are seen to be particularly sensitive to model points with light-flavour squark or gluino coannihilators. One would expect such model points, which have at least one coloured particle near-degenerate with the LSP, to produce events with missing transverse momentum, and soft jets from the coloured sparticle decays. Such model points are difficult to observe in the inclusive analyses, but when produced in association with ISR can be observed through the monojet analyses [64, 67].

The limits from experiments searching for direct detection of dark matter were taken into account when generating the pMSSM points. Figure 16 shows the corresponding

(a) Before ATLAS Run 1.

(b) After ATLAS Run 1.
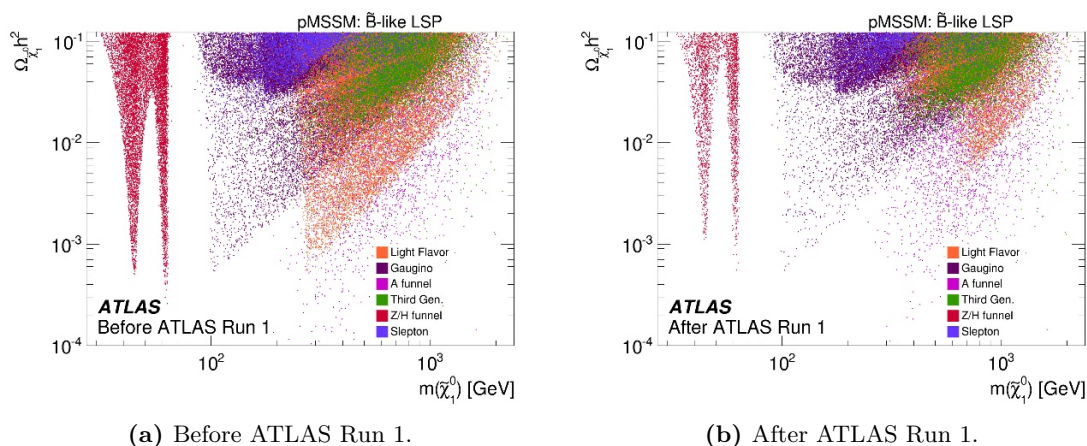
**Figure 15.** The density of pMSSM points on the plane of relic density versus LSP mass, before and after the ATLAS constraints, for the bino-like LSP models. The model points are colour coded by annihilation mechanism as described in the text. "Gaugino" refers to electroweak gaugino coannihilation, while "Light Flavour" refers to coannihilation either against squarks of the first two generations or against gluinos.

predictions together with the limits set by the measurements of the spin-independent (SI) and the proton spin-dependent (SD) cross-sections by the LUX [98] and COUPP [99] experiments respectively. The direct detection limits include the additional uncertainties described in section 3.2.2. In each case the interaction cross-section is scaled by a factor of $R_\Omega = \Omega(\tilde{\chi}_1^0)h^2/\Omega_{\text{Planck}}h^2$, since in this paper it is assumed that the LSP may be only one of a range of possible contributors[6] to the dark matter abundance, whereas direct detection experiments interpret their results in a framework in which the LSP completely saturates the relic density.

Figure 16(a) shows the model points projected onto the plane of the spin-independent interaction cross-section versus the LSP mass. The direct detection limit from the LUX experiment is shown, in which, as already mentioned, the relic density of the colliding dark matter was assumed to saturate the value measured by the Planck Collaboration. The only model points with LSP mass less than 100 GeV are those with bino-like LSPs lying in the Higgs- or Z-funnel regions. Around 15% of the bino-like model points that pass the preselection (table 3) would have been excluded by the nominal LUX limit had the additional uncertainty scaling factor of four, as mentioned in section 3.2.2, not been applied. Figure 16(b) shows the same space after removing model points excluded (at 95% CL) by the ATLAS Run 1 searches.

Figure 16(c) shows the spin-dependent cross-section, again as a function of the neutralino mass. The plot also shows the corresponding direct detection exclusion limit, this time from the COUPP experiment. The same plot is shown after ATLAS Run 1 search constraints in figure 16(d). Again one can see that sensitivity from LHC searches can stretch to regions with cross-sections several orders of magnitude below those of the current best direct detection experiments. Similar conclusions are found for spin-dependent neutron cross-sections, in this case the best direct detection limit being from Xenon-100 [100].

---

[6]These other possible contributors are not described by the pMSSM points considered in this study.

(a) Spin independent, before ATLAS Run 1.

(b) Spin independent, after ATLAS Run 1.

(c) Spin dependent, before ATLAS Run 1.

(d) Spin dependent, after ATLAS Run 1.
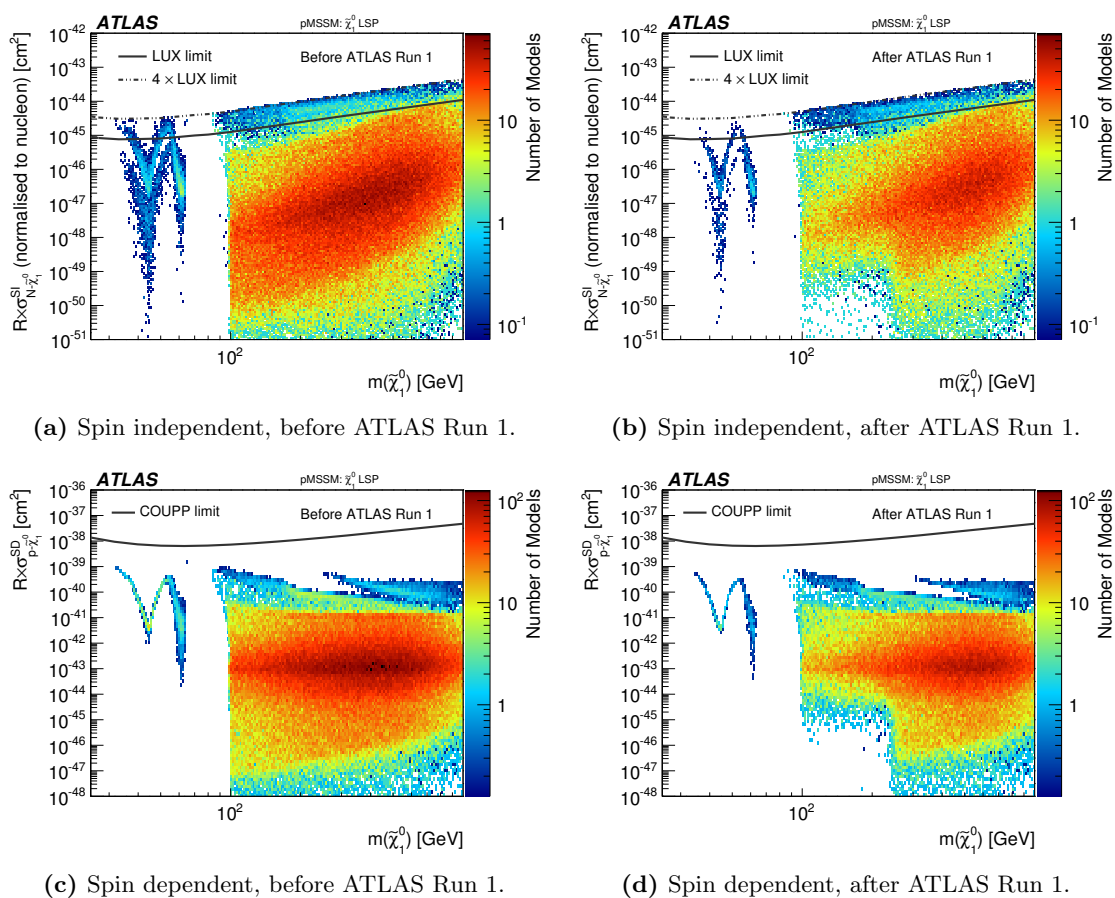
Figure 16. Left, the distribution of model points generated; right, the distribution of model points not excluded by ATLAS Run 1 searches, as projected onto the scaled spin-independent (SI) interaction cross-section of nucleons with the neutralino versus the neutralino mass. The cross-sections are scaled by a factor of $R_\Omega = \Omega(\tilde{\chi}_1^0)h^2/\Omega_{\mathrm{Planck}}h^2$. The calculated spin-independent interaction cross-sections are a weighted average of the contributions from proton and neutron scattering, corresponding to the Xenon atom (the target nucleus of the LUX experiment) and normalised to one nucleon. The 90% confidence limit [98] from the LUX direct detection experiment is overlaid, in which it is assumed that the dark matter comprises only the LSP, with relic density as measured by the Planck Collaboration [97]. For the spin-dependent cross-sections, the calculated proton cross-section is shown. It is compared to the direct detection limit from the COUPP experiment [99].

Figure 16(b) shows a roughly rectangular region excluded by ATLAS searches, bounded approximately by $m(\tilde{\chi}_1^0) \lesssim 220\,\mathrm{GeV}$ and $R_\Omega \times \sigma_{N-\tilde{\chi}_1^0}^{\mathrm{SI}} \lesssim 10^{-48}\mathrm{cm}^2$. A similar region is excluded in the SD case (figure 16(d)), this time for $R_\Omega \times \sigma_{N-\tilde{\chi}_1^0}^{\mathrm{SI}} \lesssim 10^{-44}\mathrm{cm}^2$ for the same LSP mass range. These regions are dominated by models with an LSP that is almost pure wino. The winos, having only very small Higgsino admixtures and thus little interaction with the Higgs boson, have small direct detection cross-sections. Such model points then have small $\tilde{\chi}_1^\pm$-$\tilde{\chi}_1^0$ mass splittings, and are tightly constrained by the Disappearing Track analysis, since the lightest chargino (the charged wino) is sufficiently long-lived to be de-

(a) Light Higgs boson κ_b.　　　　**(b)** Light Higgs boson BR to $\tilde{\chi}_1^0 \tilde{\chi}_1^0$.
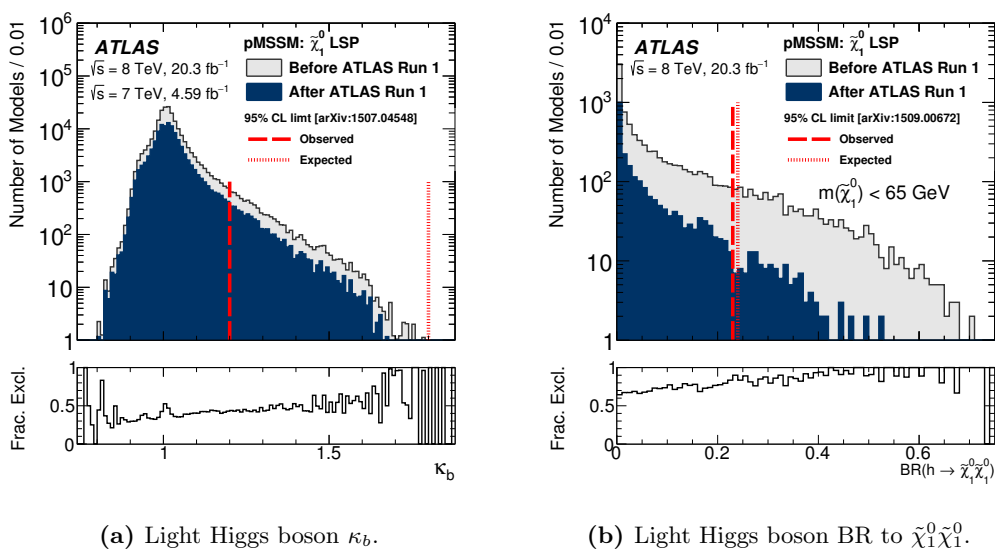
Figure 17. Distributions of pMSSM points before and after the constraints from the ATLAS direct searches for observables related to the decays of the observed Higgs boson. (a) Higgs-b-quark coupling ratio κ_b, for all LSP types. (b) Branching ratio of the Higgs boson to the LSP, only for those pMSSM points with bino-like LSPs and $m(\tilde{\chi}_1^0) < 65\,\text{GeV}$. The dashed lines show the observed and expected upper bounds of the 95% confidence limits on those parameters. The subplots show the fraction of model points excluded by the ATLAS direct searches.

tectable in that analysis. As the degree of Higgsino mixing increases, the direct detection cross-sections increase, and so does the LSP-NLSP mass splitting. This results in a more rapid NLSP decay, and lack of sensitivity by ATLAS.

As one would expect, the direct detection and LHC search techniques are found to be very complementary. The ATLAS searches have sensitivity for $m(\tilde{\chi}_1^0)$ up to about $800\,\text{GeV}$, and are particularly effective in constraining low-mass LSPs. ATLAS shows sensitivity to many SUSY models with direct detection cross-sections several orders of magnitude below current direct detection limits. On the other hand, direct detection experiments rule out large $R_\Omega \times \sigma$ up to higher LSP masses than the LHC can access.

5.3　Effect of ATLAS Higgs boson coupling measurements

Direct searches for SUSY particles are complemented by indirect searches for the effects of new particles and fields. In SUSY models the presence of the second Higgs doublet generally results in light Higgs boson couplings that are modified with respect to their SM values. For example, enhancements to the couplings to down-type quarks and charged leptons are predicted at large $\tan\beta$. In addition, loop contributions from virtual SUSY particles can produce an observable effect on lower-energy observables, including Higgs boson decay rates.

Combined fits by ATLAS to the measured Higgs boson production and decay rates provide a sensitive probe for such additional Higgs fields and for SUSY particles contributing either through loop effects or through invisible decays of the Higgs boson to unobserved neutralinos. The relevant ATLAS analyses, statistical methods, and systematic uncertain-

ties are described in refs. [143, 144]. These measurements are based on up to $4.8\,\mathrm{fb}^{-1}$ of pp collision data at $\sqrt{s} = 7\,\mathrm{TeV}$ and up to $20.3\,\mathrm{fb}^{-1}$ at $\sqrt{s} = 8\,\mathrm{TeV}$. They are used to constrain coupling scale factors

$$\kappa_i = \sqrt{\frac{\Gamma_h}{\Gamma_{h,\mathrm{SM}}} \times \frac{\mathrm{BR}(h \to i + i)}{\mathrm{BR}(h \to i + i)_{\mathrm{SM}}}},$$

where Γ_h represents the total width of the observed Higgs boson, BR indicates its branching ratio, and a SM subscript indicates the Standard Model prediction. The measurements of these scale factors were derived using the observed Higgs boson's visible decay channels as reported in ref. [144]. The upper limit on the invisible branching ratio, taking account of both visible and invisible Higgs boson decay channels is reported in ref. [145].[7] Most of the coupling parameters are not yet sufficiently well measured to have an effect on the SUSY parameter space. The exceptions — those two parameters which are already sufficiently well measured to constrain the pMSSM — are discussed below.

The parameter κ_b corresponds to the coupling of the Higgs field to b-quarks. Measuring a value of κ_b differing significantly from unity would be a clear indication of physics beyond the SM, and an important constraint on the allowed pMSSM parameter space. For the current ATLAS fit, the expected 95% CL range is $|\kappa_b| < 1.8$. This expected region contains almost all the pMSSM points not excluded by the direct searches, so the expected constraint from κ_b is negligible. The current ATLAS observed fitted value for κ_b is 0.62 ± 0.28 at 68% CL [145]. This value is lower than, but consistent with, the SM value. The corresponding observed 95% CL spans the range $|\kappa_b| < 1.2$, and is more restrictive than the expected range. As a result the observed fit disfavours those pMSSM points (see figure 17(a)) with $\kappa_b > 1.2$, which typically are those with large $\tan\beta$. Those models that are disfavoured at the 95% CL represent a weighted fraction of 3.1% of all the pMSSM points. This fraction is rather similar before and after the ATLAS Run 1 direct searches are considered.

The observed Higgs boson can decay to a pair of LSPs if those LSPs are sufficiently light. This can lead to an enhanced branching ratio of the h to the invisible final state. The expected branching ratio for decay of a light Higgs boson via ZZ^* to neutrinos is $\mathcal{O}(10^{-3})$, much smaller than the present experimental uncertainties, and so is negligible in this context. No models with a sufficiently light wino- or Higgsino-like LSP satisfied the initial constraints of section 3.2, so only models with a bino-dominated LSP need be considered in this context. All such LSPs have some wino and Higgsino admixture, allowing them to couple to the Higgs boson. Figure 17(b) shows the calculated distribution of the lightest Higgs boson's invisible branching ratio for those pMSSM points with bino-like LSPs and having $m(\tilde{\chi}_1^0) < 65\,\mathrm{GeV}$. To account for finite-width effects, this selection allows for models with LSP masses a little above $m(h)/2$. These light-LSP models represent 4.5% of the model points with bino-like LSPs that survive the ATLAS searches in table 1. The observed ATLAS bound on the h invisible branching ratio is $\mathrm{BR}(h \to \tilde{\chi}_1^0 + \tilde{\chi}_1^0) < 0.23$ at the 95% CL [145]. This observed value is close to the expected upper limit of 0.24. Considering only

---

[7]These constraints are based directly on the log-likelihood test statistic, rather than a calculation of CL_s, hence these particular limits are not protected against disfavouring models where there is little sensitivity.

those pMSSM points with a bino-like LSP lighter than 65 GeV, and which were not excluded by the direct searches, the fraction disfavoured at the 95% CL by the invisible branching ratio fit is 6.4%. The disfavoured points correspond to a weighted fraction of 0.0056% of all the pMSSM points (with any LSP type) not excluded by the ATLAS direct searches. The corresponding expected fractions are 6.1% (of those surviving models having bino-like LSPs with mass less than 65 GeV) and 0.0053% (weighted by LSP type) of all surviving models.

There is no overlap between the models disfavoured by the κ_b measurement and those disfavoured by the Higgs boson invisible branching ratio. This demonstrates that these indirect searches for new physics complement the direct searches in different ways by constraining different parts of the pMSSM space.

5.4 Impact of ATLAS searches on precision observables

Loop contributions from SUSY particles can also affect lower-energy observables. The measured values of several precision observables were taken as prior constraints on the pMSSM space sampled, as explained in section 3.2.1.

The effect of the ATLAS Run 1 searches on the distribution of pMSSM points as projected onto the expected values of these precision observables is shown in figure 18. In each case the most noticeable feature is that the ATLAS direct searches remove pMSSM points rather uniformly across the space of each precision variable, demonstrating the complementarity of the searches. The direct searches from Run 1 have placed tight constraints on the strongly interacting sector of the pMSSM, whereas the precision variables depend on other sparticles, for example the smuon and electroweakino masses, which are less tightly constrained by direct searches so far.

Figure 18 supports the statement in section 3.2.3 that the exclusion power of the ATLAS searches does not depend significantly on the mass range used for the light (SM-like) Higgs boson, the fraction of excluded model points being remarkably flat. The other three distributions: $\mathrm{BR}(B_s \to \mu\mu)$, $\mathrm{BR}(b \to s\gamma)$, and the $\Delta(g-2)_\mu$ also show good exclusion by ATLAS for all values of the observables. It is noticeable that the majority of the pMSSM points have only small SUSY contributions to these observables, so those model points would not be expected to be discoverable by using those measurements in the near future. Nevertheless there exists, for each precision measurement, a small number of model points with SUSY contributions large enough to be discovered by each. One observes that ATLAS also tends to have slightly larger sensitivity to these 'tail' model points. This increased sensitivity is not surprising since these model points are generally those with some lighter SUSY particles contributing to the precision measurements via loop diagrams. This correlation becomes more clear in figure 19, which shows the number of generated model points in the plane of the $\Delta(g-2)_\mu$ versus the mass of the lighter left- or right-handed smuon ($\min(m(\tilde{\mu}_{\mathrm{L}}), m(\tilde{\mu}_{\mathrm{R}}))$). The experimentally measured value [89], represented by the hatched band, only overlaps a region where $m(\tilde{\mu}) < 1\,\mathrm{TeV}$. As noted previously in section 3.2.1, the allowed range used for $\Delta(g-2)_\mu$ in this paper is the union of the 3σ intervals around the SM value and the experimental measurement. The experimentally measured value, if confirmed, would be a powerful constraint on the space.

(a) Light Higgs boson mass.

(b) $B_s \to \mu\mu$.

(c) $b \to s + \gamma$.

(d) Muon magnetic moment.
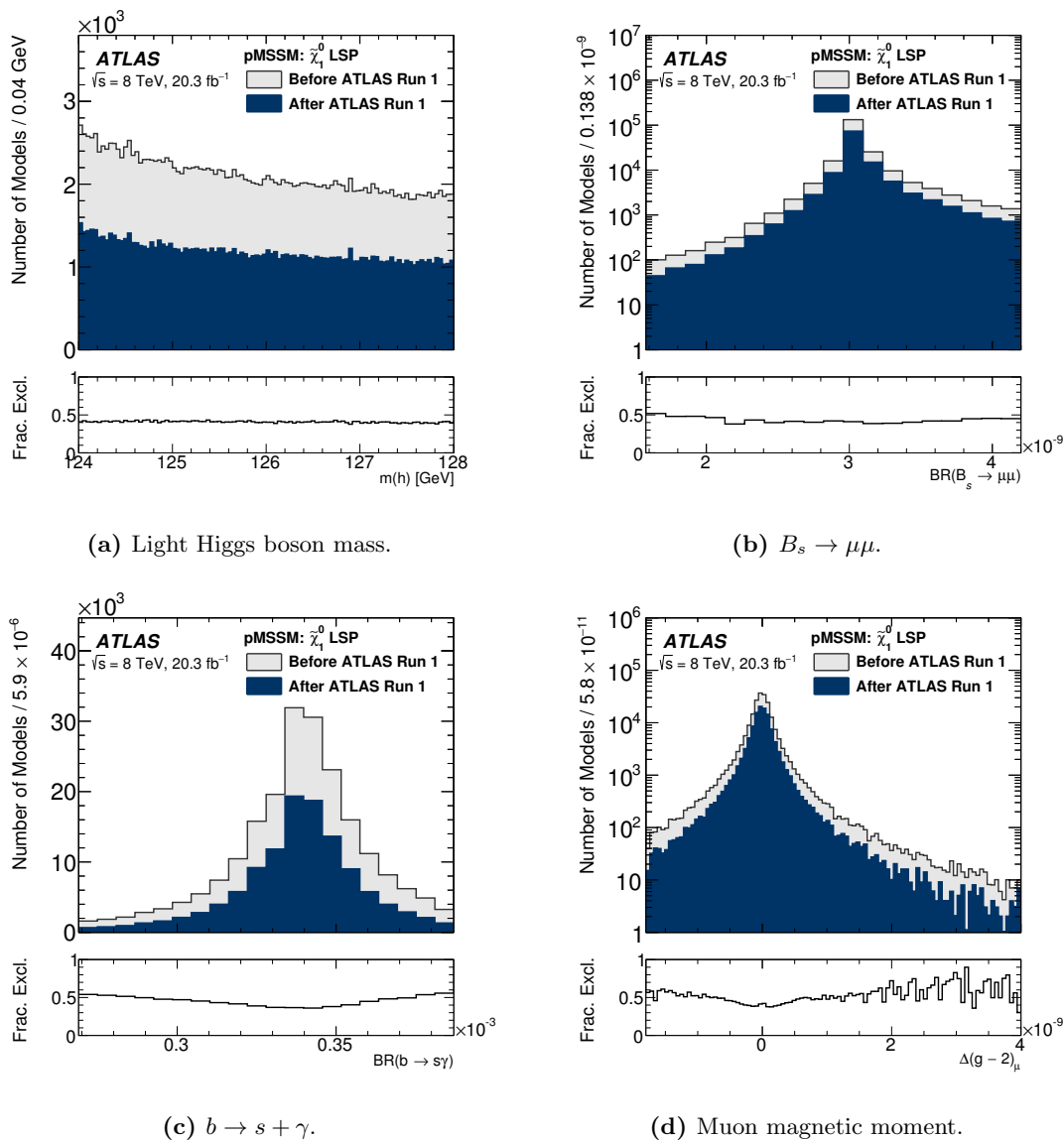
Figure 18. Distributions of model points before and after applying ATLAS searches for various precision observables. Figure (a) shows the mass of the light (SM-like) Higgs boson, $m(h)$, (b) shows the branching ratio of $B_s \to \mu + \mu$, (c) is the branching ratio of $b \to s + \gamma$ and (d) is the difference between the predicted value of $g - 2$ and the SM value, $\Delta(g - 2)_\mu$. The subplots show the fraction of model points excluded by ATLAS as a function of the observables.
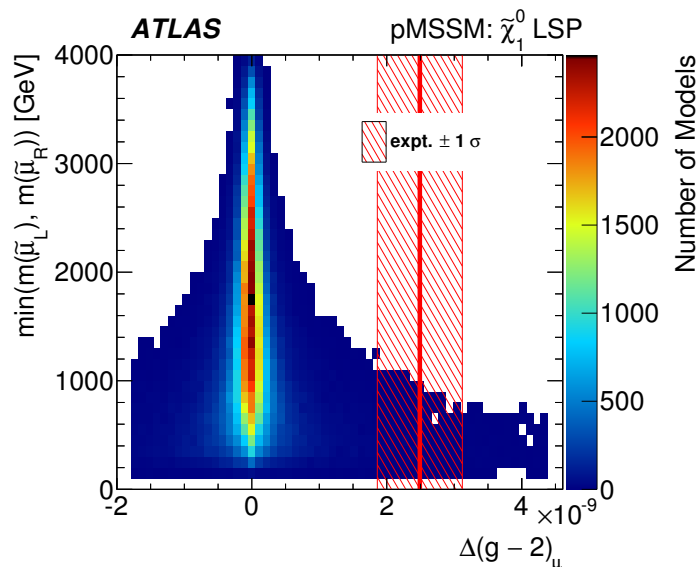
Figure 19. Distribution of model points in the plane of the mass of the lightest left- or right-handed smuon versus $\Delta(g-2)_\mu$. The experimental measurement is overlaid as the hatched band [89].

5.5 Fine-tuning

The naturalness of pMSSM points is not considered in their generation, but it is interesting to see just how fine-tuned the model points are after the ATLAS exclusion. The fine-tuning parameter adopted here is the one defined by Barbieri and Giudice [146]. Figure 20 illustrates the prediction of the fine-tuning before and after ATLAS exclusion, for all LSP types (a), and for each LSP-type separately (b)–(d). The shapes of the distributions are determined by the ranges of the pMSSM parameters considered. The dominant contributions to the fine-tuning come from μ and A_t. It can also be observed that the ATLAS Run 1 searches exclude pMSSM points with a wide range of different fine-tuning values. A decrease in sensitivity is observed with increasing fine-tuning for models with a Higgsino-like LSP. This is an artifact caused by the fact that the Higgsino is the LSP, that its mass is driven by the μ parameter, and so by requiring large fine-tuning, one is indirectly requiring that there be a heavy LSP, reducing ATLAS sensitivity.

The lowest fine-tuning parameter value for a surviving model point is 56. A representation of the sparticle spectrum of this point can be found in figure 21(a). As expected for a generic model point with low fine-tuning, the top squarks have sub-TeV masses. The model point has a wino-dominated LSP with a mass of 107 GeV, which is lighter by 1.6 GeV than its charged partner. This mass difference is sufficient to ensure that the chargino lifetime is short enough ($< 1\,\mathrm{ps}$) to evade the Disappearing Track analysis. The lower part of the mass spectrum includes a Higgsino-dominated $\{\tilde{\chi}_2^0, \tilde{\chi}_3^0, \tilde{\chi}_2^\pm\}$ multiplet with masses around 230 GeV which are mixed with the winos at about the 10% level. Most strongly interacting sparticles, particularly the gluino and left-squark doublet, have large masses of around 3 TeV, which is beyond the Run 1 search reach. The heavy Higgs bosons are also beyond the Run 1 search reach.
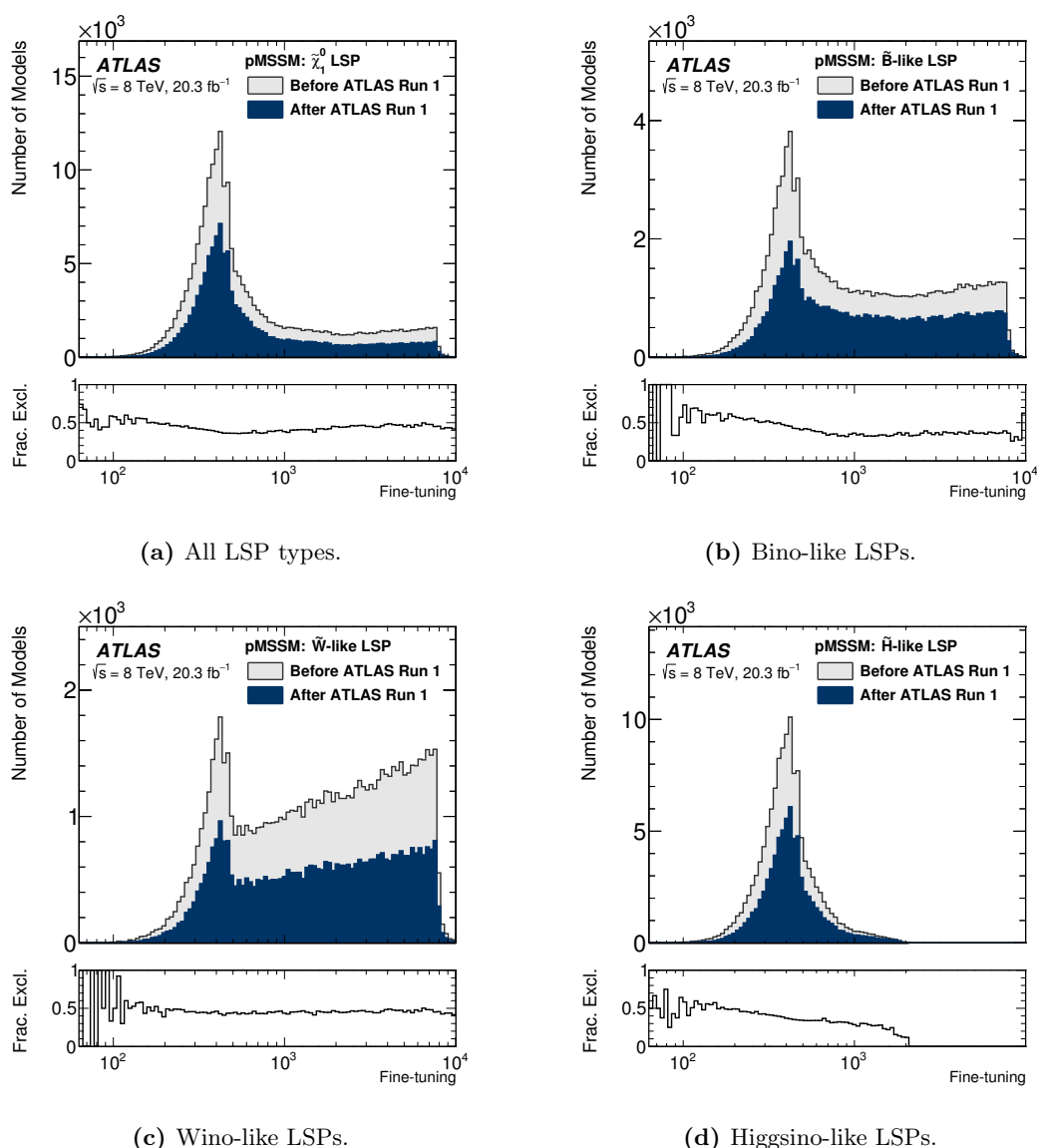
Figure 20. Distribution of fine-tuning (as defined in ref. [146]), before and after ATLAS exclusion. The subplots show the fractions of model points excluded by the ATLAS Run 1 searches.

Similar model points survive with a Higgsino-like LSP, for example as shown in figure 21(b), which has a fine-tuning of 57. Model points such as those in both figure 21(a) and figure 21(b) would be expected to produce observable signals at LHC Run 2 through a variety of channels. In particular in both cases the lighter top squark, with mass of about 800 GeV is not far from the current ATLAS Run 1 sensitivity.

Aside from model points with a wino-dominated or a Higgsino-dominated LSP there also remain model points with low fine-tuning and a mixed LSP. For example, figure 21(c) shows a model point with a mixed bino-Higgsino LSP a so-called 'well-tempered' neutralino case [105]. This model has a bottom squark with mass of about 650 GeV, not far above the Run 1 direct search sensitivity.
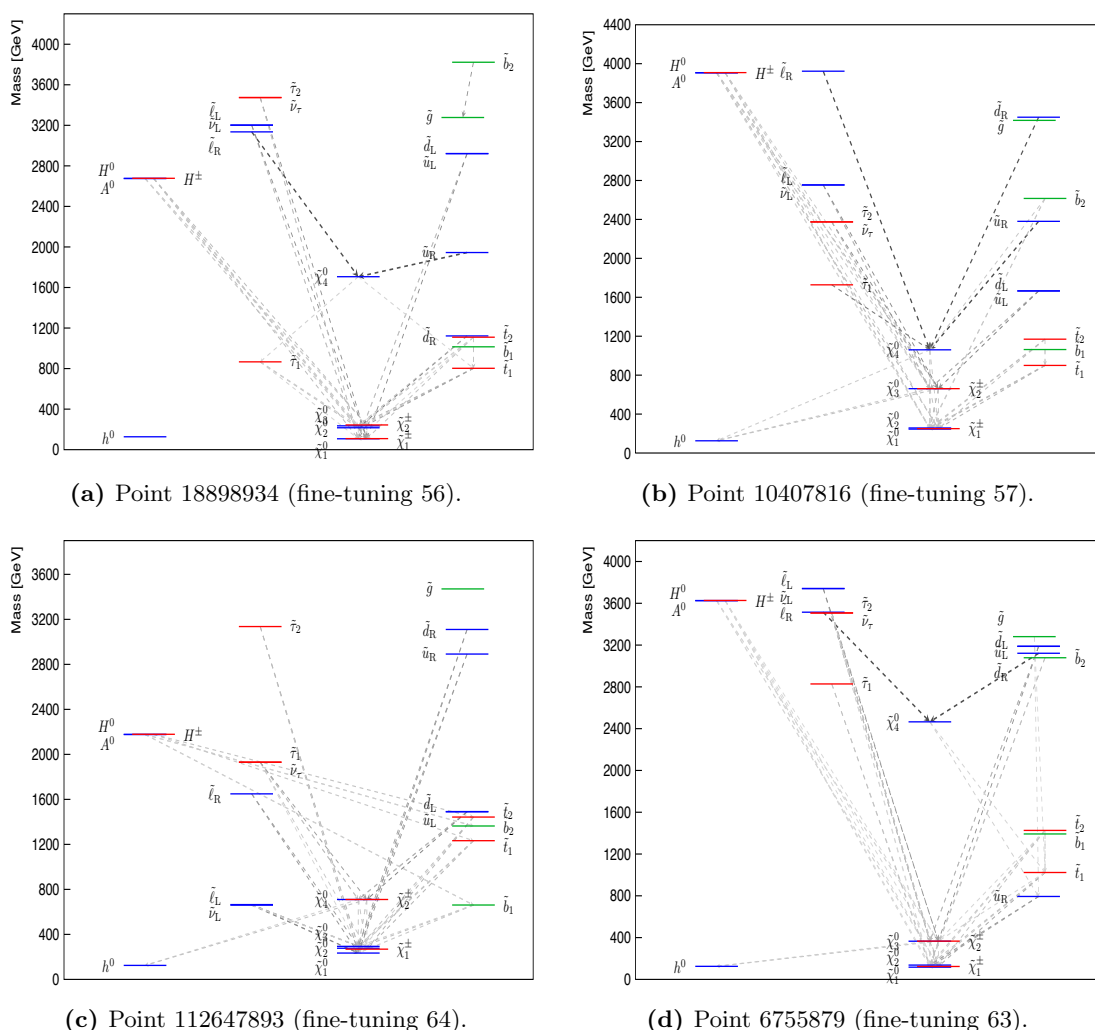
Figure 21. The sparticle spectra for some of the pMSSM-19 model points with the smallest fine-tuning not to have been excluded by the ATLAS Run 1 searches. The dashed lines indicate the dominant decay modes. For more details see the text.

Models with a small number of low-mass squarks of the first two generations also survive. For example, figure 21(d) shows a spectrum of a model point with a $\tilde{u}_R$ squark with a mass around $800\,\text{GeV}$, which again would be likely to be discoverable at LHC Run 2.

6 Conclusion

The ATLAS Collaboration has performed a wide range of direct searches for supersymmetry during the first run of the LHC, using pp collisions with centre-of-mass energy up to $8\,\text{TeV}$ and an integrated luminosity of up to $20.3\,\text{fb}^{-1}$. The interpretation of those results within the wider framework of the pMSSM gives insights into the breadth of sensitivity of those searches.

From an initial random sampling of 500 million pMSSM points, generated from the 19-parameter pMSSM, a total of 310,327 model points with $\tilde{\chi}_1^0$ LSP are selected each of which satisfies constraints from previous collider searches, precision measurements, cold dark matter energy density measurements and direct dark matter searches. The models are importance-sampled so that there are roughly equal numbers of models with a bino-like, wino-like or Higgsino-like LSP. For these model points, more than 30 billion signal events are generated, of which more than 600 million events from 44,559 different model points are passed through a GEANT4-based fast detector simulation and full reconstruction to accurately determine which have been excluded (at 95% CL) by ATLAS searches.

The impact of the ATLAS Run 1 searches on this space is presented, showing their overall effect in constraining such supersymmetric models. The results are particularly clear when considering the fraction of model points surviving, after projection into two-dimensional spaces of sparticle masses. The constraints on the masses of squarks (including third generation squarks), gluinos, electroweakinos, sleptons and heavy neutral Higgs bosons are all presented.

For the energy and luminosity achieved in LHC Run 1 the ATLAS constraints are most effective for strongly interacting sparticles, with weaker constraints on electroweakinos and sleptons. A general congruence is observed between the pMSSM points excluded and the limits determined previously in the context of simplified models. Nevertheless, significant differences are observed depending, for example, on the number of kinematically accessible squarks, and on their flavour and couplings, particularly for direct sleptons production.

The most constraining ATLAS analyses — for the model points generated — were the 0-lepton + 2–6 jets + $E_{\mathrm{T}}^{\mathrm{miss}}$ analysis, and the Disappearing Track analysis, the latter being especially powerful in the case of model points with a light wino-like LSP. Good complementarity is observed between different ATLAS analyses, with almost all showing regions of unique sensitivity.

When considering dark matter predictions, the LHC experiments are very complementary to the direct detection experiments. The two techniques have different sensitivities across the pMSSM-19 parameter space, with the ATLAS searches having more sensitivity at lower LSP mass (with significant sensitivity for $m(\tilde{\chi}_1^0) \lesssim 800\,\mathrm{GeV}$) and the direct detection experiments providing bounds at larger LSP-nucleon scattering cross-section. Similarly, the ATLAS experiment provides constraints which are complementary to those of precision measurements of $BR(B_s \to \mu\mu)$, $BR(b \to s\gamma)$, and $\Delta(g-2)_\mu$.

Model points with relatively low fine-tuning (of order 50) remain viable after LHC Run 1. Those with the lowest fine-tuning have relatively light top squarks, which indicates that one would expect them to be accessible by ATLAS searches with the LHC Run 2 dataset.

Acknowledgments

A Model point calculation

The calculation of model point properties proceeds as follows. First, `SoftSUSY` `3.4.0` [147] is used, embedded in `micrOMEGAs` `3.5.5` [77, 78], to calculate the sparticle spectrum. This spectrum is used as an input to `FeynHiggs` `2.10.0` [103, 104], which recalculates the light CP-even Higgs boson mass including important 3-loop corrections not present in `SoftSUSY`. For sparticle decay tables, a modified version of the program `SUSY-HIT` `1.3` [148] is used, updated to use `HDECAY` `5.11` [149] for the Higgs decays. In some cases, where relevant or even dominant decay modes are not included in the `SUSY-HIT` output, `MadGraph5_aMC@NLO` `2.1.1` [150] is instead used to recalculate those decays as described in detail below. `MicrOMEGAs` `3.5.5` is used to calculate the dark matter relic abundance along with the spin-independent and spin-dependent scattering cross-sections in direct detection experiments. `MicrOMEGAs` is also used to calculate the following flavour physics and precision electroweak observables: $\Delta\rho$, $\Delta(g-2)_\mu$, $\mathrm{BR}(b \to s\gamma)$ and $\mathrm{BR}(B_s \to \mu^+\mu^-)$. Finally, analytic formulas are used to calculate $\mathrm{BR}(B^+ \to \tau^+\nu_\tau)$ and the Z boson invisible width, and to check the stability of the vacuum.

B Sparticle decay calculation

The calculation of sparticle decays is performed as follows. First, the publicly available version of `SUSY-HIT` is modified by: (*i*) Incorporating light quark and lepton masses in the calculation of branching ratios and lifetimes for the various sparticles. Two-body decays implement the full mass corrections, while three-body decays only include a modified phase-space cut-off. The mass of the lightest meson of the appropriate type is included in the relevant phase space calculations to account for hadronisation effects. (*ii*) Employing full analytic expressions from ref. [151] for chargino decays when the chargino-neutralino mass splitting is $\lesssim 1$ GeV, in which case a careful treatment of hadronisation is important and can significantly affect the model phenomenology. (*iii*) Removing QCD corrections to decays involving top and bottom squarks due to their tendency to result in negative decay widths. (*iv*) Separating the Higgs decays to τ sneutrinos from those to electron and muon sneutrinos (the public version of `HDECAY` calculates them separately but then averages them).

Several cases have been identified in which `SUSY-HIT` does not calculate important decay channels or predicts a value that differs significantly from the full matrix element prediction, which are detailed in the following.

B.1 Right-handed sfermion decays

For right-handed sfermions, `SUSY-HIT` only calculates two-body decays of the form $\tilde{f}_R \to f\tilde{\chi}^0$ (and $\tilde{f}_R \to f\tilde{g}$ for right-handed squarks). If the bino component of the kinematically accessible neutralinos is very small, these decays can be highly suppressed. As a result, it is common for three-body decays of the form $\tilde{f}_R \to f\tilde{\chi}B$, where B is an electroweak gauge boson, to dominate over the two-body decays. In cases where the splitting between $\tilde{f}_R$ and the LSP is small, the three-body decay modes can be forbidden and a four-body decay (with B off-shell) can potentially be dominant, although numerically this turns out to be uncommon. Therefore `MadGraph5_aMC@NLO` is employed to calculate the decays of any right-handed sfermion satisfying the following selection criteria (designed to select all model points for which the multi-body decays would be significant while minimising the number of model points selected):

1) The bino content of the LSP is less than 10%.

2) Any accessible neutralinos with a bino content above 10% have a mass splitting with $\tilde{f}_R$ that is less than $100\,\mathrm{GeV}$ or below 20% of the $\tilde{f}_R$-LSP mass splitting.

3) For squarks, if the gluino is accessible it must have a mass splitting with $\tilde{f}_R$ that is less than 100 GeV or below 10% of the $\tilde{f}_R$-LSP mass splitting.

For model points with a $\tilde{f}_R$ — LSP mass splitting above $100\,\mathrm{GeV}$, all possible three-body decays are calculated with `MadGraph5_aMC@NLO` and added to the existing two-body decays. This can lead to double-counting when three-body decay diagrams contain intermediate particles which can go on shell. In this case, the on-shell component of the three-body decay is already included in the two-body decay width (as a tree-level two-body decay in which the SUSY decay product also undergoes a tree-level two-body decay).

This is resolved by selectively removing redundant decays. First, the sum of the combined three-body decay modes is compared with the sum of tree-level two-body decays for which the SUSY decay product has tree-level two-body decays (the "on-shell component"). In the case where the on-shell component comprised over 80% of the total three-body width, the three-body decays are discarded and only the two-body decays kept, since the sequential two-body decays give a more accurate representation of the decay kinematics. If the on-shell component is less than 80% of the total three-body width, the off-shell component of the three-body decays is deemed significant and the redundant on-shell component (the selected two-body decays) is discarded.

For model points with a $\tilde{f}_{\rm R}$-LSP mass splitting below $100\,{\rm GeV}$, four-body decays could be important. Here use was made of the MadWidth package in `MadGraph5_aMC@NLO` [150] by calling the `compute_widths` function; this function automatically determines whether three-body and four-body decays are required and includes an automatic mechanism for removing the degeneracy. It is found that MadWidth reproduces the results obtained using the procedure described above for several test cases with three-body decays.

In total the three-body decays are recalculated for at least 1 sparticle decay in 160482 model points. For 86109 model points, $\tilde{u}_{\rm R}$ decays are recalculated, while for 86791 model points the $\tilde{d}_{\rm R}$ decays are recalculated and for 122127 model points the $\tilde{e}_{\rm R}$ decays are recalculated. The four-body decays are calculated for 11633 model points, although this ends up making a significant contribution only for a few model points.

B.2 Wino and Higgsino decays to sfermions

Although `SUSY-HIT` normally calculates three-body decays of neutralinos and charginos that have mass splittings with the LSP below the Z or W boson masses, it does not calculate these decays when other two-body decay modes are available (to avoid the sort of double-counting described above). This can be a problem when the available two-body decays are suppressed by a small mixing angle (which can occur if the decaying gaugino is a neutral wino or Higgsino and the two-body decay is to a right-handed sfermion) or by kinematics. For this reason `MadGraph5_aMC@NLO` was employed to calculate the full three-body decays in cases where the decaying gaugino has a bino content below 10% and a right-handed sfermion is accessible, or has an accessible decay to any sfermion where the sfermion-gaugino splitting is below 20% of the gaugino-LSP splitting. This occurs in 716 model points with wino or Higgsino LSP and 2080 model points with bino LSP. Once again the issue with double-counting between the two-body and three-body decays is resolved; in this case any tree-level two-body decays where the product has a tree-level two-body decay are removed, since the off-shell three-body decays are expected to be important in nearly all of the selected scenarios.

B.3 Four-body top squark decays

Although `SUSY-HIT` includes a calculation of the four-body top squark decays, a significant discrepancy is observed between the `SUSY-HIT` results and the decay width calculated by `CalcHEP` in a previous model set. Therefore `MadGraph5_aMC@NLO` is used to recalculate the top squark decays for any model point in which `SUSY-HIT` predicts a non-zero four-body

decay rate for the light top squark. In this case, there are no concerns about overlap with other top squark decay modes. This procedure is employed for 15 model points with wino or Higgsino LSP and 5127 model points with bino LSP.

C   Calculational pathologies

To ensure that the spectrum is calculable, any model point with the following `SOFTSUSY` errors is discarded: "No acceptable solution found", "Non-perturbative", "No convergence", "Inaccurate Higgs mass", "Numerical problemThrown", and "Not achieved desired accuracy". Additionally the accuracy of the spectrum generation is tested by re-generating the spectrum with `SuSpect` [32] and ensuring that `SuSpect` does not produce any fatal errors or predict any sparticle masses to differ by more than 50% from the `SoftSUSY` prediction. Since `FeynHiggs` is used for the light CP-even Higgs boson mass, any model point for which `FeynHiggs` indicates an error or fails to write an output file, is discarded. Additionally it is required that $m(h)$ be within $5\,\mathrm{GeV}$ of the `SOFTSUSY` prediction, since a small tail of model points is observed for which this deviation is extremely large, suggesting that the calculation may have been unreliable. `FeynHiggs` also gives its own estimate of the uncertainty in the Higgs boson mass calculation. When this uncertainty is larger than $5\,\mathrm{GeV}$ the model points are discarded as being unreliable. Finally, the reliability of the `SUSY-HIT` decays is asserted by discarding model points for which any particle has a width larger than $1\,\mathrm{TeV}$ or a negative branching ratio.

C.1   Theoretical constraints

In addition to the numerical pathologies described above, model points that produced the following `SoftSUSY` errors are discarded as being theoretically inconsistent: "tachyon", "MuSqWrongsign", "m3sq-problem", and "Higgs potential ufb". Additionally it is checked that the scalar potential does not break colour or charge, using Equation (6) of ref. [152] for A_t and analogous formulas for A_b and A_τ. It should be noted that Equation (6) of ref. [152] uses $m(t_L)$ and $m(t_R)$, while this paper uses the Lagrangian parameters $m(Q_3)$ and $m(u_3)$.

D   Importance sampling by LSP type

As described in section 3.3, the model points generated are categorised according to LSP type (see table 4), and importance sampled so that approximately equal numbers of model points are available for each LSP type.

There are various ways in which over-production of dark matter can be achieved. A neutralino LSP can annihilate through s-channel exchange of a Z or Higgs boson or through t-channel exchange of a chargino or sfermion. If another sparticle is nearly degenerate with the LSP, that sparticle can also enhance the effective LSP annihilation rate through coannihilation. In general, sparticles with the strongest self-interactions (particularly coloured sparticles) make the most effective coannihilators. Supersymmetric models with a wino-like LSP or Higgsino-like LSP (see table 4) have a chargino that is nearly degenerate with the LSP, resulting in a sizeable annihilation rate through chargino exchange; the degenerate

chargino also serves as a coannihilator. The relic density constraint is therefore satisfied as long as the wino (Higgsino) mass is below 2.7 TeV (1 TeV) [153–155]. On the other hand, bino-like LSPs ($N_{11}^2 > \max(N_{12}^2, N_{13}^2 + N_{14}^2)$) have no guaranteed annihilation mechanism. One possibility is for the LSP to mix with the Higgsino [156], giving couplings to the Z and Higgs bosons and to the charginos. In order for the annihilation rate to be large enough, the Higgsino must be somewhat degenerate with the LSP (resulting in a large mixing angle) or the LSP must be approximately half the mass of the Z or MSSM Higgs bosons (termed a "funnel" region), producing a resonantly enhanced annihilation rate that compensates for the mixing-angle-suppressed couplings. Alternatively, a chargino or sfermion can be nearly degenerate with the LSP, resulting in a sizeable t-channel annihilation rate and/or significant coannihilation [157].

Correcting the undersampling of model points with bino-like LSPs is important for two reasons. First, they are the only model points in which the observed relic abundance can be obtained with an LSP light enough to be seen at the 8 TeV LHC, making them particularly interesting from the dark matter perspective. Second, the absence of an associated chargino can significantly alter the available decay modes. As an example, top squark decays to $W^+ b \tilde\chi_1^0$ only occur in models with bino-like LSPs, since the top squark can simply decay to $b \tilde\chi^+$ in wino or Higgsino LSP models.

Open Access. This article is distributed under the terms of the Creative Commons Attribution License (CC-BY 4.0), which permits any use, distribution and reproduction in any medium, provided the original author(s) and source are credited.

References

[1] ATLAS collaboration, *The ATLAS experiment at the CERN Large Hadron Collider*, 2008 *JINST* **3** S08003 [INSPIRE].

[2] CMS collaboration, *The CMS experiment at the CERN LHC*, 2008 *JINST* **3** S08004 [INSPIRE].

[3] H. Miyazawa, *Baryon number changing currents*, *Prog. Theor. Phys.* **36** (1966) 1266 [INSPIRE].

[4] P. Ramond, *Dual theory for free fermions*, *Phys. Rev.* **D 3** (1971) 2415 [INSPIRE].

[5] Yu. A. Golfand and E.P. Likhtman, *Extension of the algebra of Poincaré group generators and violation of p invariance*, JETP Lett. **13** (1971) 323 [*Pisma Zh. Eksp. Teor. Fiz.* **13** (1971) 452] [INSPIRE].

[6] A. Neveu and J.H. Schwarz, *Factorizable dual model of pions*, *Nucl. Phys.* **B 31** (1971) 86 [INSPIRE].

[7] A. Neveu and J.H. Schwarz, *Quark model of dual pions*, *Phys. Rev.* **D 4** (1971) 1109 [INSPIRE].

[8] J.-L. Gervais and B. Sakita, *Field theory interpretation of supergauges in dual models*, *Nucl. Phys.* **B 34** (1971) 632 [INSPIRE].

[9] D.V. Volkov and V.P. Akulov, *Is the neutrino a Goldstone particle?*, *Phys. Lett.* **B 46** (1973) 109 [INSPIRE].

[10] J. Wess and B. Zumino, *A Lagrangian model invariant under supergauge transformations*, *Phys. Lett.* **B 49** (1974) 52 [INSPIRE].

[11] J. Wess and B. Zumino, *Supergauge transformations in four-dimensions*, *Nucl. Phys.* **B 70** (1974) 39 [INSPIRE].

[12] S. Weinberg, *Implications of dynamical symmetry breaking*, *Phys. Rev.* **D 13** (1976) 974 [INSPIRE].

[13] E. Gildener, *Gauge symmetry hierarchies*, *Phys. Rev.* **D 14** (1976) 1667 [INSPIRE].

[14] S. Weinberg, *Implications of dynamical symmetry breaking: an addendum*, *Phys. Rev.* **D 19** (1979) 1277 [INSPIRE].

[15] L. Susskind, *Dynamics of spontaneous symmetry breaking in the Weinberg-Salam theory*, *Phys. Rev.* **D 20** (1979) 2619 [INSPIRE].

[16] H. Goldberg, *Constraint on the photino mass from cosmology*, *Phys. Rev. Lett.* **50** (1983) 1419 [*Erratum ibid.* **103** (2009) 099905] [INSPIRE].

[17] J.R. Ellis, J.S. Hagelin, D.V. Nanopoulos, K.A. Olive and M. Srednicki, *Supersymmetric relics from the big bang*, *Nucl. Phys.* **B 238** (1984) 453 [INSPIRE].

[18] S. Dimopoulos, S. Raby and F. Wilczek, *Supersymmetry and the scale of unification*, *Phys. Rev.* **D 24** (1981) 1681 [INSPIRE].

[19] N. Sakai, *Naturalness in supersymmetric GUTS*, *Z. Phys.* **C 11** (1981) 153 [INSPIRE].

[20] L.E. Ibáñez and G.G. Ross, *Low-energy predictions in supersymmetric Grand Unified Theories*, *Phys. Lett.* **B 105** (1981) 439 [INSPIRE].

[21] M.B. Einhorn and D.R.T. Jones, *The weak mixing angle and unification mass in supersymmetric* SU(5), *Nucl. Phys.* **B 196** (1982) 475 [INSPIRE].

[22] W.J. Marciano and G. Senjanović, *Predictions of supersymmetric Grand Unified Theories*, *Phys. Rev.* **D 25** (1982) 3092 [INSPIRE].

[23] C. Giunti, C.W. Kim and U.W. Lee, *Running coupling constants and grand unification models*, *Mod. Phys. Lett.* **A 6** (1991) 1745 [INSPIRE].

[24] J.R. Ellis, S. Kelley and D.V. Nanopoulos, *Probing the desert using gauge coupling unification*, *Phys. Lett.* **B 260** (1991) 131 [INSPIRE].

[25] U. Amaldi, W. de Boer and H. Furstenau, *Comparison of grand unified theories with electroweak and strong coupling constants measured at LEP*, *Phys. Lett.* **B 260** (1991) 447 [INSPIRE].

[26] P. Langacker and M.-X. Luo, *Implications of precision electroweak experiments for* M_t, ρ_0, $\sin^2 \theta_W$ *and grand unification*, *Phys. Rev.* **D 44** (1991) 817 [INSPIRE].

[27] P. Fayet, *Supersymmetry and weak, electromagnetic and strong interactions*, *Phys. Lett.* **B 64** (1976) 159 [INSPIRE].

[28] P. Fayet, *Spontaneously broken supersymmetric theories of weak, electromagnetic and strong interactions*, *Phys. Lett.* **B 69** (1977) 489 [INSPIRE].

[29] G.R. Farrar and P. Fayet, *Phenomenology of the production, decay and detection of new hadronic states associated with supersymmetry*, *Phys. Lett.* **B 76** (1978) 575 [INSPIRE].

[30] P. Fayet, *Relations between the masses of the superpartners of leptons and quarks, the Goldstino couplings and the neutral currents*, *Phys. Lett.* **B 84** (1979) 416 [INSPIRE].

[31] S. Dimopoulos and H. Georgi, *Softly broken supersymmetry and* SU(5), *Nucl. Phys.* **B 193** (1981) 150 [INSPIRE].

[32] A. Djouadi, J.-L. Kneur and G. Moultaka, *SuSpect: a fortran code for the supersymmetric and Higgs particle spectrum in the MSSM, Comput. Phys. Commun.* **176** (2007) 426 [hep-ph/0211331] [INSPIRE].

[33] C.F. Berger, J.S. Gainer, J.L. Hewett and T.G. Rizzo, *Supersymmetry without prejudice, JHEP* **02** (2009) 023 [arXiv:0812.0980] [INSPIRE].

[34] M.W. Cahill-Rowley, J.L. Hewett, S. Hoeche, A. Ismail and T.G. Rizzo, *The new look pMSSM with neutralino and gravitino LSPs, Eur. Phys. J.* **C 72** (2012) 2156 [arXiv:1206.4321] [INSPIRE].

[35] K.J. de Vries et al., *The pMSSM10 after LHC Run* 1, *Eur. Phys. J.* **C 75** (2015) 422 [arXiv:1504.03260] [INSPIRE].

[36] C. Strege et al., *Profile likelihood maps of a* 15-*dimensional MSSM, JHEP* **09** (2014) 081 [arXiv:1405.0622] [INSPIRE].

[37] S. Henrot-Versillé et al., *Constraining supersymmetry using the relic density and the Higgs boson, Phys. Rev.* **D 89** (2014) 055017 [arXiv:1309.6958] [INSPIRE].

[38] M. Cahill-Rowley, J. Hewett, A. Ismail and T. Rizzo, *Higgs boson coupling measurements and direct searches as complementary probes of the phenomenological MSSM, Phys. Rev.* **D 90** (2014) 095017 [arXiv:1407.7021] [INSPIRE].

[39] M. Cahill-Rowley et al., *Complementarity of dark matter searches in the phenomenological MSSM, Phys. Rev.* **D 91** (2015) 055011 [arXiv:1405.6716] [INSPIRE].

[40] M. Chakraborti, U. Chattopadhyay, A. Choudhury, A. Datta and S. Poddar, *The electroweak sector of the pMSSM in the light of LHC-8 TeV and other data, JHEP* **07** (2014) 019 [arXiv:1404.4841] [INSPIRE].

[41] M.W. Cahill-Rowley, J.L. Hewett, A. Ismail and T.G. Rizzo, *More energy, more searches, but the phenomenological MSSM lives on, Phys. Rev.* **D 88** (2013) 035002 [arXiv:1211.1981] [INSPIRE].

[42] S.S. AbdusSalam, *LHC-7 supersymmetry search interpretation within the phenomenological MSSM, Phys. Rev.* **D 87** (2013) 115012 [arXiv:1211.0999] [INSPIRE].

[43] S.S. AbdusSalam and D. Choudhury, *Higgs boson discovery versus sparticles prediction: impact on the pMSSM's posterior samples from a Bayesian global fit, Universal J. Phys. Appl.* **2** (2014) 155 [arXiv:1210.3331] [INSPIRE].

[44] M.W. Cahill-Rowley, J.L. Hewett, A. Ismail and T.G. Rizzo, *The Higgs sector and fine-tuning in the pMSSM, Phys. Rev.* **D 86** (2012) 075015 [arXiv:1206.5800] [INSPIRE].

[45] M. Carena, J. Lykken, S. Sekmen, N.R. Shah and C.E.M. Wagner, *The pMSSM interpretation of LHC results using rernormalization group invariants, Phys. Rev.* **D 86** (2012) 075025 [arXiv:1205.5903] [INSPIRE].

[46] A. Arbey, M. Battaglia and F. Mahmoudi, *Light neutralino dark matter in the pMSSM: implications of LEP, LHC and dark matter searches on SUSY particle spectra, Eur. Phys. J.* **C 72** (2012) 2169 [arXiv:1205.2557] [INSPIRE].

[47] A. Strubig, S. Caron and M. Rammensee, *Constraints on the pMSSM from searches for squarks and gluinos by ATLAS, JHEP* **05** (2012) 150 [arXiv:1202.6244] [INSPIRE].

[48] A. Arbey, M. Battaglia and F. Mahmoudi, *Implications of LHC searches on SUSY particle spectra: the pMSSM parameter space with neutralino dark matter*, *Eur. Phys. J.* **C 72** (2012) 1847 [arXiv:1110.3726] [INSPIRE].

[49] S. Sekmen et al., *Interpreting LHC SUSY searches in the phenomenological MSSM*, *JHEP* **02** (2012) 075 [arXiv:1109.5119] [INSPIRE].

[50] B.C. Allanach, A.J. Barr, A. Dafinca and C. Gwenlan, *Discovery reach for generic supersymmetry at the LHC: MT2 versus missing transverse momentum selections for pMSSM searches*, *JHEP* **07** (2011) 104 [arXiv:1105.1024] [INSPIRE].

[51] J.A. Conley, J.S. Gainer, J.L. Hewett, M.P. Le and T.G. Rizzo, *Supersymmetry without prejudice at the LHC*, *Eur. Phys. J.* **C 71** (2011) 1697 [arXiv:1009.2539] [INSPIRE].

[52] S.S. AbdusSalam, B.C. Allanach, F. Quevedo, F. Feroz and M. Hobson, *Fitting the phenomenological MSSM*, *Phys. Rev.* **D 81** (2010) 095012 [arXiv:0904.2548] [INSPIRE].

[53] ATLAS collaboration, *Search for direct production of charginos and neutralinos in events with three leptons and missing transverse momentum in $\sqrt{s} = 8\,TeV$ pp collisions with the ATLAS detector*, *JHEP* **04** (2014) 169 [arXiv:1402.7029] [INSPIRE].

[54] ATLAS collaboration, *Search for direct production of charginos, neutralinos and sleptons in final states with two leptons and missing transverse momentum in pp collisions at $\sqrt{s} = 8\,TeV$ with the ATLAS detector*, *JHEP* **05** (2014) 071 [arXiv:1403.5294] [INSPIRE].

[55] ATLAS collaboration, *Search for the direct production of charginos, neutralinos and staus in final states with at least two hadronically decaying taus and missing transverse momentum in pp collisions at $\sqrt{s} = 8\,TeV$ with the ATLAS detector*, *JHEP* **10** (2014) 96 [arXiv:1407.0350] [INSPIRE].

[56] ATLAS collaboration, *Search for top squark pair production in final states with one isolated lepton, jets and missing transverse momentum in $\sqrt{s} = 8\,TeV$ pp collisions with the ATLAS detector*, *JHEP* **11** (2014) 118 [arXiv:1407.0583] [INSPIRE].

[57] ATLAS collaboration, *ATLAS Run 1 searches for direct pair production of third-generation squarks at the Large Hadron Collider*, arXiv:1506.08616 [INSPIRE].

[58] ATLAS collaboration, *Search for squarks and gluinos with the ATLAS detector in final states with jets and missing transverse momentum using $\sqrt{s} = 8\,TeV$ proton-proton collision data*, *JHEP* **09** (2014) 176 [arXiv:1405.7875] [INSPIRE].

[59] ATLAS collaboration, *Search for new phenomena in final states with large jet multiplicities and missing transverse momentum at $\sqrt{s} = 8\,TeV$ proton-proton collisions using the ATLAS experiment*, *JHEP* **10** (2013) 130 [*Erratum ibid.* **01** (2014) 109] [arXiv:1308.1841] [INSPIRE].

[60] ATLAS collaboration, *Search for squarks and gluinos in events with isolated leptons, jets and missing transverse momentum at $\sqrt{s} = 8\,TeV$ with the ATLAS detector*, *JHEP* **04** (2015) 116 [arXiv:1501.03555] [INSPIRE].

[61] ATLAS collaboration, *Search for supersymmetry in events with large missing transverse momentum, jets and at least one tau lepton in $20\,fb^{-1}$ of $\sqrt{s} = 8\,TeV$ proton-proton collision data with the ATLAS detector*, *JHEP* **09** (2014) 103 [arXiv:1407.0603] [INSPIRE].

[62] ATLAS collaboration, *Search for supersymmetry at $\sqrt{s} = 8\,TeV$ in final states with jets and two same-sign leptons or three leptons with the ATLAS detector*, *JHEP* **06** (2014) 035 [arXiv:1404.2500] [INSPIRE].

[63] ATLAS collaboration, *Search for strong production of supersymmetric particles in final states with missing transverse momentum and at least three b-jets at $\sqrt{s} = 8\,TeV$ proton-proton collisions with the ATLAS detector*, *JHEP* **10** (2014) 24 [arXiv:1407.0600] [INSPIRE].

[64] ATLAS collaboration, *Search for new phenomena in final states with an energetic jet and large missing transverse momentum in pp collisions at $\sqrt{s} = 8\,TeV$ with the ATLAS detector*, *Eur. Phys. J.* **C 75** (2015) 299 [*Erratum ibid.* **C 75** (2015) 408] [arXiv:1502.01518] [INSPIRE].

[65] ATLAS collaboration, *Search for direct pair production of the top squark in all-hadronic final states in proton-proton collisions at $\sqrt{s} = 8\,TeV$ with the ATLAS detector*, *JHEP* **09** (2014) 015 [arXiv:1406.1122] [INSPIRE].

[66] ATLAS collaboration, *Search for direct top-squark pair production in final states with two leptons in pp collisions at $\sqrt{s} = 8\,TeV$ with the ATLAS detector*, *JHEP* **06** (2014) 124 [arXiv:1403.4853] [INSPIRE].

[67] ATLAS collaboration, *Search for pair-produced third-generation squarks decaying via charm quarks or in compressed supersymmetric scenarios in pp collisions at $\sqrt{s} = 8\,TeV$ with the ATLAS detector*, *Phys. Rev.* **D 90** (2014) 052008 [arXiv:1407.0608] [INSPIRE].

[68] ATLAS collaboration, *Search for direct top squark pair production in events with a Z boson, b-jets and missing transverse momentum in $\sqrt{s} = 8\,TeV$ pp collisions with the ATLAS detector*, *Eur. Phys. J.* **C 74** (2014) 2883 [arXiv:1403.5222] [INSPIRE].

[69] ATLAS collaboration, *Search for direct third-generation squark pair production in final states with missing transverse momentum and two b-jets in $\sqrt{s} = 8\,TeV$ pp collisions with the ATLAS detector*, *JHEP* **10** (2013) 189 [arXiv:1308.2631] [INSPIRE].

[70] ATLAS collaboration, *Search for direct pair production of a chargino and a neutralino decaying to the $125\,GeV$ Higgs boson in $\sqrt{s} = 8\,TeV$ pp collisions with the ATLAS detector*, *Eur. Phys. J.* **C 75** (2015) 208 [arXiv:1501.07110] [INSPIRE].

[71] ATLAS collaboration, *Search for supersymmetry in events with four or more leptons in $\sqrt{s} = 8\,TeV$ pp collisions with the ATLAS detector*, *Phys. Rev.* **D 90** (2014) 052001 [arXiv:1405.5086] [INSPIRE].

[72] ATLAS collaboration, *Search for charginos nearly mass degenerate with the lightest neutralino based on a disappearing-track signature in pp collisions at $\sqrt{s} = 8\,TeV$ with the ATLAS detector*, *Phys. Rev.* **D 88** (2013) 112006 [arXiv:1310.3675] [INSPIRE].

[73] ATLAS collaboration, *Searches for heavy long-lived sleptons and R-hadrons with the ATLAS detector in pp collisions at $\sqrt{s} = 7\,TeV$*, *Phys. Lett.* **B 720** (2013) 277 [arXiv:1211.1597] [INSPIRE].

[74] ATLAS collaboration, *Searches for heavy long-lived charged particles with the ATLAS detector in proton-proton collisions at $\sqrt{s} = 8\,TeV$*, *JHEP* **01** (2015) 068 [arXiv:1411.6795] [INSPIRE].

[75] ATLAS collaboration, *Search for neutral Higgs bosons of the minimal supersymmetric Standard Model in pp collisions at $\sqrt{s} = 8\,TeV$ with the ATLAS detector*, *JHEP* **11** (2014) 056 [arXiv:1409.6064] [INSPIRE].

[76] G. D'Ambrosio, G.F. Giudice, G. Isidori and A. Strumia, *Minimal flavor violation: an effective field theory approach*, *Nucl. Phys.* **B 645** (2002) 155 [hep-ph/0207036] [INSPIRE].

[77] G. Bélanger, F. Boudjema, A. Pukhov and A. Semenov, *MicrOMEGAs 2.0: a program to calculate the relic density of dark matter in a generic model*, *Comput. Phys. Commun.* **176** (2007) 367 [hep-ph/0607059] [INSPIRE].

[78] G. Bélanger, F. Boudjema, A. Pukhov and A. Semenov, *MicrOMEGAs: a tool for dark matter studies*, *Nuovo Cim.* **C 033N2** (2010) 111 [arXiv:1005.4133] [INSPIRE].

[79] M. Baak et al., *The electroweak fit of the Standard Model after the discovery of a new boson at the LHC*, *Eur. Phys. J.* **C 72** (2012) 2205 [arXiv:1209.2716] [INSPIRE].

[80] HEAVY FLAVOR AVERAGING GROUP collaboration, Y. Amhis et al., *Averages of b-hadron, c-hadron and τ-lepton properties as of early* 2012, arXiv:1207.1158 [INSPIRE].

[81] K. De Bruyn et al., *Probing new physics via the $B_s^0 \to \mu^+\mu^-$ effective lifetime*, *Phys. Rev. Lett.* **109** (2012) 041801 [arXiv:1204.1737] [INSPIRE].

[82] LHCb and CMS collaborations, *Observation of the rare $B_s^0 \to \mu^+\mu^-$ decay from the combined analysis of CMS and LHCb data*, *Nature* **522** (2015) 68 [arXiv:1411.4413] [INSPIRE].

[83] F. Mahmoudi, *SuperIso v2.3: a program for calculating flavor physics observables in supersymmetry*, *Comput. Phys. Commun.* **180** (2009) 1579 [arXiv:0808.3144] [INSPIRE].

[84] BaBar collaboration, B. Aubert et al., *A search for $B^+ \to \ell^+\nu_\ell$ recoiling against $B^- \to D^0\ell^-\bar\nu X$*, *Phys. Rev.* **D 81** (2010) 051101 [arXiv:0912.2453] [INSPIRE].

[85] BELLE collaboration, K. Hara et al., *Evidence for $B^- \to \tau^-\bar\nu$ with a semileptonic tagging method*, *Phys. Rev.* **D 82** (2010) 071101 [arXiv:1006.4201] [INSPIRE].

[86] BELLE collaboration, I. Adachi et al., *Evidence for $B^- \to \tau^-\bar\nu_\tau$ with a hadronic tagging method using the full data sample of Belle*, *Phys. Rev. Lett.* **110** (2013) 131801 [arXiv:1208.4678] [INSPIRE].

[87] BaBar collaboration, J.P. Lees et al., *Evidence of $B^+ \to \tau^+\nu$ decays with hadronic B tags*, *Phys. Rev.* **D 88** (2013) 031102 [arXiv:1207.0698] [INSPIRE].

[88] CKMFITTER GROUP collaboration, J. Charles et al., *CP violation and the CKM matrix: assessing the impact of the asymmetric B factories*, *Eur. Phys. J.* **C 41** (2005) 1 [hep-ph/0406184] [INSPIRE].

[89] T. Aoyama, M. Hayakawa, T. Kinoshita and M. Nio, *Complete tenth-order QED contribution to the muon g-2*, *Phys. Rev. Lett.* **109** (2012) 111808 [arXiv:1205.5370] [INSPIRE].

[90] K. Hagiwara, R. Liao, A.D. Martin, D. Nomura and T. Teubner, *$(g-2)_\mu$ and $\alpha(M_Z^2)$ re-evaluated using new precise data*, *J. Phys.* **G 38** (2011) 085003 [arXiv:1105.3149] [INSPIRE].

[91] A. Nyffeler, *Hadronic light-by-light scattering in the muon g − 2: a new short-distance constraint on pion-exchange*, *Phys. Rev.* **D 79** (2009) 073012 [arXiv:0901.1172] [INSPIRE].

[92] A. Czarnecki, W.J. Marciano and A. Vainshtein, *Refinements in electroweak contributions to the muon anomalous magnetic moment*, *Phys. Rev.* **D 67** (2003) 073006 [*Erratum ibid.* **D 73** (2006) 119901] [hep-ph/0212229] [INSPIRE].

[93] MUON G-2 collaboration, G.W. Bennett et al., *Measurement of the negative muon anomalous magnetic moment to 0.7 ppm*, *Phys. Rev. Lett.* **92** (2004) 161802 [hep-ex/0401008] [INSPIRE].

[94] MUON G-2 collaboration, G.W. Bennett et al., *Final report of the muon E821 anomalous magnetic moment measurement at BNL*, *Phys. Rev.* **D 73** (2006) 072003 [`hep-ex/0602035`] [INSPIRE].

[95] P.J. Mohr, B.N. Taylor and D.B. Newell, *CODATA recommended values of the fundamental physical constants:* 2006, *Rev. Mod. Phys.* **80** (2008) 633 [`arXiv:0801.0028`] [INSPIRE].

[96] B.L. Roberts, *Status of the Fermilab muon* $(g-2)$ *experiment*, *Chin. Phys.* **C 34** (2010) 741 [`arXiv:1001.2898`] [INSPIRE].

[97] PLANCK collaboration, P.A.R. Ade et al., *Planck* 2015 *results. XIII. Cosmological parameters*, `arXiv:1502.01589` [INSPIRE].

[98] LUX collaboration, D.S. Akerib et al., *First results from the LUX dark matter experiment at the Sanford Underground Research Facility*, *Phys. Rev. Lett.* **112** (2014) 091303 [`arXiv:1310.8214`] [INSPIRE].

[99] COUPP collaboration, E. Behnke et al., *First dark matter search results from a* 4 kg CF_3I *bubble chamber operated in a deep underground site*, *Phys. Rev.* **D 86** (2012) 052001 [`arXiv:1204.3094`] [INSPIRE].

[100] XENON100 collaboration, E. Aprile et al., *Limits on spin-dependent WIMP-nucleon cross sections from* 225 *live days of XENON*100 *data*, *Phys. Rev. Lett.* **111** (2013) 021301 [`arXiv:1301.6620`] [INSPIRE].

[101] SLD ELECTROWEAK GROUP, DELPHI, ALEPH, SLD, SLD HEAVY FLAVOUR GROUP, OPAL, LEP ELECTROWEAK WORKING GROUP and L3 collaborations, S. Schael et al., *Precision electroweak measurements on the Z resonance*, *Phys. Rept.* **427** (2006) 257 [`hep-ex/0509008`] [INSPIRE].

[102] LEP2 SUSY WORKING GROUP, ALEPH, DELPHI, L3 and OPAL collaborations, *Combined LEP chargino results, up to* 208 *GeV for large* m0, note LEPSUSYWG/01-03.1, http://lepsusy.web.cern.ch/lepsusy.

[103] S. Heinemeyer, W. Hollik and G. Weiglein, *FeynHiggs: a program for the calculation of the masses of the neutral CP even Higgs bosons in the MSSM*, *Comput. Phys. Commun.* **124** (2000) 76 [`hep-ph/9812320`] [INSPIRE].

[104] T. Hahn, S. Heinemeyer, W. Hollik, H. Rzehak and G. Weiglein, *High-precision predictions for the light CP-even Higgs boson mass of the minimal supersymmetric Standard Model*, *Phys. Rev. Lett.* **112** (2014) 141801 [`arXiv:1312.4937`] [INSPIRE].

[105] N. Arkani-Hamed, A. Delgado and G.F. Giudice, *The well-tempered neutralino*, *Nucl. Phys.* **B 741** (2006) 108 [`hep-ph/0601041`] [INSPIRE].

[106] W. Beenakker, R. Hopker, M. Spira and P.M. Zerwas, *Squark and gluino production at hadron colliders*, *Nucl. Phys.* **B 492** (1997) 51 [`hep-ph/9610490`] [INSPIRE].

[107] W. Beenakker, M. Krämer, T. Plehn, M. Spira and P.M. Zerwas, *Stop production at hadron colliders*, *Nucl. Phys.* **B 515** (1998) 3 [`hep-ph/9710451`] [INSPIRE].

[108] W. Beenakker, M. Klasen, M. Krämer, T. Plehn, M. Spira and P.M. Zerwas, *The production of charginos/neutralinos and sleptons at hadron colliders*, *Phys. Rev. Lett.* **83** (1999) 3780 [*Erratum ibid.* **100** (2008) 029901] [`hep-ph/9906298`] [INSPIRE].

[109] M. Spira, *Higgs and SUSY particle production at hadron colliders*, `hep-ph/0211145` [INSPIRE].

[110] T. Plehn, *Measuring the MSSM Lagrangean*, *Czech. J. Phys.* **55** (2005) B213 [hep-ph/0410063] [INSPIRE].

[111] J. Alwall, M. Herquet, F. Maltoni, O. Mattelaer and T. Stelzer, *MadGraph 5: going beyond*, *JHEP* **06** (2011) 128 [arXiv:1106.0522] [INSPIRE].

[112] J. Pumplin, D.R. Stump, J. Huston, H.L. Lai, P.M. Nadolsky and W.K. Tung, *New generation of parton distributions with uncertainties from global QCD analysis*, *JHEP* **07** (2002) 012 [hep-ph/0201195] [INSPIRE].

[113] T. Sjöstrand, S. Mrenna and P.Z. Skands, *PYTHIA 6.4 physics and manual*, *JHEP* **05** (2006) 026 [hep-ph/0603175] [INSPIRE].

[114] ATLAS collaboration, *ATLAS tunes of PYTHIA 6 and PYTHIA 8 for MC11*, ATL-PHYS-PUB-2011-009, CERN, Geneva Switzerland (2011).

[115] M.L. Mangano, M. Moretti, F. Piccinini and M. Treccani, *Matching matrix elements and shower evolution for top-quark production in hadronic collisions*, *JHEP* **01** (2007) 013 [hep-ph/0611129] [INSPIRE].

[116] S. Jadach, Z. Was, R. Decker and J.H. Kuhn, *The τ decay library TAUOLA: version* 2.4, *Comput. Phys. Commun.* **76** (1993) 361 [INSPIRE].

[117] P. Golonka and Z. Was, *PHOTOS Monte Carlo: a precision tool for QED corrections in Z and W decays*, *Eur. Phys. J.* **C 45** (2006) 97 [hep-ph/0506026] [INSPIRE].

[118] GEANT4 collaboration, S. Agostinelli et al., *GEANT4: a simulation toolkit*, *Nucl. Instrum. Meth.* **A 506** (2003) 250 [INSPIRE].

[119] ATLAS collaboration, *The ATLAS simulation infrastructure*, *Eur. Phys. J.* **C 70** (2010) 823 [arXiv:1005.4568] [INSPIRE].

[120] M. Krämer et al., *Supersymmetry production cross sections in pp collisions at $\sqrt{s} = 7\ TeV$*, arXiv:1206.2892 [INSPIRE].

[121] A. Kulesza and L. Motyka, *Threshold resummation for squark-antisquark and gluino-pair production at the LHC*, *Phys. Rev. Lett.* **102** (2009) 111802 [arXiv:0807.2405] [INSPIRE].

[122] A. Kulesza and L. Motyka, *Soft gluon resummation for the production of gluino-gluino and squark-antisquark pairs at the LHC*, *Phys. Rev.* **D 80** (2009) 095004 [arXiv:0905.4749] [INSPIRE].

[123] W. Beenakker, S. Brensing, M. Krämer, A. Kulesza, E. Laenen and I. Niessen, *Soft-gluon resummation for squark and gluino hadroproduction*, *JHEP* **12** (2009) 041 [arXiv:0909.4418] [INSPIRE].

[124] W. Beenakker et al., *Squark and gluino hadroproduction*, *Int. J. Mod. Phys.* **A 26** (2011) 2637 [arXiv:1105.1110] [INSPIRE].

[125] M. Baak, G.J. Besjes, D. Côte, A. Koutsman, J. Lorenz and D. Short, *HistFitter software framework for statistical data analysis*, *Eur. Phys. J.* **C 75** (2015) 153 [arXiv:1410.1280] [INSPIRE].

[126] A.L. Read, *Presentation of search results: the CL_s technique*, *J. Phys.* **G 28** (2002) 2693 [INSPIRE].

[127] LHC HIGGS CROSS SECTION WORKING GROUP collaboration, S. Dittmaier et al., *Handbook of LHC Higgs cross sections: 1. Inclusive observables*, arXiv:1101.0593 [INSPIRE].

[128] LHC Higgs Cross section Working Group collaboration, S. Dittmaier et al., *Handbook of LHC Higgs cross sections: 2. Differential distributions*, `arXiv:1201.3084` [inSPIRE].

[129] LHC Higgs Cross section Working Group collaboration, J.R. Andersen et al., *Handbook of LHC Higgs cross sections: 3. Higgs properties*, `arXiv:1307.1347` [inSPIRE].

[130] R.V. Harlander, S. Liebler and H. Mantler, *SusHi: a program for the calculation of Higgs production in gluon fusion and bottom-quark annihilation in the Standard Model and the MSSM*, *Comput. Phys. Commun.* **184** (2013) 1605 [`arXiv:1212.3249`] [inSPIRE].

[131] R.V. Harlander and W.B. Kilgore, *Next-to-next-to-leading order Higgs production at hadron colliders*, *Phys. Rev. Lett.* **88** (2002) 201801 [`hep-ph/0201206`] [inSPIRE].

[132] R.V. Harlander and W.B. Kilgore, *Higgs boson production in bottom quark fusion at next-to-next-to leading order*, *Phys. Rev.* **D 68** (2003) 013001 [`hep-ph/0304035`] [inSPIRE].

[133] U. Aglietti, R. Bonciani, G. Degrassi and A. Vicini, *Two loop light fermion contribution to Higgs production and decays*, *Phys. Lett.* **B 595** (2004) 432 [`hep-ph/0404071`] [inSPIRE].

[134] R. Bonciani, G. Degrassi and A. Vicini, *On the generalized harmonic polylogarithms of one complex variable*, *Comput. Phys. Commun.* **182** (2011) 1253 [`arXiv:1007.1891`] [inSPIRE].

[135] G. Degrassi and P. Slavich, *NLO QCD bottom corrections to Higgs boson production in the MSSM*, *JHEP* **11** (2010) 044 [`arXiv:1007.3465`] [inSPIRE].

[136] G. Degrassi, S. Di Vita and P. Slavich, *NLO QCD corrections to pseudoscalar Higgs production in the MSSM*, *JHEP* **08** (2011) 128 [`arXiv:1107.0914`] [inSPIRE].

[137] G. Degrassi, S. Di Vita and P. Slavich, *On the NLO QCD corrections to the production of the heaviest neutral Higgs scalar in the MSSM*, *Eur. Phys. J.* **C 72** (2012) 2032 [`arXiv:1204.1016`] [inSPIRE].

[138] S. Heinemeyer, W. Hollik and G. Weiglein, *The masses of the neutral CP-even Higgs bosons in the MSSM: accurate analysis at the two loop level*, *Eur. Phys. J.* **C 9** (1999) 343 [`hep-ph/9812472`] [inSPIRE].

[139] G. Degrassi, S. Heinemeyer, W. Hollik, P. Slavich and G. Weiglein, *Towards high precision predictions for the MSSM Higgs sector*, *Eur. Phys. J.* **C 28** (2003) 133 [`hep-ph/0212020`] [inSPIRE].

[140] M. Frank, T. Hahn, S. Heinemeyer, W. Hollik, H. Rzehak and G. Weiglein, *The Higgs boson masses and mixings of the complex MSSM in the Feynman-diagrammatic approach*, *JHEP* **02** (2007) 047 [`hep-ph/0611326`] [inSPIRE].

[141] R. Harlander and P. Kant, *Higgs production and decay: analytic results at next-to-leading order QCD*, *JHEP* **12** (2005) 015 [`hep-ph/0509189`] [inSPIRE].

[142] ATLAS collaboration, *Summary of the ATLAS experiment's sensitivity to supersymmetry after LHC Run1 — interpreted in the phenomenological MSSM*, https://atlas.web.cern.ch/Atlas/GROUPS/PHYSICS/PAPERS/SUSY-2014-08/, (2015).

[143] ATLAS collaboration, *Measurements of Higgs boson production and couplings in diboson final states with the ATLAS detector at the LHC*, *Phys. Lett.* **B 726** (2013) 88 [*Erratum ibid.* **B 734** (2014) 406] [`arXiv:1307.1427`] [inSPIRE].

[144] ATLAS collaboration, *Measurements of the Higgs boson production and decay rates and coupling strengths using pp collision data at $\sqrt{s} = 7$ and 8 TeV in the ATLAS experiment,* `arXiv:1507.04548` [INSPIRE].

[145] ATLAS collaboration, *Constraints on new phenomena via Higgs boson couplings and invisible decays with the ATLAS detector,* `arXiv:1509.00672` [INSPIRE].

[146] R. Barbieri and G.F. Giudice, *Upper bounds on supersymmetric particle masses,* *Nucl. Phys.* **B 306** (1988) 63 [INSPIRE].

[147] B.C. Allanach, *SOFTSUSY: a program for calculating supersymmetric spectra,* *Comput. Phys. Commun.* **143** (2002) 305 [`hep-ph/0104145`] [INSPIRE].

[148] A. Djouadi, M.M. Muhlleitner and M. Spira, *Decays of supersymmetric particles: the program SUSY-HIT (SUspect-SdecaY-HDECAY-InTerface),* *Acta Phys. Polon.* **B 38** (2007) 635 [`hep-ph/0609292`] [INSPIRE].

[149] A. Djouadi, J. Kalinowski and M. Spira, *HDECAY: a program for Higgs boson decays in the Standard Model and its supersymmetric extension,* *Comput. Phys. Commun.* **108** (1998) 56 [`hep-ph/9704448`] [INSPIRE].

[150] J. Alwall et al., *The automated computation of tree-level and next-to-leading order differential cross sections and their matching to parton shower simulations,* *JHEP* **07** (2014) 079 [`arXiv:1405.0301`] [INSPIRE].

[151] C.H. Chen, M. Drees and J.F. Gunion, *Addendum/erratum for 'searching for invisible and almost invisible particles at e^+e^- colliders' [hep-ph/9512230] and 'a nonstandard string/SUSY scenario and its phenomenological implications' [hep-ph/9607421],* `hep-ph/9902309` [INSPIRE].

[152] D. Chowdhury, R.M. Godbole, K.A. Mohan and S.K. Vempati, *Charge and color breaking constraints in MSSM after the Higgs discovery at LHC,* *JHEP* **02** (2014) 110 [`arXiv:1310.1932`] [INSPIRE].

[153] M. Cirelli, N. Fornengo and A. Strumia, *Minimal dark matter,* *Nucl. Phys.* **B 753** (2006) 178 [`hep-ph/0512090`] [INSPIRE].

[154] M. Cirelli, A. Strumia and M. Tamburini, *Cosmology and astrophysics of minimal dark matter,* *Nucl. Phys.* **B 787** (2007) 152 [`arXiv:0706.4071`] [INSPIRE].

[155] J. Hisano, S. Matsumoto, M. Nagai, O. Saito and M. Senami, *Non-perturbative effect on thermal relic abundance of dark matter,* *Phys. Lett.* **B 646** (2007) 34 [`hep-ph/0610249`] [INSPIRE].

[156] J.L. Feng, K.T. Matchev and F. Wilczek, *Neutralino dark matter in focus point supersymmetry,* *Phys. Lett.* **B 482** (2000) 388 [`hep-ph/0004043`] [INSPIRE].

[157] J. Edsjo, M. Schelke, P. Ullio and P. Gondolo, *Accurate relic densities with neutralino, chargino and sfermion coannihilations in mSUGRA,* *JCAP* **04** (2003) 001 [`hep-ph/0301106`] [INSPIRE].

The ATLAS collaboration

G. Aad[85], B. Abbott[113], J. Abdallah[151], O. Abdinov[11], R. Aben[107], M. Abolins[90],
O.S. AbouZeid[158], H. Abramowicz[153], H. Abreu[152], R. Abreu[116], Y. Abulaiti[146a,146b],
B.S. Acharya[164a,164b,a], L. Adamczyk[38a], D.L. Adams[25], J. Adelman[108], S. Adomeit[100],
T. Adye[131], A.A. Affolder[74], T. Agatonovic-Jovin[13], J. Agricola[54], J.A. Aguilar-Saavedra[126a,126f],
S.P. Ahlen[22], F. Ahmadov[65,b], G. Aielli[133a,133b], H. Akerstedt[146a,146b], T.P.A. Åkesson[81],
A.V. Akimov[96], G.L. Alberghi[20a,20b], J. Albert[169], S. Albrand[55], M.J. Alconada Verzini[71],
M. Aleksa[30], I.N. Aleksandrov[65], C. Alexa[26b], G. Alexander[153], T. Alexopoulos[10], M. Alhroob[113],
G. Alimonti[91a], L. Alio[85], J. Alison[31], S.P. Alkire[35], B.M.M. Allbrooke[149], P.P. Allport[18],
A. Aloisio[104a,104b], A. Alonso[36], F. Alonso[71], C. Alpigiani[138], A. Altheimer[35],
B. Alvarez Gonzalez[30], D. Álvarez Piqueras[167], M.G. Alviggi[104a,104b], B.T. Amadio[15],
K. Amako[66], Y. Amaral Coutinho[24a], C. Amelung[23], D. Amidei[89], S.P. Amor Dos Santos[126a,126c],
A. Amorim[126a,126b], S. Amoroso[48], N. Amram[153], G. Amundsen[23], C. Anastopoulos[139],
L.S. Ancu[49], N. Andari[108], T. Andeen[35], C.F. Anders[58b], G. Anders[30], J.K. Anders[74],
K.J. Anderson[31], A. Andreazza[91a,91b], V. Andrei[58a], S. Angelidakis[9], I. Angelozzi[107], P. Anger[44],
A. Angerami[35], F. Anghinolfi[30], A.V. Anisenkov[109,c], N. Anjos[12], A. Annovi[124a,124b],
M. Antonelli[47], A. Antonov[98], J. Antos[144b], F. Anulli[132a], M. Aoki[66], L. Aperio Bella[18],
G. Arabidze[90], Y. Arai[66], J.P. Araque[126a], A.T.H. Arce[45], F.A. Arduh[71], J-F. Arguin[95],
S. Argyropoulos[63], M. Arik[19a], A.J. Armbruster[30], O. Arnaez[30], H. Arnold[48], M. Arratia[28],
O. Arslan[21], A. Artamonov[97], G. Artoni[23], S. Asai[155], N. Asbah[42], A. Ashkenazi[153],
B. Åsman[146a,146b], L. Asquith[149], K. Assamagan[25], R. Astalos[144a], M. Atkinson[165], N.B. Atlay[141],
K. Augsten[128], M. Aurousseau[145b], G. Avolio[30], B. Axen[15], M.K. Ayoub[117], G. Azuelos[95,d],
M.A. Baak[30], A.E. Baas[58a], M.J. Baca[18], C. Bacci[134a,134b], H. Bachacou[136], K. Bachas[154],
M. Backes[30], M. Backhaus[30], P. Bagiacchi[132a,132b], P. Bagnaia[132a,132b], Y. Bai[33a], T. Bain[35],
J.T. Baines[131], O.K. Baker[176], E.M. Baldin[109,c], P. Balek[129], T. Balestri[148], F. Balli[84],
W.K. Balunas[122], E. Banas[39], Sw. Banerjee[173], A.A.E. Bannoura[175], L. Barak[30], E.L. Barberio[88],
D. Barberis[50a,50b], M. Barbero[85], T. Barillari[101], M. Barisonzi[164a,164b], T. Barklow[143],
N. Barlow[28], S.L. Barnes[84], B.M. Barnett[131], R.M. Barnett[15], Z. Barnovska[5], A. Baroncelli[134a],
G. Barone[23], A.J. Barr[120], F. Barreiro[82], J. Barreiro Guimarães da Costa[57], R. Bartoldus[143],
A.E. Barton[72], P. Bartos[144a], A. Basalaev[123], A. Bassalat[117], A. Basye[165], R.L. Bates[53],
S.J. Batista[158], J.R. Batley[28], M. Battaglia[137], M. Bauce[132a,132b], F. Bauer[136], H.S. Bawa[143,e],
J.B. Beacham[111], M.D. Beattie[72], T. Beau[80], P.H. Beauchemin[161], R. Beccherle[124a,124b],
P. Bechtle[21], H.P. Beck[17,f], K. Becker[120], M. Becker[83], M. Beckingham[170], C. Becot[117],
A.J. Beddall[19b], A. Beddall[19b], V.A. Bednyakov[65], C.P. Bee[148], L.J. Beemster[107],
T.A. Beermann[30], M. Begel[25], J.K. Behr[120], C. Belanger-Champagne[87], W.H. Bell[49], G. Bella[153],
L. Bellagamba[20a], A. Bellerive[29], M. Bellomo[86], K. Belotskiy[98], O. Beltramello[30], O. Benary[153],
D. Benchekroun[135a], M. Bender[100], K. Bendtz[146a,146b], N. Benekos[10], Y. Benhammou[153],
E. Benhar Noccioli[49], J.A. Benitez Garcia[159b], D.P. Benjamin[45], J.R. Bensinger[23],
S. Bentvelsen[107], L. Beresford[120], M. Beretta[47], D. Berge[107], E. Bergeaas Kuutmann[166],
N. Berger[5], F. Berghaus[169], J. Beringer[15], C. Bernard[22], N.R. Bernard[86], C. Bernius[110],
F.U. Bernlochner[21], T. Berry[77], P. Berta[129], C. Bertella[83], G. Bertoli[146a,146b],
F. Bertolucci[124a,124b], C. Bertsche[113], D. Bertsche[113], M.I. Besana[91a], G.J. Besjes[36],
O. Bessidskaia Bylund[146a,146b], M. Bessner[42], N. Besson[136], C. Betancourt[48], S. Bethke[101],
A.J. Bevan[76], W. Bhimji[15], R.M. Bianchi[125], L. Bianchini[23], M. Bianco[30], O. Biebel[100],
D. Biedermann[16], S.P. Bieniek[78], N.V. Biesuz[124a,124b], M. Biglietti[134a],
J. Bilbao De Mendizabal[49], H. Bilokon[47], M. Bindi[54], S. Binet[117], A. Bingul[19b], C. Bini[132a,132b],
S. Biondi[20a,20b], D.M. Bjergaard[45], C.W. Black[150], J.E. Black[143], K.M. Black[22], D. Blackburn[138],

R.E. Blair[6], J.-B. Blanchard[136], J.E. Blanco[77], T. Blazek[144a], I. Bloch[42], C. Blocker[23],
W. Blum[83,*], U. Blumenschein[54], S. Blunier[32a], G.J. Bobbink[107], V.S. Bobrovnikov[109,c],
S.S. Bocchetta[81], A. Bocci[45], C. Bock[100], M. Boehler[48], J.A. Bogaerts[30], D. Bogavac[13],
A.G. Bogdanchikov[109], C. Bohm[146a], V. Boisvert[77], T. Bold[38a], V. Boldea[26b], A.S. Boldyrev[99],
M. Bomben[80], M. Bona[76], M. Boonekamp[136], A. Borisov[130], G. Borissov[72], S. Borroni[42],
J. Bortfeldt[100], V. Bortolotto[60a,60b,60c], K. Bos[107], D. Boscherini[20a], M. Bosman[12],
J. Boudreau[125], J. Bouffard[2], E.V. Bouhova-Thacker[72], D. Boumediene[34], C. Bourdarios[117],
N. Bousson[114], S.K. Boutle[53], A. Boveia[30], J. Boyd[30], I.R. Boyko[65], I. Bozic[13], J. Bracinik[18],
A. Brandt[8], G. Brandt[54], O. Brandt[58a], U. Bratzler[156], B. Brau[86], J.E. Brau[116], H.M. Braun[175,*],
W.D. Breaden Madden[53], K. Brendlinger[122], A.J. Brennan[88], L. Brenner[107], R. Brenner[166],
S. Bressler[172], K. Bristow[145c], T.M. Bristow[46], D. Britton[53], D. Britzger[42], F.M. Brochu[28],
I. Brock[21], R. Brock[90], J. Bronner[101], G. Brooijmans[35], T. Brooks[77], W.K. Brooks[32b],
J. Brosamer[15], E. Brost[116], P.A. Bruckman de Renstrom[39], D. Bruncko[144b], R. Bruneliere[48],
A. Bruni[20a], G. Bruni[20a], M. Bruschi[20a], N. Bruscino[21], L. Bryngemark[81], T. Buanes[14],
Q. Buat[142], P. Buchholz[141], A.G. Buckley[53], S.I. Buda[26b], I.A. Budagov[65], F. Buehrer[48],
L. Bugge[119], M.K. Bugge[119], O. Bulekov[98], D. Bullock[8], H. Burckhart[30], S. Burdin[74],
C.D. Burgard[48], B. Burghgrave[108], S. Burke[131], I. Burmeister[43], E. Busato[34], D. Büscher[48],
V. Büscher[83], P. Bussey[53], J.M. Butler[22], A.I. Butt[3], C.M. Buttar[53], J.M. Butterworth[78],
P. Butti[107], W. Buttinger[25], A. Buzatu[53], A.R. Buzykaev[109,c], S. Cabrera Urbán[167],
D. Caforio[128], V.M. Cairo[37a,37b], O. Cakir[4a], N. Calace[49], P. Calafiura[15], A. Calandri[136],
G. Calderini[80], P. Calfayan[100], L.P. Caloba[24a], D. Calvet[34], S. Calvet[34], R. Camacho Toro[31],
S. Camarda[42], P. Camarri[133a,133b], D. Cameron[119], R. Caminal Armadans[165], S. Campana[30],
M. Campanelli[78], A. Campoverde[148], V. Canale[104a,104b], A. Canepa[159a], M. Cano Bret[33e],
J. Cantero[82], R. Cantrill[126a], T. Cao[40], M.D.M. Capeans Garrido[30], I. Caprini[26b], M. Caprini[26b],
M. Capua[37a,37b], R. Caputo[83], R.M. Carbone[35], R. Cardarelli[133a], F. Cardillo[48], T. Carli[30],
G. Carlino[104a], L. Carminati[91a,91b], S. Caron[106], E. Carquin[32a], G.D. Carrillo-Montoya[30],
J.R. Carter[28], J. Carvalho[126a,126c], D. Casadei[78], M.P. Casado[12], M. Casolino[12],
E. Castaneda-Miranda[145a], A. Castelli[107], V. Castillo Gimenez[167], N.F. Castro[126a,g],
P. Catastini[57], A. Catinaccio[30], J.R. Catmore[119], A. Cattai[30], J. Caudron[83], V. Cavaliere[165],
D. Cavalli[91a], M. Cavalli-Sforza[12], V. Cavasinni[124a,124b], F. Ceradini[134a,134b], B.C. Cerio[45],
K. Cerny[129], A.S. Cerqueira[24b], A. Cerri[149], L. Cerrito[76], F. Cerutti[15], M. Cerv[30], A. Cervelli[17],
S.A. Cetin[19c], A. Chafaq[135a], D. Chakraborty[108], I. Chalupkova[129], P. Chang[165],
J.D. Chapman[28], D.G. Charlton[18], C.C. Chau[158], C.A. Chavez Barajas[149], S. Cheatham[152],
A. Chegwidden[90], S. Chekanov[6], S.V. Chekulaev[159a], G.A. Chelkov[65,h], M.A. Chelstowska[89],
C. Chen[64], H. Chen[25], K. Chen[148], L. Chen[33d,i], S. Chen[33c], S. Chen[155], X. Chen[33f], Y. Chen[67],
H.C. Cheng[89], Y. Cheng[31], A. Cheplakov[65], E. Cheremushkina[130], R. Cherkaoui El Moursli[135e],
V. Chernyatin[25,*], E. Cheu[7], L. Chevalier[136], V. Chiarella[47], G. Chiarelli[124a,124b], G. Chiodini[73a],
A.S. Chisholm[18], R.T. Chislett[78], A. Chitan[26b], M.V. Chizhov[65], K. Choi[61], S. Chouridou[9],
B.K.B. Chow[100], V. Christodoulou[78], D. Chromek-Burckhart[30], J. Chudoba[127], A.J. Chuinard[87],
J.J. Chwastowski[39], L. Chytka[115], G. Ciapetti[132a,132b], A.K. Ciftci[4a], D. Cinca[53], V. Cindro[75],
I.A. Cioara[21], A. Ciocio[15], F. Cirotto[104a,104b], Z.H. Citron[172], M. Ciubancan[26b], A. Clark[49],
B.L. Clark[57], P.J. Clark[46], R.N. Clarke[15], C. Clement[146a,146b], Y. Coadou[85], M. Cobal[164a,164c],
A. Coccaro[49], J. Cochran[64], L. Coffey[23], J.G. Cogan[143], L. Colasurdo[106], B. Cole[35], S. Cole[108],
A.P. Colijn[107], J. Collot[55], T. Colombo[58c], G. Compostella[101], P. Conde Muiño[126a,126b],
E. Coniavitis[48], S.H. Connell[145b], I.A. Connelly[77], V. Consorti[48], S. Constantinescu[26b],
C. Conta[121a,121b], G. Conti[30], F. Conventi[104a,j], M. Cooke[15], B.D. Cooper[78],
A.M. Cooper-Sarkar[120], T. Cornelissen[175], M. Corradi[20a], F. Corriveau[87,k], A. Corso-Radu[163],
A. Cortes-Gonzalez[12], G. Cortiana[101], G. Costa[91a], M.J. Costa[167], D. Costanzo[139], D. Côté[8],

G. Cottin[28], G. Cowan[77], B.E. Cox[84], K. Cranmer[110], G. Cree[29], S. Crépé-Renaudin[55],
F. Crescioli[80], W.A. Cribbs[146a,146b], M. Crispin Ortuzar[120], M. Cristinziani[21], V. Croft[106],
G. Crosetti[37a,37b], T. Cuhadar Donszelmann[139], J. Cummings[176], M. Curatolo[47], J. Cúth[83],
C. Cuthbert[150], H. Czirr[141], P. Czodrowski[3], S. D'Auria[53], M. D'Onofrio[74],
M.J. Da Cunha Sargedas De Sousa[126a,126b], C. Da Via[84], W. Dabrowski[38a], A. Dafinca[120],
T. Dai[89], O. Dale[14], F. Dallaire[95], C. Dallapiccola[86], M. Dam[36], J.R. Dandoy[31], N.P. Dang[48],
A.C. Daniells[18], M. Danninger[168], M. Dano Hoffmann[136], V. Dao[48], G. Darbo[50a], S. Darmora[8],
J. Dassoulas[3], A. Dattagupta[61], W. Davey[21], C. David[169], T. Davidek[129], E. Davies[120,l],
M. Davies[153], P. Davison[78], Y. Davygora[58a], E. Dawe[88], I. Dawson[139],
R.K. Daya-Ishmukhametova[86], K. De[8], R. de Asmundis[104a], A. De Benedetti[113],
S. De Castro[20a,20b], S. De Cecco[80], N. De Groot[106], P. de Jong[107], H. De la Torre[82],
F. De Lorenzi[64], D. De Pedis[132a], A. De Salvo[132a], U. De Sanctis[149], A. De Santo[149],
J.B. De Vivie De Regie[117], W.J. Dearnaley[72], R. Debbe[25], C. Debenedetti[137], D.V. Dedovich[65],
I. Deigaard[107], J. Del Peso[82], T. Del Prete[124a,124b], D. Delgove[117], F. Deliot[136], C.M. Delitzsch[49],
M. Deliyergiyev[75], A. Dell'Acqua[30], L. Dell'Asta[22], M. Dell'Orso[124a,124b], M. Della Pietra[104a,j],
D. della Volpe[49], M. Delmastro[5], P.A. Delsart[55], C. Deluca[107], D.A. DeMarco[158], S. Demers[176],
M. Demichev[65], A. Demilly[80], S.P. Denisov[130], D. Derendarz[39], J.E. Derkaoui[135d], F. Derue[80],
P. Dervan[74], K. Desch[21], C. Deterre[42], P.O. Deviveiros[30], A. Dewhurst[131], S. Dhaliwal[23],
A. Di Ciaccio[133a,133b], L. Di Ciaccio[5], A. Di Domenico[132a,132b], C. Di Donato[104a,104b],
A. Di Girolamo[30], B. Di Girolamo[30], A. Di Mattia[152], B. Di Micco[134a,134b], R. Di Nardo[47],
A. Di Simone[48], R. Di Sipio[158], D. Di Valentino[29], C. Diaconu[85], M. Diamond[158], F.A. Dias[46],
M.A. Diaz[32a], E.B. Diehl[89], J. Dietrich[16], S. Diglio[85], A. Dimitrievska[13], J. Dingfelder[21],
P. Dita[26b], S. Dita[26b], F. Dittus[30], F. Djama[85], T. Djobava[51b], J.I. Djuvsland[58a],
M.A.B. do Vale[24c], D. Dobos[30], M. Dobre[26b], C. Doglioni[81], T. Dohmae[155], J. Dolejsi[129],
Z. Dolezal[129], B.A. Dolgoshein[98,*], M. Donadelli[24d], S. Donati[124a,124b], P. Dondero[121a,121b],
J. Donini[34], J. Dopke[131], A. Doria[104a], M.T. Dova[71], A.T. Doyle[53], E. Drechsler[54], M. Dris[10],
E. Dubreuil[34], E. Duchovni[172], G. Duckeck[100], O.A. Ducu[26b,85], D. Duda[107], A. Dudarev[30],
L. Duflot[117], L. Duguid[77], M. Dührssen[30], M. Dunford[58a], H. Duran Yildiz[4a], M. Düren[52],
A. Durglishvili[51b], D. Duschinger[44], B. Dutta[42], M. Dyndal[38a], C. Eckardt[42], K.M. Ecker[101],
R.C. Edgar[89], W. Edson[2], N.C. Edwards[46], W. Ehrenfeld[21], T. Eifert[30], G. Eigen[14],
K. Einsweiler[15], T. Ekelof[166], M. El Kacimi[135c], M. Ellert[166], S. Elles[5], F. Ellinghaus[175],
A.A. Elliot[169], N. Ellis[30], J. Elmsheuser[100], M. Elsing[30], D. Emeliyanov[131], Y. Enari[155],
O.C. Endner[83], M. Endo[118], J. Erdmann[43], A. Ereditato[17], G. Ernis[175], J. Ernst[2], M. Ernst[25],
S. Errede[165], E. Ertel[83], M. Escalier[117], H. Esch[43], C. Escobar[125], B. Esposito[47], A.I. Etienvre[136],
E. Etzion[153], H. Evans[61], A. Ezhilov[123], L. Fabbri[20a,20b], G. Facini[31], R.M. Fakhrutdinov[130],
S. Falciano[132a], R.J. Falla[78], J. Faltova[129], Y. Fang[33a], M. Fanti[91a,91b], A. Farbin[8], A. Farilla[134a],
T. Farooque[12], S. Farrell[15], S.M. Farrington[170], P. Farthouat[30], F. Fassi[135e], P. Fassnacht[30],
D. Fassouliotis[9], M. Faucci Giannelli[77], A. Favareto[50a,50b], W.J. Fawcett[120], L. Fayard[117],
O.L. Fedin[123,m], W. Fedorko[168], S. Feigl[30], L. Feligioni[85], C. Feng[33d], E.J. Feng[30], H. Feng[89],
A.B. Fenyuk[130], L. Feremenga[8], P. Fernandez Martinez[167], S. Fernandez Perez[30], J. Ferrando[53],
A. Ferrari[166], P. Ferrari[107], R. Ferrari[121a], D.E. Ferreira de Lima[53], A. Ferrer[167], D. Ferrere[49],
C. Ferretti[89], A. Ferretto Parodi[50a,50b], M. Fiascaris[31], F. Fiedler[83], A. Filipčič[75], M. Filipuzzi[42],
F. Filthaut[106], M. Fincke-Keeler[169], K.D. Finelli[150], M.C.N. Fiolhais[126a,126c], L. Fiorini[167],
A. Firan[40], A. Fischer[2], C. Fischer[12], J. Fischer[175], W.C. Fisher[90], N. Flaschel[42], I. Fleck[141],
P. Fleischmann[89], G.T. Fletcher[139], G. Fletcher[76], R.R.M. Fletcher[122], T. Flick[175], A. Floderus[81],
L.R. Flores Castillo[60a], M.J. Flowerdew[101], A. Formica[136], A. Forti[84], D. Fournier[117], H. Fox[72],
S. Fracchia[12], P. Francavilla[80], M. Franchini[20a,20b], D. Francis[30], L. Franconi[119], M. Franklin[57],
M. Frate[163], M. Fraternali[121a,121b], D. Freeborn[78], S.T. French[28], F. Friedrich[44], D. Froidevaux[30],

J.A. Frost[120], C. Fukunaga[156], E. Fullana Torregrosa[83], B.G. Fulsom[143], T. Fusayasu[102],
J. Fuster[167], C. Gabaldon[55], O. Gabizon[175], A. Gabrielli[20a,20b], A. Gabrielli[15], G.P. Gach[18],
S. Gadatsch[30], S. Gadomski[49], G. Gagliardi[50a,50b], P. Gagnon[61], C. Galea[106],
B. Galhardo[126a,126c], E.J. Gallas[120], B.J. Gallop[131], P. Gallus[128], G. Galster[36], K.K. Gan[111],
J. Gao[33b,85], Y. Gao[46], Y.S. Gao[143,e], F.M. Garay Walls[46], F. Garberson[176], C. García[167],
J.E. García Navarro[167], M. Garcia-Sciveres[15], R.W. Gardner[31], N. Garelli[143], V. Garonne[119],
C. Gatti[47], A. Gaudiello[50a,50b], G. Gaudio[121a], B. Gaur[141], L. Gauthier[95], P. Gauzzi[132a,132b],
I.L. Gavrilenko[96], C. Gay[168], G. Gaycken[21], E.N. Gazis[10], P. Ge[33d], Z. Gecse[168], C.N.P. Gee[131],
Ch. Geich-Gimbel[21], M.P. Geisler[58a], C. Gemme[50a], M.H. Genest[55], S. Gentile[132a,132b],
M. George[54], S. George[77], D. Gerbaudo[163], A. Gershon[153], S. Ghasemi[141], H. Ghazlane[135b],
B. Giacobbe[20a], S. Giagu[132a,132b], V. Giangiobbe[12], P. Giannetti[124a,124b], B. Gibbard[25],
S.M. Gibson[77], M. Gignac[168], M. Gilchriese[15], T.P.S. Gillam[28], D. Gillberg[30], G. Gilles[34],
D.M. Gingrich[3,d], N. Giokaris[9], M.P. Giordani[164a,164c], F.M. Giorgi[20a], F.M. Giorgi[16],
P.F. Giraud[136], P. Giromini[47], D. Giugni[91a], C. Giuliani[48], M. Giulini[58b], B.K. Gjelsten[119],
S. Gkaitatzis[154], I. Gkialas[154], E.L. Gkougkousis[117], L.K. Gladilin[99], C. Glasman[82], J. Glatzer[30],
P.C.F. Glaysher[46], A. Glazov[42], M. Goblirsch-Kolb[101], J.R. Goddard[76], J. Godlewski[39],
S. Goldfarb[89], T. Golling[49], D. Golubkov[130], A. Gomes[126a,126b,126d], R. Gonçalo[126a],
J. Goncalves Pinto Firmino Da Costa[136], L. Gonella[21], S. González de la Hoz[167],
G. Gonzalez Parra[12], S. Gonzalez-Sevilla[49], L. Goossens[30], P.A. Gorbounov[97], H.A. Gordon[25],
I. Gorelov[105], B. Gorini[30], E. Gorini[73a,73b], A. Gorišek[75], E. Gornicki[39], A.T. Goshaw[45],
C. Gössling[43], M.I. Gostkin[65], D. Goujdami[135c], A.G. Goussiou[138], N. Govender[145b], E. Gozani[152],
H.M.X. Grabas[137], L. Graber[54], I. Grabowska-Bold[38a], P.O.J. Gradin[166], P. Grafström[20a,20b],
K-J. Grahn[42], J. Gramling[49], E. Gramstad[119], S. Grancagnolo[16], V. Gratchev[123], H.M. Gray[30],
E. Graziani[134a], Z.D. Greenwood[79,n], C. Grefe[21], K. Gregersen[78], I.M. Gregor[42], P. Grenier[143],
J. Griffiths[8], A.A. Grillo[137], K. Grimm[72], S. Grinstein[12,o], Ph. Gris[34], J.-F. Grivaz[117],
J.P. Grohs[44], A. Grohsjean[42], E. Gross[172], J. Grosse-Knetter[54], G.C. Grossi[79], Z.J. Grout[149],
L. Guan[89], J. Guenther[128], F. Guescini[49], D. Guest[176], O. Gueta[153], E. Guido[50a,50b],
T. Guillemin[117], S. Guindon[2], U. Gul[53], C. Gumpert[44], J. Guo[33e], Y. Guo[33b,p], S. Gupta[120],
G. Gustavino[132a,132b], P. Gutierrez[113], N.G. Gutierrez Ortiz[78], C. Gutschow[44], C. Guyot[136],
C. Gwenlan[120], C.B. Gwilliam[74], A. Haas[110], C. Haber[15], H.K. Hadavand[8], N. Haddad[135e],
P. Haefner[21], S. Hageböck[21], Z. Hajduk[39], H. Hakobyan[177], M. Haleem[42], J. Haley[114], D. Hall[120],
G. Halladjian[90], G.D. Hallewell[85], K. Hamacher[175], P. Hamal[115], K. Hamano[169], A. Hamilton[145a],
G.N. Hamity[139], P.G. Hamnett[42], L. Han[33b], K. Hanagaki[66,q], K. Hanawa[155], M. Hance[137],
B. Haney[122], P. Hanke[58a], R. Hanna[136], J.B. Hansen[36], J.D. Hansen[36], M.C. Hansen[21],
P.H. Hansen[36], K. Hara[160], A.S. Hard[173], T. Harenberg[175], F. Hariri[117], S. Harkusha[92],
R.D. Harrington[46], P.F. Harrison[170], F. Hartjes[107], M. Hasegawa[67], Y. Hasegawa[140], A. Hasib[113],
S. Hassani[136], S. Haug[17], R. Hauser[90], L. Hauswald[44], M. Havranek[127], C.M. Hawkes[18],
R.J. Hawkings[30], A.D. Hawkins[81], T. Hayashi[160], D. Hayden[90], C.P. Hays[120], J.M. Hays[76],
H.S. Hayward[74], S.J. Haywood[131], S.J. Head[18], T. Heck[83], V. Hedberg[81], L. Heelan[8], S. Heim[122],
T. Heim[175], B. Heinemann[15], L. Heinrich[110], J. Hejbal[127], L. Helary[22], S. Hellman[146a,146b],
D. Hellmich[21], C. Helsens[12], J. Henderson[120], R.C.W. Henderson[72], Y. Heng[173], C. Hengler[42],
S. Henkelmann[168], A. Henrichs[176], A.M. Henriques Correia[30], S. Henrot-Versille[117],
G.H. Herbert[16], Y. Hernández Jiménez[167], G. Herten[48], R. Hertenberger[100], L. Hervas[30],
G.G. Hesketh[78], N.P. Hessey[107], J.W. Hetherly[40], R. Hickling[76], E. Higón-Rodriguez[167],
E. Hill[169], J.C. Hill[28], K.H. Hiller[42], S.J. Hillier[18], I. Hinchliffe[15], E. Hines[122], R.R. Hinman[15],
M. Hirose[157], D. Hirschbuehl[175], J. Hobbs[148], N. Hod[107], M.C. Hodgkinson[139], P. Hodgson[139],
A. Hoecker[30], M.R. Hoeferkamp[105], F. Hoenig[100], M. Hohlfeld[83], D. Hohn[21], T.R. Holmes[15],
M. Homann[43], T.M. Hong[125], W.H. Hopkins[116], Y. Horii[103], A.J. Horton[142], J-Y. Hostachy[55],

S. Hou[151], A. Hoummada[135a], J. Howard[120], J. Howarth[42], M. Hrabovsky[115], I. Hristova[16],
J. Hrivnac[117], T. Hryn'ova[5], A. Hrynevich[93], C. Hsu[145c], P.J. Hsu[151,r], S.-C. Hsu[138], D. Hu[35],
Q. Hu[33b], X. Hu[89], Y. Huang[42], Z. Hubacek[128], F. Hubaut[85], F. Huegging[21], T.B. Huffman[120],
E.W. Hughes[35], G. Hughes[72], M. Huhtinen[30], T.A. Hülsing[83], N. Huseynov[65,b], J. Huston[90],
J. Huth[57], G. Iacobucci[49], G. Iakovidis[25], I. Ibragimov[141], L. Iconomidou-Fayard[117], E. Ideal[176],
Z. Idrissi[135e], P. Iengo[30], O. Igonkina[107], T. Iizawa[171], Y. Ikegami[66], K. Ikematsu[141], M. Ikeno[66],
Y. Ilchenko[31,s], D. Iliadis[154], N. Ilic[143], T. Ince[101], G. Introzzi[121a,121b], P. Ioannou[9], M. Iodice[134a],
K. Iordanidou[35], V. Ippolito[57], A. Irles Quiles[167], C. Isaksson[166], M. Ishino[68], M. Ishitsuka[157],
R. Ishmukhametov[111], C. Issever[120], S. Istin[19a], J.M. Iturbe Ponce[84], R. Iuppa[133a,133b],
J. Ivarsson[81], W. Iwanski[39], H. Iwasaki[66], J.M. Izen[41], V. Izzo[104a], S. Jabbar[3], B. Jackson[122],
M. Jackson[74], P. Jackson[1], M.R. Jaekel[30], V. Jain[2], K. Jakobs[48], S. Jakobsen[30], T. Jakoubek[127],
J. Jakubek[128], D.O. Jamin[114], D.K. Jana[79], E. Jansen[78], R. Jansky[62], J. Janssen[21], M. Janus[54],
G. Jarlskog[81], N. Javadov[65,b], T. Javůrek[48], L. Jeanty[15], J. Jejelava[51a,t], G.-Y. Jeng[150],
D. Jennens[88], P. Jenni[48,u], J. Jentzsch[43], C. Jeske[170], S. Jézéquel[5], H. Ji[173], J. Jia[148], Y. Jiang[33b],
S. Jiggins[78], J. Jimenez Pena[167], S. Jin[33a], A. Jinaru[26b], O. Jinnouchi[157], M.D. Joergensen[36],
P. Johansson[139], K.A. Johns[7], W.J. Johnson[138], K. Jon-And[146a,146b], G. Jones[170],
R.W.L. Jones[72], T.J. Jones[74], J. Jongmanns[58a], P.M. Jorge[126a,126b], K.D. Joshi[84],
J. Jovicevic[159a], X. Ju[173], P. Jussel[62], A. Juste Rozas[12,o], M. Kaci[167], A. Kaczmarska[39],
M. Kado[117], H. Kagan[111], M. Kagan[143], S.J. Kahn[85], E. Kajomovitz[45], C.W. Kalderon[120],
S. Kama[40], A. Kamenshchikov[130], N. Kanaya[155], S. Kaneti[28], V.A. Kantserov[98], J. Kanzaki[66],
B. Kaplan[110], L.S. Kaplan[173], A. Kapliy[31], D. Kar[145c], K. Karakostas[10], A. Karamaoun[3],
N. Karastathis[10,107], M.J. Kareem[54], E. Karentzos[10], M. Karnevskiy[83], S.N. Karpov[65],
Z.M. Karpova[65], K. Karthik[110], V. Kartvelishvili[72], A.N. Karyukhin[130], K. Kasahara[160],
L. Kashif[173], R.D. Kass[111], A. Kastanas[14], Y. Kataoka[155], C. Kato[155], A. Katre[49], J. Katzy[42],
K. Kawade[103], K. Kawagoe[70], T. Kawamoto[155], G. Kawamura[54], S. Kazama[155],
V.F. Kazanin[109,c], R. Keeler[169], R. Kehoe[40], J.S. Keller[42], J.J. Kempster[77], H. Keoshkerian[84],
O. Kepka[127], B.P. Kerševan[75], S. Kersten[175], R.A. Keyes[87], F. Khalil-zada[11],
H. Khandanyan[146a,146b], A. Khanov[114], A.G. Kharlamov[109,c], T.J. Khoo[28], V. Khovanskiy[97],
E. Khramov[65], J. Khubua[51b,v], S. Kido[67], H.Y. Kim[8], S.H. Kim[160], Y.K. Kim[31], N. Kimura[154],
O.M. Kind[16], B.T. King[74], M. King[167], S.B. King[168], J. Kirk[131], A.E. Kiryunin[101],
T. Kishimoto[67], D. Kisielewska[38a], F. Kiss[48], K. Kiuchi[160], O. Kivernyk[136], E. Kladiva[144b],
M.H. Klein[35], M. Klein[74], U. Klein[74], K. Kleinknecht[83], P. Klimek[146a,146b], A. Klimentov[25],
R. Klingenberg[43], J.A. Klinger[139], T. Klioutchnikova[30], E.-E. Kluge[58a], P. Kluit[107], S. Kluth[101],
J. Knapik[39], E. Kneringer[62], E.B.F.G. Knoops[85], A. Knue[53], A. Kobayashi[155], D. Kobayashi[157],
T. Kobayashi[155], M. Kobel[44], M. Kocian[143], P. Kodys[129], T. Koffas[29], E. Koffeman[107],
L.A. Kogan[120], S. Kohlmann[175], Z. Kohout[128], T. Kohriki[66], T. Koi[143], H. Kolanoski[16],
M. Kolb[58b], I. Koletsou[5], A.A. Komar[96,*], Y. Komori[155], T. Kondo[66], N. Kondrashova[42],
K. Köneke[48], A.C. König[106], T. Kono[66], R. Konoplich[110,w], N. Konstantinidis[78],
R. Kopeliansky[152], S. Koperny[38a], L. Köpke[83], A.K. Kopp[48], K. Korcyl[39], K. Kordas[154],
A. Korn[78], A.A. Korol[109,c], I. Korolkov[12], E.V. Korolkova[139], O. Kortner[101], S. Kortner[101],
T. Kosek[129], V.V. Kostyukhin[21], V.M. Kotov[65], A. Kotwal[45], A. Kourkoumeli-Charalampidi[154],
C. Kourkoumelis[9], V. Kouskoura[25], A. Koutsman[159a], R. Kowalewski[169], T.Z. Kowalski[38a],
W. Kozanecki[136], A.S. Kozhin[130], V.A. Kramarenko[99], G. Kramberger[75], D. Krasnopevtsev[98],
M.W. Krasny[80], A. Krasznahorkay[30], J.K. Kraus[21], A. Kravchenko[25], S. Kreiss[110], M. Kretz[58c],
J. Kretzschmar[74], K. Kreutzfeldt[52], P. Krieger[158], K. Krizka[31], K. Kroeninger[43], H. Kroha[101],
J. Kroll[122], J. Kroseberg[21], J. Krstic[13], U. Kruchonak[65], H. Krüger[21], N. Krumnack[64],
A. Kruse[173], M.C. Kruse[45], M. Kruskal[22], T. Kubota[88], H. Kucuk[78], S. Kuday[4b], S. Kuehn[48],
A. Kugel[58c], F. Kuger[174], A. Kuhl[137], T. Kuhl[42], V. Kukhtin[65], R. Kukla[136], Y. Kulchitsky[92],

S. Kuleshov[32b], M. Kuna[132a,132b], T. Kunigo[68], A. Kupco[127], H. Kurashige[67], Y.A. Kurochkin[92],
V. Kus[127], E.S. Kuwertz[169], M. Kuze[157], J. Kvita[115], T. Kwan[169], D. Kyriazopoulos[139],
A. La Rosa[137], J.L. La Rosa Navarro[24d], L. La Rotonda[37a,37b], C. Lacasta[167], F. Lacava[132a,132b],
J. Lacey[29], H. Lacker[16], D. Lacour[80], V.R. Lacuesta[167], E. Ladygin[65], R. Lafaye[5], B. Laforge[80],
T. Lagouri[176], S. Lai[54], L. Lambourne[78], S. Lammers[61], C.L. Lampen[7], W. Lampl[7], E. Lançon[136],
U. Landgraf[48], M.P.J. Landon[76], V.S. Lang[58a], J.C. Lange[12], A.J. Lankford[163], F. Lanni[25],
K. Lantzsch[21], A. Lanza[121a], S. Laplace[80], C. Lapoire[30], J.F. Laporte[136], T. Lari[91a],
F. Lasagni Manghi[20a,20b], M. Lassnig[30], P. Laurelli[47], W. Lavrijsen[15], A.T. Law[137], P. Laycock[74],
T. Lazovich[57], O. Le Dortz[80], E. Le Guirriec[85], E. Le Menedeu[12], M. LeBlanc[169], T. LeCompte[6],
F. Ledroit-Guillon[55], C.A. Lee[145a], S.C. Lee[151], L. Lee[1], G. Lefebvre[80], M. Lefebvre[169],
F. Legger[100], C. Leggett[15], A. Lehan[74], G. Lehmann Miotto[30], X. Lei[7], W.A. Leight[29],
A. Leisos[154,x], A.G. Leister[176], M.A.L. Leite[24d], R. Leitner[129], D. Lellouch[172], B. Lemmer[54],
K.J.C. Leney[78], T. Lenz[21], B. Lenzi[30], R. Leone[7], S. Leone[124a,124b], C. Leonidopoulos[46],
S. Leontsinis[10], C. Leroy[95], C.G. Lester[28], M. Levchenko[123], J. Levêque[5], D. Levin[89],
L.J. Levinson[172], M. Levy[18], A. Lewis[120], A.M. Leyko[21], M. Leyton[41], B. Li[33b,y], H. Li[148],
H.L. Li[31], L. Li[45], L. Li[33e], S. Li[45], X. Li[84], Y. Li[33c,z], Z. Liang[137], H. Liao[34], B. Liberti[133a],
A. Liblong[158], P. Lichard[30], K. Lie[165], J. Liebal[21], W. Liebig[14], C. Limbach[21], A. Limosani[150],
S.C. Lin[151,aa], T.H. Lin[83], F. Linde[107], B.E. Lindquist[148], J.T. Linnemann[90], E. Lipeles[122],
A. Lipniacka[14], M. Lisovyi[58b], T.M. Liss[165], D. Lissauer[25], A. Lister[168], A.M. Litke[137],
B. Liu[151,ab], D. Liu[151], H. Liu[89], J. Liu[85], J.B. Liu[33b], K. Liu[85], L. Liu[165], M. Liu[45], M. Liu[33b],
Y. Liu[33b], M. Livan[121a,121b], A. Lleres[55], J. Llorente Merino[82], S.L. Lloyd[76], F. Lo Sterzo[151],
E. Lobodzinska[42], P. Loch[7], W.S. Lockman[137], F.K. Loebinger[84], A.E. Loevschall-Jensen[36],
K.M. Loew[23], A. Loginov[176], T. Lohse[16], K. Lohwasser[42], M. Lokajicek[127], B.A. Long[22],
J.D. Long[165], R.E. Long[72], K.A. Looper[111], L. Lopes[126a], D. Lopez Mateos[57],
B. Lopez Paredes[139], I. Lopez Paz[12], J. Lorenz[100], N. Lorenzo Martinez[61], M. Losada[162],
P.J. Lösel[100], X. Lou[33a], A. Lounis[117], J. Love[6], P.A. Love[72], N. Lu[89], H.J. Lubatti[138],
C. Luci[132a,132b], A. Lucotte[55], C. Luedtke[48], F. Luehring[61], W. Lukas[62], L. Luminari[132a],
O. Lundberg[146a,146b], B. Lund-Jensen[147], D. Lynn[25], R. Lysak[127], E. Lytken[81], H. Ma[25],
L.L. Ma[33d], G. Maccarrone[47], A. Macchiolo[101], C.M. Macdonald[139], B. Maček[75],
J. Machado Miguens[122,126b], D. Macina[30], D. Madaffari[85], R. Madar[34], H.J. Maddocks[72],
W.F. Mader[44], A. Madsen[166], J. Maeda[67], S. Maeland[14], T. Maeno[25], A. Maevskiy[99],
E. Magradze[54], K. Mahboubi[48], J. Mahlstedt[107], C. Maiani[136], C. Maidantchik[24a], A.A. Maier[101],
T. Maier[100], A. Maio[126a,126b,126d], S. Majewski[116], Y. Makida[66], N. Makovec[117], B. Malaescu[80],
Pa. Malecki[39], V.P. Maleev[123], F. Malek[55], U. Mallik[63], D. Malon[6], C. Malone[143], S. Maltezos[10],
V.M. Malyshev[109], S. Malyukov[30], J. Mamuzic[42], G. Mancini[47], B. Mandelli[30], L. Mandelli[91a],
I. Mandić[75], R. Mandrysch[63], J. Maneira[126a,126b], A. Manfredini[101],
L. Manhaes de Andrade Filho[24b], J. Manjarres Ramos[159b], A. Mann[100],
A. Manousakis-Katsikakis[9], B. Mansoulie[136], R. Mantifel[87], M. Mantoani[54], L. Mapelli[30],
L. March[145c], G. Marchiori[80], M. Marcisovsky[127], C.P. Marino[169], M. Marjanovic[13],
D.E. Marley[89], F. Marroquim[24a], S.P. Marsden[84], Z. Marshall[15], L.F. Marti[17], S. Marti-Garcia[167],
B. Martin[90], T.A. Martin[170], V.J. Martin[46], B. Martin dit Latour[14], M. Martinez[12,o],
S. Martin-Haugh[131], V.S. Martoiu[26b], A.C. Martyniuk[78], M. Marx[138], F. Marzano[132a],
A. Marzin[30], L. Masetti[83], T. Mashimo[155], R. Mashinistov[96], J. Masik[84], A.L. Maslennikov[109,c],
I. Massa[20a,20b], L. Massa[20a,20b], P. Mastrandrea[5], A. Mastroberardino[37a,37b], T. Masubuchi[155],
P. Mättig[175], J. Mattmann[83], J. Maurer[26b], S.J. Maxfield[74], D.A. Maximov[109,c], R. Mazini[151],
S.M. Mazza[91a,91b], G. Mc Goldrick[158], S.P. Mc Kee[89], A. McCarn[89], R.L. McCarthy[148],
T.G. McCarthy[29], N.A. McCubbin[131], K.W. McFarlane[56,*], J.A. Mcfayden[78], G. Mchedlidze[54],
S.J. McMahon[131], R.A. McPherson[169,k], M. Medinnis[42], S. Meehan[145a], S. Mehlhase[100],

A. Mehta[74], K. Meier[58a], C. Meineck[100], B. Meirose[41], B.R. Mellado Garcia[145c], F. Meloni[17],
A. Mengarelli[20a,20b], S. Menke[101], E. Meoni[161], K.M. Mercurio[57], S. Mergelmeyer[21], P. Mermod[49],
L. Merola[104a,104b], C. Meroni[91a], F.S. Merritt[31], A. Messina[132a,132b], J. Metcalfe[25], A.S. Mete[163],
C. Meyer[83], C. Meyer[122], J-P. Meyer[136], J. Meyer[107], H. Meyer Zu Theenhausen[58a],
R.P. Middleton[131], S. Miglioranzi[164a,164c], L. Mijović[21], G. Mikenberg[172], M. Mikestikova[127],
M. Mikuž[75], M. Milesi[88], A. Milic[30], D.W. Miller[31], C. Mills[46], A. Milov[172],
D.A. Milstead[146a,146b], A.A. Minaenko[130], Y. Minami[155], I.A. Minashvili[65], A.I. Mincer[110],
B. Mindur[38a], M. Mineev[65], Y. Ming[173], L.M. Mir[12], K.P. Mistry[122], T. Mitani[171], J. Mitrevski[100],
V.A. Mitsou[167], A. Miucci[49], P.S. Miyagawa[139], J.U. Mjörnmark[81], T. Moa[146a,146b],
K. Mochizuki[85], S. Mohapatra[35], W. Mohr[48], S. Molander[146a,146b], R. Moles-Valls[21],
R. Monden[68], K. Mönig[42], C. Monini[55], J. Monk[36], E. Monnier[85], A. Montalbano[148],
J. Montejo Berlingen[12], F. Monticelli[71], S. Monzani[132a,132b], R.W. Moore[3], N. Morange[117],
D. Moreno[162], M. Moreno Llácer[54], P. Morettini[50a], D. Mori[142], T. Mori[155], M. Morii[57],
M. Morinaga[155], V. Morisbak[119], S. Moritz[83], A.K. Morley[150], G. Mornacchi[30], J.D. Morris[76],
S.S. Mortensen[36], A. Morton[53], L. Morvaj[103], M. Mosidze[51b], J. Moss[143], K. Motohashi[157],
R. Mount[143], E. Mountricha[25], S.V. Mouraviev[96,*], E.J.W. Moyse[86], S. Muanza[85], R.D. Mudd[18],
F. Mueller[101], J. Mueller[125], R.S.P. Mueller[100], T. Mueller[28], D. Muenstermann[49], P. Mullen[53],
G.A. Mullier[17], J.A. Murillo Quijada[18], W.J. Murray[170,131], H. Musheghyan[54], E. Musto[152],
A.G. Myagkov[130,ac], M. Myska[128], B.P. Nachman[143], O. Nackenhorst[54], J. Nadal[54], K. Nagai[120],
R. Nagai[157], Y. Nagai[85], K. Nagano[66], A. Nagarkar[111], Y. Nagasaka[59], K. Nagata[160], M. Nagel[101],
E. Nagy[85], A.M. Nairz[30], Y. Nakahama[30], K. Nakamura[66], T. Nakamura[155], I. Nakano[112],
H. Namasivayam[41], R.F. Naranjo Garcia[42], R. Narayan[31], D.I. Narrias Villar[58a], T. Naumann[42],
G. Navarro[162], R. Nayyar[7], H.A. Neal[89], P.Yu. Nechaeva[96], T.J. Neep[84], P.D. Nef[143],
A. Negri[121a,121b], M. Negrini[20a], S. Nektarijevic[106], C. Nellist[117], A. Nelson[163], S. Nemecek[127],
P. Nemethy[110], A.A. Nepomuceno[24a], M. Nessi[30,ad], M.S. Neubauer[165], M. Neumann[175],
R.M. Neves[110], P. Nevski[25], P.R. Newman[18], D.H. Nguyen[6], R.B. Nickerson[120], R. Nicolaidou[136],
B. Nicquevert[30], J. Nielsen[137], N. Nikiforou[35], A. Nikiforov[16], V. Nikolaenko[130,ac],
I. Nikolic-Audit[80], K. Nikolopoulos[18], J.K. Nilsen[119], P. Nilsson[25], Y. Ninomiya[155], A. Nisati[132a],
R. Nisius[101], T. Nobe[155], M. Nomachi[118], I. Nomidis[29], T. Nooney[76], S. Norberg[113],
M. Nordberg[30], O. Novgorodova[44], S. Nowak[101], M. Nozaki[66], L. Nozka[115], K. Ntekas[10],
G. Nunes Hanninger[88], T. Nunnemann[100], E. Nurse[78], F. Nuti[88], B.J. O'Brien[46], F. O'grady[7],
D.C. O'Neil[142], V. O'Shea[53], F.G. Oakham[29,d], H. Oberlack[101], T. Obermann[21], J. Ocariz[80],
A. Ochi[67], I. Ochoa[35], J.P. Ochoa-Ricoux[32a], S. Oda[70], S. Odaka[66], H. Ogren[61], A. Oh[84],
S.H. Oh[45], C.C. Ohm[15], H. Ohman[166], H. Oide[30], W. Okamura[118], H. Okawa[160], Y. Okumura[31],
T. Okuyama[66], A. Olariu[26b], S.A. Olivares Pino[46], D. Oliveira Damazio[25], A. Olszewski[39],
J. Olszowska[39], A. Onofre[126a,126e], K. Onogi[103], P.U.E. Onyisi[31,s], C.J. Oram[159a], M.J. Oreglia[31],
Y. Oren[153], D. Orestano[134a,134b], N. Orlando[154], C. Oropeza Barrera[53], R.S. Orr[158],
B. Osculati[50a,50b], R. Ospanov[84], G. Otero y Garzon[27], H. Otono[70], M. Ouchrif[135d],
F. Ould-Saada[119], A. Ouraou[136], K.P. Oussoren[107], Q. Ouyang[33a], A. Ovcharova[15], M. Owen[53],
R.E. Owen[18], V.E. Ozcan[19a], N. Ozturk[8], K. Pachal[142], A. Pacheco Pages[12], C. Padilla Aranda[12],
M. Pagáčová[48], S. Pagan Griso[15], E. Paganis[139], F. Paige[25], P. Pais[86], K. Pajchel[119],
G. Palacino[159b], S. Palestini[30], M. Palka[38b], D. Pallin[34], A. Palma[126a,126b], Y.B. Pan[173],
E.St. Panagiotopoulou[10], C.E. Pandini[80], J.G. Panduro Vazquez[77], P. Pani[146a,146b], S. Panitkin[25],
D. Pantea[26b], L. Paolozzi[49], Th.D. Papadopoulou[10], K. Papageorgiou[154], A. Paramonov[6],
D. Paredes Hernandez[154], M.A. Parker[28], K.A. Parker[139], F. Parodi[50a,50b], J.A. Parsons[35],
U. Parzefall[48], E. Pasqualucci[132a], S. Passaggio[50a], F. Pastore[134a,134b,*], Fr. Pastore[77],
G. Pásztor[29], S. Pataraia[175], N.D. Patel[150], J.R. Pater[84], T. Pauly[30], J. Pearce[169], B. Pearson[113],
L.E. Pedersen[36], M. Pedersen[119], S. Pedraza Lopez[167], R. Pedro[126a,126b], S.V. Peleganchuk[109,c],

D. Pelikan[166], O. Penc[127], C. Peng[33a], H. Peng[33b], B. Penning[31], J. Penwell[61], D.V. Perepelitsa[25],
E. Perez Codina[159a], M.T. Pérez García-Estañ[167], L. Perini[91a,91b], H. Pernegger[30],
S. Perrella[104a,104b], R. Peschke[42], V.D. Peshekhonov[65], K. Peters[30], R.F.Y. Peters[84],
B.A. Petersen[30], T.C. Petersen[36], E. Petit[42], A. Petridis[1], C. Petridou[154], P. Petroff[117],
E. Petrolo[132a], F. Petrucci[134a,134b], N.E. Pettersson[157], R. Pezoa[32b], P.W. Phillips[131],
G. Piacquadio[143], E. Pianori[170], A. Picazio[49], E. Piccaro[76], M. Piccinini[20a,20b], M.A. Pickering[120],
R. Piegaia[27], D.T. Pignotti[111], J.E. Pilcher[31], A.D. Pilkington[84], A.W.J. Pin[84],
J. Pina[126a,126b,126d], M. Pinamonti[164a,164c,ae], J.L. Pinfold[3], A. Pingel[36], S. Pires[80], H. Pirumov[42],
M. Pitt[172], C. Pizio[91a,91b], L. Plazak[144a], M.-A. Pleier[25], V. Pleskot[129], E. Plotnikova[65],
P. Plucinski[146a,146b], D. Pluth[64], R. Poettgen[146a,146b], L. Poggioli[117], D. Pohl[21], G. Polesello[121a],
A. Poley[42], A. Policicchio[37a,37b], R. Polifka[158], A. Polini[20a], C.S. Pollard[53], V. Polychronakos[25],
K. Pommès[30], L. Pontecorvo[132a], B.G. Pope[90], G.A. Popeneciu[26c], D.S. Popovic[13],
A. Poppleton[30], S. Pospisil[128], K. Potamianos[15], I.N. Potrap[65], C.J. Potter[149], C.T. Potter[116],
G. Poulard[30], J. Poveda[30], V. Pozdnyakov[65], P. Pralavorio[85], A. Pranko[15], S. Prasad[30], S. Prell[64],
D. Price[84], L.E. Price[6], M. Primavera[73a], S. Prince[87], M. Proissl[46], K. Prokofiev[60c],
F. Prokoshin[32b], E. Protopapadaki[136], S. Protopopescu[25], J. Proudfoot[6], M. Przybycien[38a],
E. Ptacek[116], D. Puddu[134a,134b], E. Pueschel[86], D. Puldon[148], M. Purohit[25,af], P. Puzo[117],
J. Qian[89], G. Qin[53], Y. Qin[84], A. Quadt[54], D.R. Quarrie[15], W.B. Quayle[164a,164b],
M. Queitsch-Maitland[84], D. Quilty[53], S. Raddum[119], V. Radeka[25], V. Radescu[42],
S.K. Radhakrishnan[148], P. Radloff[116], P. Rados[88], F. Ragusa[91a,91b], G. Rahal[178],
S. Rajagopalan[25], M. Rammensee[30], C. Rangel-Smith[166], F. Rauscher[100], S. Rave[83],
T. Ravenscroft[53], M. Raymond[30], A.L. Read[119], N.P. Readioff[74], D.M. Rebuzzi[121a,121b],
A. Redelbach[174], G. Redlinger[25], R. Reece[137], K. Reeves[41], L. Rehnisch[16], J. Reichert[122],
H. Reisin[27], C. Rembser[30], H. Ren[33a], A. Renaud[117], M. Rescigno[132a], S. Resconi[91a],
O.L. Rezanova[109,c], P. Reznicek[129], R. Rezvani[95], R. Richter[101], S. Richter[78], E. Richter-Was[38b],
O. Ricken[21], M. Ridel[80], P. Rieck[16], C.J. Riegel[175], J. Rieger[54], O. Rifki[113], M. Rijssenbeek[148],
A. Rimoldi[121a,121b], L. Rinaldi[20a], B. Ristić[49], E. Ritsch[30], I. Riu[12], F. Rizatdinova[114], E. Rizvi[76],
T.G. Rizzo[ag], S.H. Robertson[87,k], A. Robichaud-Veronneau[87], D. Robinson[28], J.E.M. Robinson[42],
A. Robson[53], C. Roda[124a,124b], S. Roe[30], O. Røhne[119], S. Rolli[161], A. Romaniouk[98],
M. Romano[20a,20b], S.M. Romano Saez[34], E. Romero Adam[167], N. Rompotis[138], M. Ronzani[48],
L. Roos[80], E. Ros[167], S. Rosati[132a], K. Rosbach[48], P. Rose[137], P.L. Rosendahl[14], O. Rosenthal[141],
V. Rossetti[146a,146b], E. Rossi[104a,104b], L.P. Rossi[50a], J.H.N. Rosten[28], R. Rosten[138], M. Rotaru[26b],
I. Roth[172], J. Rothberg[138], D. Rousseau[117], C.R. Royon[136], A. Rozanov[85], Y. Rozen[152],
X. Ruan[145c], F. Rubbo[143], I. Rubinskiy[42], V.I. Rud[99], C. Rudolph[44], M.S. Rudolph[158], F. Rühr[48],
A. Ruiz-Martinez[30], Z. Rurikova[48], N.A. Rusakovich[65], A. Ruschke[100], H.L. Russell[138],
J.P. Rutherfoord[7], N. Ruthmann[30], Y.F. Ryabov[123], M. Rybar[165], G. Rybkin[117], N.C. Ryder[120],
A.F. Saavedra[150], G. Sabato[107], S. Sacerdoti[27], A. Saddique[3], H.F-W. Sadrozinski[137],
R. Sadykov[65], F. Safai Tehrani[132a], P. Saha[108], M. Sahinsoy[58a], M. Saimpert[136], T. Saito[155],
H. Sakamoto[155], Y. Sakurai[171], G. Salamanna[134a,134b], A. Salamon[133a], J.E. Salazar Loyola[32b],
M. Saleem[113], D. Salek[107], P.H. Sales De Bruin[138], D. Salihagic[101], A. Salnikov[143], J. Salt[167],
D. Salvatore[37a,37b], F. Salvatore[149], A. Salvucci[60a], A. Salzburger[30], D. Sammel[48],
D. Sampsonidis[154], A. Sanchez[104a,104b], J. Sánchez[167], V. Sanchez Martinez[167], H. Sandaker[119],
R.L. Sandbach[76], H.G. Sander[83], M.P. Sanders[100], M. Sandhoff[175], C. Sandoval[162],
R. Sandstroem[101], D.P.C. Sankey[131], M. Sannino[50a,50b], A. Sansoni[47], C. Santoni[34],
R. Santonico[133a,133b], H. Santos[126a], I. Santoyo Castillo[149], K. Sapp[125], A. Sapronov[65],
J.G. Saraiva[126a,126d], B. Sarrazin[21], O. Sasaki[66], Y. Sasaki[155], K. Sato[160], G. Sauvage[5,*],
E. Sauvan[5], G. Savage[77], P. Savard[158,d], C. Sawyer[131], L. Sawyer[79,n], J. Saxon[31], C. Sbarra[20a],
A. Sbrizzi[20a,20b], T. Scanlon[78], D.A. Scannicchio[163], M. Scarcella[150], V. Scarfone[37a,37b],

J. Schaarschmidt[172], P. Schacht[101], D. Schaefer[30], R. Schaefer[42], J. Schaeffer[83], S. Schaepe[21],
S. Schaetzel[58b], U. Schäfer[83], A.C. Schaffer[117], D. Schaile[100], R.D. Schamberger[148], V. Scharf[58a],
V.A. Schegelsky[123], D. Scheirich[129], M. Schernau[163], C. Schiavi[50a,50b], C. Schillo[48],
M. Schioppa[37a,37b], S. Schlenker[30], K. Schmieden[30], C. Schmitt[83], S. Schmitt[58b], S. Schmitt[42],
B. Schneider[159a], Y.J. Schnellbach[74], U. Schnoor[44], L. Schoeffel[136], A. Schoening[58b],
B.D. Schoenrock[90], E. Schopf[21], A.L.S. Schorlemmer[54], M. Schott[83], D. Schouten[159a],
J. Schovancova[8], S. Schramm[49], M. Schreyer[174], N. Schuh[83], M.J. Schultens[21],
H.-C. Schultz-Coulon[58a], H. Schulz[16], M. Schumacher[48], B.A. Schumm[137], Ph. Schune[136],
C. Schwanenberger[84], A. Schwartzman[143], T.A. Schwarz[89], Ph. Schwegler[101], H. Schweiger[84],
Ph. Schwemling[136], R. Schwienhorst[90], J. Schwindling[136], T. Schwindt[21], F.G. Sciacca[17],
E. Scifo[117], G. Sciolla[23], F. Scuri[124a,124b], F. Scutti[21], J. Searcy[89], G. Sedov[42], E. Sedykh[123],
P. Seema[21], S.C. Seidel[105], A. Seiden[137], F. Seifert[128], J.M. Seixas[24a], G. Sekhniaidze[104a],
K. Sekhon[89], S.J. Sekula[40], D.M. Seliverstov[123,*], N. Semprini-Cesari[20a,20b], C. Serfon[30],
L. Serin[117], L. Serkin[164a,164b], T. Serre[85], M. Sessa[134a,134b], R. Seuster[159a], H. Severini[113],
T. Sfiligoj[75], F. Sforza[30], A. Sfyrla[30], E. Shabalina[54], M. Shamim[116], L.Y. Shan[33a], R. Shang[165],
J.T. Shank[22], M. Shapiro[15], P.B. Shatalov[97], K. Shaw[164a,164b], S.M. Shaw[84],
A. Shcherbakova[146a,146b], C.Y. Shehu[149], P. Sherwood[78], L. Shi[151,ah], S. Shimizu[67],
C.O. Shimmin[163], M. Shimojima[102], M. Shiyakova[65], A. Shmeleva[96], D. Shoaleh Saadi[95],
M.J. Shochet[31], S. Shojaii[91a,91b], S. Shrestha[111], E. Shulga[98], M.A. Shupe[7], S. Shushkevich[42],
P. Sicho[127], P.E. Sidebo[147], O. Sidiropoulou[174], D. Sidorov[114], A. Sidoti[20a,20b], F. Siegert[44],
Dj. Sijacki[13], J. Silva[126a,126d], Y. Silver[153], S.B. Silverstein[146a], V. Simak[128], O. Simard[5],
Lj. Simic[13], S. Simion[117], E. Simioni[83], B. Simmons[78], D. Simon[34], P. Sinervo[158], N.B. Sinev[116],
M. Sioli[20a,20b], G. Siragusa[174], A.N. Sisakyan[65,*], S.Yu. Sivoklokov[99], J. Sjölin[146a,146b],
T.B. Sjursen[14], M.B. Skinner[72], H.P. Skottowe[57], P. Skubic[113], M. Slater[18], T. Slavicek[128],
M. Slawinska[107], K. Sliwa[161], V. Smakhtin[172], B.H. Smart[46], L. Smestad[14], S.Yu. Smirnov[98],
Y. Smirnov[98], L.N. Smirnova[99,ai], O. Smirnova[81], M.N.K. Smith[35], R.W. Smith[35],
M. Smizanska[72], K. Smolek[128], A.A. Snesarev[96], G. Snidero[76], S. Snyder[25], R. Sobie[169,k],
F. Socher[44], A. Soffer[153], D.A. Soh[151,ah], G. Sokhrannyi[75], C.A. Solans[30], M. Solar[128], J. Solc[128],
E.Yu. Soldatov[98], U. Soldevila[167], A.A. Solodkov[130], A. Soloshenko[65], O.V. Solovyanov[130],
V. Solovyev[123], P. Sommer[48], H.Y. Song[33b,y], N. Soni[1], A. Sood[15], A. Sopczak[128], B. Sopko[128],
V. Sopko[128], V. Sorin[12], D. Sosa[58b], M. Sosebee[8], C.L. Sotiropoulou[124a,124b], R. Soualah[164a,164c],
A.M. Soukharev[109,c], D. South[42], B.C. Sowden[77], S. Spagnolo[73a,73b], M. Spalla[124a,124b],
M. Spangenberg[170], F. Spanò[77], W.R. Spearman[57], D. Sperlich[16], F. Spettel[101], R. Spighi[20a],
G. Spigo[30], L.A. Spiller[88], M. Spousta[129], R.D. St. Denis[53,*], A. Stabile[91a], S. Staerz[44],
J. Stahlman[122], R. Stamen[58a], S. Stamm[16], E. Stanecka[39], C. Stanescu[134a], M. Stanescu-Bellu[42],
M.M. Stanitzki[42], S. Stapnes[119], E.A. Starchenko[130], J. Stark[55], P. Staroba[127], P. Starovoitov[58a],
R. Staszewski[39], P. Steinberg[25], B. Stelzer[142], H.J. Stelzer[30], O. Stelzer-Chilton[159a], H. Stenzel[52],
G.A. Stewart[53], J.A. Stillings[21], M.C. Stockton[87], M. Stoebe[87], G. Stoicea[26b], P. Stolte[54],
S. Stonjek[101], A.R. Stradling[8], A. Straessner[44], M.E. Stramaglia[17], J. Strandberg[147],
S. Strandberg[146a,146b], A. Strandlie[119], E. Strauss[143], M. Strauss[113], P. Strizenec[144b],
R. Ströhmer[174], D.M. Strom[116], R. Stroynowski[40], A. Strubig[106], S.A. Stucci[17], B. Stugu[14],
N.A. Styles[42], D. Su[143], J. Su[125], R. Subramaniam[79], A. Succurro[12], Y. Sugaya[118], M. Suk[128],
V.V. Sulin[96], S. Sultansoy[4c], T. Sumida[68], S. Sun[57], X. Sun[33a], J.E. Sundermann[48], K. Suruliz[149],
G. Susinno[37a,37b], M.R. Sutton[149], S. Suzuki[66], M. Svatos[127], M. Swiatlowski[143], I. Sykora[144a],
T. Sykora[129], D. Ta[48], C. Taccini[134a,134b], K. Tackmann[42], J. Taenzer[158], A. Taffard[163],
R. Tafirout[159a], N. Taiblum[153], H. Takai[25], R. Takashima[69], H. Takeda[67], T. Takeshita[140],
Y. Takubo[66], M. Talby[85], A.A. Talyshev[109,c], J.Y.C. Tam[174], K.G. Tan[88], J. Tanaka[155],
R. Tanaka[117], S. Tanaka[66], B.B. Tannenwald[111], N. Tannoury[21], S. Tapia Araya[32b],

S. Tapprogge[83], S. Tarem[152], F. Tarrade[29], G.F. Tartarelli[91a], P. Tas[129], M. Tasevsky[127],
T. Tashiro[68], E. Tassi[37a,37b], A. Tavares Delgado[126a,126b], Y. Tayalati[135d], F.E. Taylor[94],
G.N. Taylor[88], P.T.E. Taylor[88], W. Taylor[159b], F.A. Teischinger[30],
M. Teixeira Dias Castanheira[76], P. Teixeira-Dias[77], K.K. Temming[48], D. Temple[142],
H. Ten Kate[30], P.K. Teng[151], J.J. Teoh[118], F. Tepel[175], S. Terada[66], K. Terashi[155], J. Terron[82],
S. Terzo[101], M. Testa[47], R.J. Teuscher[158,k], T. Theveneaux-Pelzer[34], J.P. Thomas[18],
J. Thomas-Wilsker[77], E.N. Thompson[35], P.D. Thompson[18], R.J. Thompson[84], A.S. Thompson[53],
L.A. Thomsen[176], E. Thomson[122], M. Thomson[28], R.P. Thun[89,*], M.J. Tibbetts[15],
R.E. Ticse Torres[85], V.O. Tikhomirov[96,aj], Yu.A. Tikhonov[109,c], S. Timoshenko[98],
E. Tiouchichine[85], P. Tipton[176], S. Tisserant[85], K. Todome[157], T. Todorov[5,*],
S. Todorova-Nova[129], J. Tojo[70], S. Tokár[144a], K. Tokushuku[66], K. Tollefson[90], E. Tolley[57],
L. Tomlinson[84], M. Tomoto[103], L. Tompkins[143,ak], K. Toms[105], E. Torrence[116], H. Torres[142],
E. Torró Pastor[138], J. Toth[85,al], F. Touchard[85], D.R. Tovey[139], T. Trefzger[174], L. Tremblet[30],
A. Tricoli[30], I.M. Trigger[159a], S. Trincaz-Duvoid[80], M.F. Tripiana[12], W. Trischuk[158], B. Trocmé[55],
C. Troncon[91a], M. Trottier-McDonald[15], M. Trovatelli[169], L. Truong[164a,164c], M. Trzebinski[39],
A. Trzupek[39], C. Tsarouchas[30], J.C-L. Tseng[120], P.V. Tsiareshka[92], D. Tsionou[154],
G. Tsipolitis[10], N. Tsirintanis[9], S. Tsiskaridze[12], V. Tsiskaridze[48], E.G. Tskhadadze[51a],
I.I. Tsukerman[97], V. Tsulaia[15], S. Tsuno[66], D. Tsybychev[148], A. Tudorache[26b], V. Tudorache[26b],
A.N. Tuna[57], S.A. Tupputi[20a,20b], S. Turchikhin[99,ai], D. Turecek[128], R. Turra[91a,91b],
A.J. Turvey[40], P.M. Tuts[35], A. Tykhonov[49], M. Tylmad[146a,146b], M. Tyndel[131], I. Ueda[155],
R. Ueno[29], M. Ughetto[146a,146b], M. Ugland[14], F. Ukegawa[160], G. Unal[30], A. Undrus[25],
G. Unel[163], F.C. Ungaro[48], Y. Unno[66], C. Unverdorben[100], J. Urban[144b], P. Urquijo[88],
P. Urrejola[83], G. Usai[8], A. Usanova[62], L. Vacavant[85], V. Vacek[128], B. Vachon[87], C. Valderanis[83],
N. Valencic[107], S. Valentinetti[20a,20b], A. Valero[167], L. Valery[12], S. Valkar[129], S. Vallecorsa[49],
J.A. Valls Ferrer[167], W. Van Den Wollenberg[107], P.C. Van Der Deijl[107], R. van der Geer[107],
H. van der Graaf[107], N. van Eldik[152], P. van Gemmeren[6], J. Van Nieuwkoop[142], I. van Vulpen[107],
M.C. van Woerden[30], M. Vanadia[132a,132b], W. Vandelli[30], R. Vanguri[122], A. Vaniachine[6],
F. Vannucci[80], G. Vardanyan[177], R. Vari[132a], E.W. Varnes[7], T. Varol[40], D. Varouchas[80],
A. Vartapetian[8], K.E. Varvell[150], F. Vazeille[34], T. Vazquez Schroeder[87], J. Veatch[7],
L.M. Veloce[158], F. Veloso[126a,126c], T. Velz[21], S. Veneziano[132a], A. Ventura[73a,73b], D. Ventura[86],
M. Venturi[169], N. Venturi[158], A. Venturini[23], V. Vercesi[121a], M. Verducci[132a,132b], W. Verkerke[107],
J.C. Vermeulen[107], A. Vest[44], M.C. Vetterli[142,d], O. Viazlo[81], I. Vichou[165], T. Vickey[139],
O.E. Vickey Boeriu[139], G.H.A. Viehhauser[120], S. Viel[15], R. Vigne[62], M. Villa[20a,20b],
M. Villaplana Perez[91a,91b], E. Vilucchi[47], M.G. Vincter[29], V.B. Vinogradov[65], I. Vivarelli[149],
F. Vives Vaque[3], S. Vlachos[10], D. Vladoiu[100], M. Vlasak[128], M. Vogel[32a], P. Vokac[128],
G. Volpi[124a,124b], M. Volpi[88], H. von der Schmitt[101], H. von Radziewski[48], E. von Toerne[21],
V. Vorobel[129], K. Vorobev[98], M. Vos[167], R. Voss[30], J.H. Vossebeld[74], N. Vranjes[13],
M. Vranjes Milosavljevic[13], V. Vrba[127], M. Vreeswijk[107], R. Vuillermet[30], I. Vukotic[31],
Z. Vykydal[128], P. Wagner[21], W. Wagner[175], H. Wahlberg[71], S. Wahrmund[44], J. Wakabayashi[103],
J. Walder[72], R. Walker[100], W. Walkowiak[141], C. Wang[151], F. Wang[173], H. Wang[15], H. Wang[40],
J. Wang[42], J. Wang[150], K. Wang[87], R. Wang[6], S.M. Wang[151], T. Wang[21], T. Wang[35],
X. Wang[176], C. Wanotayaroj[116], A. Warburton[87], C.P. Ward[28], D.R. Wardrope[78],
A. Washbrook[46], C. Wasicki[42], P.M. Watkins[18], A.T. Watson[18], I.J. Watson[150], M.F. Watson[18],
G. Watts[138], S. Watts[84], B.M. Waugh[78], S. Webb[84], M.S. Weber[17], S.W. Weber[174],
J.S. Webster[31], A.R. Weidberg[120], B. Weinert[61], J. Weingarten[54], C. Weiser[48], H. Weits[107],
P.S. Wells[30], T. Wenaus[25], T. Wengler[30], S. Wenig[30], N. Wermes[21], M. Werner[48], P. Werner[30],
M. Wessels[58a], J. Wetter[161], K. Whalen[116], A.M. Wharton[72], A. White[8], M.J. White[1],
R. White[32b], S. White[124a,124b], D. Whiteson[163], F.J. Wickens[131], W. Wiedenmann[173],

JHEP10(2015)134

M. Wielers[131], P. Wienemann[21], C. Wiglesworth[36], L.A.M. Wiik-Fuchs[21], A. Wildauer[101],
H.G. Wilkens[30], H.H. Williams[122], S. Williams[107], C. Willis[90], S. Willocq[86], A. Wilson[89],
J.A. Wilson[18], I. Wingerter-Seez[5], F. Winklmeier[116], B.T. Winter[21], M. Wittgen[143],
J. Wittkowski[100], S.J. Wollstadt[83], M.W. Wolter[39], H. Wolters[126a,126c], B.K. Wosiek[39],
J. Wotschack[30], M.J. Woudstra[84], K.W. Wozniak[39], M. Wu[55], M. Wu[31], S.L. Wu[173], X. Wu[49],
Y. Wu[89], T.R. Wyatt[84], B.M. Wynne[46], S. Xella[36], D. Xu[33a], L. Xu[25], B. Yabsley[150],
S. Yacoob[145a], R. Yakabe[67], M. Yamada[66], D. Yamaguchi[157], Y. Yamaguchi[118], A. Yamamoto[66],
S. Yamamoto[155], T. Yamanaka[155], K. Yamauchi[103], Y. Yamazaki[67], Z. Yan[22], H. Yang[33e],
H. Yang[173], Y. Yang[151], W-M. Yao[15], Y.C. Yap[80], Y. Yasu[66], E. Yatsenko[5], K.H. Yau Wong[21],
J. Ye[40], S. Ye[25], I. Yeletskikh[65], A.L. Yen[57], E. Yildirim[42], K. Yorita[171], R. Yoshida[6],
K. Yoshihara[122], C. Young[143], C.J.S. Young[30], S. Youssef[22], D.R. Yu[15], J. Yu[8], J.M. Yu[89],
J. Yu[114], L. Yuan[67], S.P.Y. Yuen[21], A. Yurkewicz[108], I. Yusuff[28,am], B. Zabinski[39], R. Zaidan[63],
A.M. Zaitsev[130,ac], J. Zalieckas[14], A. Zaman[148], S. Zambito[57], L. Zanello[132a,132b], D. Zanzi[88],
C. Zeitnitz[175], M. Zeman[128], A. Zemla[38a], Q. Zeng[143], K. Zengel[23], O. Zenin[130], T. Ženiš[144a],
D. Zerwas[117], D. Zhang[89], F. Zhang[173], G. Zhang[33b], H. Zhang[33c], J. Zhang[6], L. Zhang[48],
R. Zhang[33b,i], X. Zhang[33d], Z. Zhang[117], X. Zhao[40], Y. Zhao[33d,117], Z. Zhao[33b],
A. Zhemchugov[65], J. Zhong[120], B. Zhou[89], C. Zhou[45], L. Zhou[35], L. Zhou[40], M. Zhou[148],
N. Zhou[33f], C.G. Zhu[33d], H. Zhu[33a], J. Zhu[89], Y. Zhu[33b], X. Zhuang[33a], K. Zhukov[96],
A. Zibell[174], D. Zieminska[61], N.I. Zimine[65], C. Zimmermann[83], S. Zimmermann[48], Z. Zinonos[54],
M. Zinser[83], M. Ziolkowski[141], L. Živković[13], G. Zobernig[173], A. Zoccoli[20a,20b], M. zur Nedden[16],
G. Zurzolo[104a,104b] and L. Zwalinski[30].

¹ *Department of Physics, University of Adelaide, Adelaide, Australia*
² *Physics Department, SUNY Albany, Albany NY, United States of America*
³ *Department of Physics, University of Alberta, Edmonton AB, Canada*
⁴ *⁽ᵃ⁾ Department of Physics, Ankara University, Ankara; ⁽ᵇ⁾ Istanbul Aydin University, Istanbul; ⁽ᶜ⁾ Division of Physics, TOBB University of Economics and Technology, Ankara, Turkey*
⁵ *LAPP, CNRS/IN2P3 and Université Savoie Mont Blanc, Annecy-le-Vieux, France*
⁶ *High Energy Physics Division, Argonne National Laboratory, Argonne IL, United States of America*
⁷ *Department of Physics, University of Arizona, Tucson AZ, United States of America*
⁸ *Department of Physics, The University of Texas at Arlington, Arlington TX, United States of America*
⁹ *Physics Department, University of Athens, Athens, Greece*
¹⁰ *Physics Department, National Technical University of Athens, Zografou, Greece*
¹¹ *Institute of Physics, Azerbaijan Academy of Sciences, Baku, Azerbaijan*
¹² *Institut de Física d'Altes Energies and Departament de Física de la Universitat Autònoma de Barcelona, Barcelona, Spain*
¹³ *Institute of Physics, University of Belgrade, Belgrade, Serbia*
¹⁴ *Department for Physics and Technology, University of Bergen, Bergen, Norway*
¹⁵ *Physics Division, Lawrence Berkeley National Laboratory and University of California, Berkeley CA, United States of America*
¹⁶ *Department of Physics, Humboldt University, Berlin, Germany*
¹⁷ *Albert Einstein Center for Fundamental Physics and Laboratory for High Energy Physics, University of Bern, Bern, Switzerland*
¹⁸ *School of Physics and Astronomy, University of Birmingham, Birmingham, United Kingdom*
¹⁹ *⁽ᵃ⁾ Department of Physics, Bogazici University, Istanbul; ⁽ᵇ⁾ Department of Physics Engineering, Gaziantep University, Gaziantep; ⁽ᶜ⁾ Department of Physics, Dogus University, Istanbul, Turkey*
²⁰ *⁽ᵃ⁾ INFN Sezione di Bologna; ⁽ᵇ⁾ Dipartimento di Fisica e Astronomia, Università di Bologna, Bologna, Italy*
²¹ *Physikalisches Institut, University of Bonn, Bonn, Germany*
²² *Department of Physics, Boston University, Boston MA, United States of America*

[23] *Department of Physics, Brandeis University, Waltham MA, United States of America*

[24] [a] *Universidade Federal do Rio De Janeiro COPPE/EE/IF, Rio de Janeiro;* [b] *Electrical Circuits Department, Federal University of Juiz de Fora (UFJF), Juiz de Fora;* [c] *Federal University of Sao Joao del Rei (UFSJ), Sao Joao del Rei;* [d] *Instituto de Fisica, Universidade de Sao Paulo, Sao Paulo, Brazil*

[25] *Physics Department, Brookhaven National Laboratory, Upton NY, United States of America*

[26] [a] *Transilvania University of Brasov, Brasov, Romania;* [b] *National Institute of Physics and Nuclear Engineering, Bucharest;* [c] *National Institute for Research and Development of Isotopic and Molecular Technologies, Physics Department, Cluj Napoca;* [d] *University Politehnica Bucharest, Bucharest;* [e] *West University in Timisoara, Timisoara, Romania*

[27] *Departamento de Física, Universidad de Buenos Aires, Buenos Aires, Argentina*

[28] *Cavendish Laboratory, University of Cambridge, Cambridge, United Kingdom*

[29] *Department of Physics, Carleton University, Ottawa ON, Canada*

[30] *CERN, Geneva, Switzerland*

[31] *Enrico Fermi Institute, University of Chicago, Chicago IL, United States of America*

[32] [a] *Departamento de Física, Pontificia Universidad Católica de Chile, Santiago;* [b] *Departamento de Física, Universidad Técnica Federico Santa María, Valparaíso, Chile*

[33] [a] *Institute of High Energy Physics, Chinese Academy of Sciences, Beijing;* [b] *Department of Modern Physics, University of Science and Technology of China, Anhui;* [c] *Department of Physics, Nanjing University, Jiangsu;* [d] *School of Physics, Shandong University, Shandong;* [e] *Department of Physics and Astronomy, Shanghai Key Laboratory for Particle Physics and Cosmology, Shanghai Jiao Tong University, Shanghai;* [f] *Physics Department, Tsinghua University, Beijing 100084, China*

[34] *Laboratoire de Physique Corpusculaire, Clermont Université and Université Blaise Pascal and CNRS/IN2P3, Clermont-Ferrand, France*

[35] *Nevis Laboratory, Columbia University, Irvington NY, United States of America*

[36] *Niels Bohr Institute, University of Copenhagen, Kobenhavn, Denmark*

[37] [a] *INFN Gruppo Collegato di Cosenza, Laboratori Nazionali di Frascati;* [b] *Dipartimento di Fisica, Università della Calabria, Rende, Italy*

[38] [a] *AGH University of Science and Technology, Faculty of Physics and Applied Computer Science, Krakow;* [b] *Marian Smoluchowski Institute of Physics, Jagiellonian University, Krakow, Poland*

[39] *Institute of Nuclear Physics Polish Academy of Sciences, Krakow, Poland*

[40] *Physics Department, Southern Methodist University, Dallas TX, United States of America*

[41] *Physics Department, University of Texas at Dallas, Richardson TX, United States of America*

[42] *DESY, Hamburg and Zeuthen, Germany*

[43] *Institut für Experimentelle Physik IV, Technische Universität Dortmund, Dortmund, Germany*

[44] *Institut für Kern- und Teilchenphysik, Technische Universität Dresden, Dresden, Germany*

[45] *Department of Physics, Duke University, Durham NC, United States of America*

[46] *SUPA - School of Physics and Astronomy, University of Edinburgh, Edinburgh, United Kingdom*

[47] *INFN Laboratori Nazionali di Frascati, Frascati, Italy*

[48] *Fakultät für Mathematik und Physik, Albert-Ludwigs-Universität, Freiburg, Germany*

[49] *Section de Physique, Université de Genève, Geneva, Switzerland*

[50] [a] *INFN Sezione di Genova;* [b] *Dipartimento di Fisica, Università di Genova, Genova, Italy*

[51] [a] *E. Andronikashvili Institute of Physics, Iv. Javakhishvili Tbilisi State University, Tbilisi;* [b] *High Energy Physics Institute, Tbilisi State University, Tbilisi, Georgia*

[52] *II Physikalisches Institut, Justus-Liebig-Universität Giessen, Giessen, Germany*

[53] *SUPA - School of Physics and Astronomy, University of Glasgow, Glasgow, United Kingdom*

[54] *II Physikalisches Institut, Georg-August-Universität, Göttingen, Germany*

[55] *Laboratoire de Physique Subatomique et de Cosmologie, Université Grenoble-Alpes, CNRS/IN2P3, Grenoble, France*

[56] *Department of Physics, Hampton University, Hampton VA, United States of America*

[57] *Laboratory for Particle Physics and Cosmology, Harvard University, Cambridge MA, United States*

of America

58 *(a) Kirchhoff-Institut für Physik, Ruprecht-Karls-Universität Heidelberg, Heidelberg; (b) Physikalisches Institut, Ruprecht-Karls-Universität Heidelberg, Heidelberg; (c) ZITI Institut für technische Informatik, Ruprecht-Karls-Universität Heidelberg, Mannheim, Germany*

59 *Faculty of Applied Information Science, Hiroshima Institute of Technology, Hiroshima, Japan*

60 *(a) Department of Physics, The Chinese University of Hong Kong, Shatin, N.T., Hong Kong; (b) Department of Physics, The University of Hong Kong, Hong Kong; (c) Department of Physics, The Hong Kong University of Science and Technology, Clear Water Bay, Kowloon, Hong Kong, China*

61 *Department of Physics, Indiana University, Bloomington IN, United States of America*

62 *Institut für Astro- und Teilchenphysik, Leopold-Franzens-Universität, Innsbruck, Austria*

63 *University of Iowa, Iowa City IA, United States of America*

64 *Department of Physics and Astronomy, Iowa State University, Ames IA, United States of America*

65 *Joint Institute for Nuclear Research, JINR Dubna, Dubna, Russia*

66 *KEK, High Energy Accelerator Research Organization, Tsukuba, Japan*

67 *Graduate School of Science, Kobe University, Kobe, Japan*

68 *Faculty of Science, Kyoto University, Kyoto, Japan*

69 *Kyoto University of Education, Kyoto, Japan*

70 *Department of Physics, Kyushu University, Fukuoka, Japan*

71 *Instituto de Física La Plata, Universidad Nacional de La Plata and CONICET, La Plata, Argentina*

72 *Physics Department, Lancaster University, Lancaster, United Kingdom*

73 *(a) INFN Sezione di Lecce; (b) Dipartimento di Matematica e Fisica, Università del Salento, Lecce, Italy*

74 *Oliver Lodge Laboratory, University of Liverpool, Liverpool, United Kingdom*

75 *Department of Physics, Jožef Stefan Institute and University of Ljubljana, Ljubljana, Slovenia*

76 *School of Physics and Astronomy, Queen Mary University of London, London, United Kingdom*

77 *Department of Physics, Royal Holloway University of London, Surrey, United Kingdom*

78 *Department of Physics and Astronomy, University College London, London, United Kingdom*

79 *Louisiana Tech University, Ruston LA, United States of America*

80 *Laboratoire de Physique Nucléaire et de Hautes Energies, UPMC and Université Paris-Diderot and CNRS/IN2P3, Paris, France*

81 *Fysiska institutionen, Lunds universitet, Lund, Sweden*

82 *Departamento de Fisica Teorica C-15, Universidad Autonoma de Madrid, Madrid, Spain*

83 *Institut für Physik, Universität Mainz, Mainz, Germany*

84 *School of Physics and Astronomy, University of Manchester, Manchester, United Kingdom*

85 *CPPM, Aix-Marseille Université and CNRS/IN2P3, Marseille, France*

86 *Department of Physics, University of Massachusetts, Amherst MA, United States of America*

87 *Department of Physics, McGill University, Montreal QC, Canada*

88 *School of Physics, University of Melbourne, Victoria, Australia*

89 *Department of Physics, The University of Michigan, Ann Arbor MI, United States of America*

90 *Department of Physics and Astronomy, Michigan State University, East Lansing MI, United States of America*

91 *(a) INFN Sezione di Milano; (b) Dipartimento di Fisica, Università di Milano, Milano, Italy*

92 *B.I. Stepanov Institute of Physics, National Academy of Sciences of Belarus, Minsk, Republic of Belarus*

93 *National Scientific and Educational Centre for Particle and High Energy Physics, Minsk, Republic of Belarus*

94 *Department of Physics, Massachusetts Institute of Technology, Cambridge MA, United States of America*

95 *Group of Particle Physics, University of Montreal, Montreal QC, Canada*

96 *P.N. Lebedev Institute of Physics, Academy of Sciences, Moscow, Russia*

97 *Institute for Theoretical and Experimental Physics (ITEP), Moscow, Russia*

98 *National Research Nuclear University MEPhI, Moscow, Russia*

99 *D.V. Skobeltsyn Institute of Nuclear Physics, M.V. Lomonosov Moscow State University, Moscow, Russia*

100 *Fakultät für Physik, Ludwig-Maximilians-Universität München, München, Germany*

101 *Max-Planck-Institut für Physik (Werner-Heisenberg-Institut), München, Germany*

102 *Nagasaki Institute of Applied Science, Nagasaki, Japan*

103 *Graduate School of Science and Kobayashi-Maskawa Institute, Nagoya University, Nagoya, Japan*

104 (a) *INFN Sezione di Napoli;* (b) *Dipartimento di Fisica, Università di Napoli, Napoli, Italy*

105 *Department of Physics and Astronomy, University of New Mexico, Albuquerque NM, United States of America*

106 *Institute for Mathematics, Astrophysics and Particle Physics, Radboud University Nijmegen/Nikhef, Nijmegen, Netherlands*

107 *Nikhef National Institute for Subatomic Physics and University of Amsterdam, Amsterdam, Netherlands*

108 *Department of Physics, Northern Illinois University, DeKalb IL, United States of America*

109 *Budker Institute of Nuclear Physics, SB RAS, Novosibirsk, Russia*

110 *Department of Physics, New York University, New York NY, United States of America*

111 *Ohio State University, Columbus OH, United States of America*

112 *Faculty of Science, Okayama University, Okayama, Japan*

113 *Homer L. Dodge Department of Physics and Astronomy, University of Oklahoma, Norman OK, United States of America*

114 *Department of Physics, Oklahoma State University, Stillwater OK, United States of America*

115 *Palacký University, RCPTM, Olomouc, Czech Republic*

116 *Center for High Energy Physics, University of Oregon, Eugene OR, United States of America*

117 *LAL, Université Paris-Sud and CNRS/IN2P3, Orsay, France*

118 *Graduate School of Science, Osaka University, Osaka, Japan*

119 *Department of Physics, University of Oslo, Oslo, Norway*

120 *Department of Physics, Oxford University, Oxford, United Kingdom*

121 (a) *INFN Sezione di Pavia;* (b) *Dipartimento di Fisica, Università di Pavia, Pavia, Italy*

122 *Department of Physics, University of Pennsylvania, Philadelphia PA, United States of America*

123 *National Research Centre "Kurchatov Institute" B.P.Konstantinov Petersburg Nuclear Physics Institute, St. Petersburg, Russia*

124 (a) *INFN Sezione di Pisa;* (b) *Dipartimento di Fisica E. Fermi, Università di Pisa, Pisa, Italy*

125 *Department of Physics and Astronomy, University of Pittsburgh, Pittsburgh PA, United States of America*

126 (a) *Laboratório de Instrumentação e Física Experimental de Partículas - LIP, Lisboa;* (b) *Faculdade de Ciências, Universidade de Lisboa, Lisboa;* (c) *Department of Physics, University of Coimbra, Coimbra;* (d) *Centro de Física Nuclear da Universidade de Lisboa, Lisboa;* (e) *Departamento de Fisica, Universidade do Minho, Braga;* (f) *Departamento de Fisica Teorica y del Cosmos and CAFPE, Universidad de Granada, Granada (Spain);* (g) *Dep Fisica and CEFITEC of Faculdade de Ciencias e Tecnologia, Universidade Nova de Lisboa, Caparica, Portugal*

127 *Institute of Physics, Academy of Sciences of the Czech Republic, Praha, Czech Republic*

128 *Czech Technical University in Prague, Praha, Czech Republic*

129 *Faculty of Mathematics and Physics, Charles University in Prague, Praha, Czech Republic*

130 *State Research Center Institute for High Energy Physics, Protvino, Russia*

131 *Particle Physics Department, Rutherford Appleton Laboratory, Didcot, United Kingdom*

132 (a) *INFN Sezione di Roma;* (b) *Dipartimento di Fisica, Sapienza Università di Roma, Roma, Italy*

133 (a) *INFN Sezione di Roma Tor Vergata;* (b) *Dipartimento di Fisica, Università di Roma Tor Vergata, Roma, Italy*

134 (a) *INFN Sezione di Roma Tre;* (b) *Dipartimento di Matematica e Fisica, Università Roma Tre, Roma, Italy*

135 (a) *Faculté des Sciences Ain Chock, Réseau Universitaire de Physique des Hautes Energies - Université Hassan II, Casablanca;* (b) *Centre National de l'Energie des Sciences Techniques*

Nucleaires, Rabat; [(c)] *Faculté des Sciences Semlalia, Université Cadi Ayyad, LPHEA-Marrakech;* [(d)] *Faculté des Sciences, Université Mohamed Premier and LPTPM, Oujda;* [(e)] *Faculté des sciences, Université Mohammed V, Rabat, Morocco*

136 *DSM/IRFU (Institut de Recherches sur les Lois Fondamentales de l'Univers), CEA Saclay (Commissariat à l'Energie Atomique et aux Energies Alternatives), Gif-sur-Yvette, France*

137 *Santa Cruz Institute for Particle Physics, University of California Santa Cruz, Santa Cruz CA, United States of America*

138 *Department of Physics, University of Washington, Seattle WA, United States of America*

139 *Department of Physics and Astronomy, University of Sheffield, Sheffield, United Kingdom*

140 *Department of Physics, Shinshu University, Nagano, Japan*

141 *Fachbereich Physik, Universität Siegen, Siegen, Germany*

142 *Department of Physics, Simon Fraser University, Burnaby BC, Canada*

143 *SLAC National Accelerator Laboratory, Stanford CA, United States of America*

144 [(a)] *Faculty of Mathematics, Physics & Informatics, Comenius University, Bratislava;* [(b)] *Department of Subnuclear Physics, Institute of Experimental Physics of the Slovak Academy of Sciences, Kosice, Slovak Republic*

145 [(a)] *Department of Physics, University of Cape Town, Cape Town;* [(b)] *Department of Physics, University of Johannesburg, Johannesburg;* [(c)] *School of Physics, University of the Witwatersrand, Johannesburg, South Africa*

146 [(a)] *Department of Physics, Stockholm University;* [(b)] *The Oskar Klein Centre, Stockholm, Sweden*

147 *Physics Department, Royal Institute of Technology, Stockholm, Sweden*

148 *Departments of Physics & Astronomy and Chemistry, Stony Brook University, Stony Brook NY, United States of America*

149 *Department of Physics and Astronomy, University of Sussex, Brighton, United Kingdom*

150 *School of Physics, University of Sydney, Sydney, Australia*

151 *Institute of Physics, Academia Sinica, Taipei, Taiwan*

152 *Department of Physics, Technion: Israel Institute of Technology, Haifa, Israel*

153 *Raymond and Beverly Sackler School of Physics and Astronomy, Tel Aviv University, Tel Aviv, Israel*

154 *Department of Physics, Aristotle University of Thessaloniki, Thessaloniki, Greece*

155 *International Center for Elementary Particle Physics and Department of Physics, The University of Tokyo, Tokyo, Japan*

156 *Graduate School of Science and Technology, Tokyo Metropolitan University, Tokyo, Japan*

157 *Department of Physics, Tokyo Institute of Technology, Tokyo, Japan*

158 *Department of Physics, University of Toronto, Toronto ON, Canada*

159 [(a)] *TRIUMF, Vancouver BC;* [(b)] *Department of Physics and Astronomy, York University, Toronto ON, Canada*

160 *Faculty of Pure and Applied Sciences, and Center for Integrated Research in Fundamental Science and Engineering, University of Tsukuba, Tsukuba, Japan*

161 *Department of Physics and Astronomy, Tufts University, Medford MA, United States of America*

162 *Centro de Investigaciones, Universidad Antonio Narino, Bogota, Colombia*

163 *Department of Physics and Astronomy, University of California Irvine, Irvine CA, United States of America*

164 [(a)] *INFN Gruppo Collegato di Udine, Sezione di Trieste, Udine;* [(b)] *ICTP, Trieste;* [(c)] *Dipartimento di Chimica, Fisica e Ambiente, Università di Udine, Udine, Italy*

165 *Department of Physics, University of Illinois, Urbana IL, United States of America*

166 *Department of Physics and Astronomy, University of Uppsala, Uppsala, Sweden*

167 *Instituto de Física Corpuscular (IFIC) and Departamento de Física Atómica, Molecular y Nuclear and Departamento de Ingeniería Electrónica and Instituto de Microelectrónica de Barcelona (IMB-CNM), University of Valencia and CSIC, Valencia, Spain*

168 *Department of Physics, University of British Columbia, Vancouver BC, Canada*

169 *Department of Physics and Astronomy, University of Victoria, Victoria BC, Canada*

[170] Department of Physics, University of Warwick, Coventry, United Kingdom
[171] Waseda University, Tokyo, Japan
[172] Department of Particle Physics, The Weizmann Institute of Science, Rehovot, Israel
[173] Department of Physics, University of Wisconsin, Madison WI, United States of America
[174] Fakultät für Physik und Astronomie, Julius-Maximilians-Universität, Würzburg, Germany
[175] Fachbereich C Physik, Bergische Universität Wuppertal, Wuppertal, Germany
[176] Department of Physics, Yale University, New Haven CT, United States of America
[177] Yerevan Physics Institute, Yerevan, Armenia
[178] Centre de Calcul de l'Institut National de Physique Nucléaire et de Physique des Particules (IN2P3), Villeurbanne, France

[a] Also at Department of Physics, King's College London, London, United Kingdom
[b] Also at Institute of Physics, Azerbaijan Academy of Sciences, Baku, Azerbaijan
[c] Also at Novosibirsk State University, Novosibirsk, Russia
[d] Also at TRIUMF, Vancouver BC, Canada
[e] Also at Department of Physics, California State University, Fresno CA, United States of America
[f] Also at Department of Physics, University of Fribourg, Fribourg, Switzerland
[g] Also at Departamento de Fisica e Astronomia, Faculdade de Ciencias, Universidade do Porto, Portugal
[h] Also at Tomsk State University, Tomsk, Russia
[i] Also at CPPM, Aix-Marseille Université and CNRS/IN2P3, Marseille, France
[j] Also at Universita di Napoli Parthenope, Napoli, Italy
[k] Also at Institute of Particle Physics (IPP), Canada
[l] Also at Particle Physics Department, Rutherford Appleton Laboratory, Didcot, United Kingdom
[m] Also at Department of Physics, St. Petersburg State Polytechnical University, St. Petersburg, Russia
[n] Also at Louisiana Tech University, Ruston LA, United States of America
[o] Also at Institucio Catalana de Recerca i Estudis Avancats, ICREA, Barcelona, Spain
[p] Also at Department of Physics, The University of Michigan, Ann Arbor MI, United States of America
[q] Also at Graduate School of Science, Osaka University, Osaka, Japan
[r] Also at Department of Physics, National Tsing Hua University, Taiwan
[s] Also at Department of Physics, The University of Texas at Austin, Austin TX, United States of America
[t] Also at Institute of Theoretical Physics, Ilia State University, Tbilisi, Georgia
[u] Also at CERN, Geneva, Switzerland
[v] Also at Georgian Technical University (GTU),Tbilisi, Georgia
[w] Also at Manhattan College, New York NY, United States of America
[x] Also at Hellenic Open University, Patras, Greece
[y] Also at Institute of Physics, Academia Sinica, Taipei, Taiwan
[z] Also at LAL, Université Paris-Sud and CNRS/IN2P3, Orsay, France
[aa] Also at Academia Sinica Grid Computing, Institute of Physics, Academia Sinica, Taipei, Taiwan
[ab] Also at School of Physics, Shandong University, Shandong, China
[ac] Also at Moscow Institute of Physics and Technology State University, Dolgoprudny, Russia
[ad] Also at Section de Physique, Université de Genève, Geneva, Switzerland
[ae] Also at International School for Advanced Studies (SISSA), Trieste, Italy
[af] Also at Department of Physics and Astronomy, University of South Carolina, Columbia SC, United States of America
[ag] Associated at Theory Department, SLAC National Accelerator Laboratory, Stanford, CA, United States of America
[ah] Also at School of Physics and Engineering, Sun Yat-sen University, Guangzhou, China
[ai] Also at Faculty of Physics, M.V.Lomonosov Moscow State University, Moscow, Russia

^{aj} Also at National Research Nuclear University MEPhI, Moscow, Russia

^{ak} Also at Department of Physics, Stanford University, Stanford CA, United States of America

^{al} Also at Institute for Particle and Nuclear Physics, Wigner Research Centre for Physics, Budapest, Hungary

^{am} Also at University of Malaya, Department of Physics, Kuala Lumpur, Malaysia

* Deceased